Departamento de Ingenierías Química y Biomolecular

ETSIIyT, UNIVERSIDAD DE CANTABRIA

MEASUREMENT, CHARACTERIZATION AND SEPARATION OF HIGH ADDED VALUE BIOMOLECULES

(Medida, Caracterización y Separación de Biomoléculas con alto valor añadido)

Memoria de Tesis Doctoral presentada para optar al título de:
Doctora por la Universidad de Cantabria. Doctorado en Ingeniería Química y de Procesos

Virginia Valiño Llamazares

Santander, July 2014

Supervisors:

Dr. Raquel Ibáñez Mendizabal
Dr. Mª Fresnedo San Román San Emeterio

Programa oficial de Doctorado en Ingeniería Química y de Procesos (BOE núm. 36, de 10 de febrero de 2010) con Mención hacia la Excelencia (BOE núm. 253, de 20 de octubre de 2011. Referencia: MEE2011-0031).

The research described in this thesis was carried out at the Advanced Separation Processes Research Group in the Chemical and Biomolecular Engineering Department at University of Cantabria.

The research is financially supported by the Spanish Ministry of Economy and Competitiveness (MINECO) and the European Regional Development Fund (FEDER) through the projects CTQ2008-05545/PPQ, CTQ2008-00690/PPQ, CTQ2008-03225/PPQ, CTQ2011-25262, CTM2011-23912 and CTQ2012. Additionally, the research period was supported by a grant ECD/3628/2011 from the Ministry of Education, Culture and Sports (BOE de 14th January 2012).

There is a driving force more powerful than steam, electricity and atomic energy: the will". Albert Einstein

Virginia Valiño Llamazares

To my family,

Who have shown me courage, values and happiness.

AGRADECIMIENTOS

Quiero expresar mi más sincero agradecimiento a mis directoras, Dra. Mª Fresnedo San Román San Emeterio y Dra. Raquel Ibáñez Mendizabal, por su esfuerzo, paciencia y dedicación a esta tesis, sin ellas no hubiera sido posible.

Muchas gracias a la Catedrática Inmaculada Ortiz Uribe por haberme dado la oportunidad de trabajar en este gran grupo y orientarme en el mundo de la investigación.

Al Profesor Philip Sistat por su acogimiento y su apoyo durante la estancia en Montpellier.

A los Doctores Jose Manuel Benito e Isabel Escudero por su amable acogimiento durante mis estancias en Burgos.

Quiero hacer un especial agradecimiento al Profesor Rafael Valiente por su orientación y compañía durante los largos días de medida en la Facultad de Físicas.

Al personal de administración y servicios por estar siempre dispuestos a ayudar, en especial a Oscar y Pili.

A mis compañeros durante esta etapa, a Javi, Juancho, Gema, Jorge, Rubén, Isa, Rosa, Marta, Maria, Raquel, Axel, Elia, Vanesa, y Antía, por esos grandes momentos que nos permiten desconectar de todo.

A mis amigos, los de aquí y los de allá, por estar siempre a una llamada de distancia.

A Fonsi por ser mi mayor apoyo, en lo bueno y en lo malo, pero sobre todo por hacerme siempre sentir querida y valorada.

Quiero dedicar este trabajo a mi familia, en especial a mis padres y hermanos por confiar siempre en mí y enseñarme a no rendirme nunca.

GRACIAS!

SUMMARY

Bovine whey proteins have been increasingly used as food ingredients, mainly due to their well-balanced amino acid formulation and their functional properties, including the ability to form gels, their solubility and their foaming and emulsifying characteristics. Whey is a high and varied mixture of secreted proteins, which contain a wide range of chemical, physical, and functional properties. Among them, bovine serum albumin (BSA) presents foaming and gelling properties and bovine lactoferrin (LF) exhibits important nutraceutical and anti-inflammatory or antimicrobial properties and plays a significant role in iron metabolism. Such properties made its use interesting in food and pharmaceutical applications. The isolation of proteins from their original mixtures is usually carried out through costly downstream processes that can account for as much as 80 % of the entire production cost. For 100 years the chromatographic techniques have been applied for the quantification and industrial production of protein isolates. With this technique purities higher than 90% are obtained but with a high cost associated and relatively low throughputs. Compared to resin-based chromatography, membrane separations are simple, energy efficient and readily scalable from the laboratory to industrial settings. Despite the significant effort that has been applied toward developing new materials, conformations, and configurations, the industrial application of this technology has not met the requirements to achieve their real separation.

This thesis assesses the quantification, characterization and separation of two high added value biomolecules: Bovine serum albumin (BSA) and Lactoferrin (LF). The main results obtained along this thesis research work are presented in four chapters.

In the first section the composition of the natural medium in which this proteins are present, the whey, was analyzed. Then, a scope

of the state of the art focused on protein measurement, characterization and separation of binary mixtures of BSA and LF was performed.

In the second section two analytical methods have been developed with the objective of quantify BSA and LF in binary mixtures. Firstly a chromatographic method for mixtures in buffers with low salt concentration was obtained. Secondly a new measurement method was proposed for the individual and total protein quantification of mixtures present in high concentrated salt solutions based on fluorescence and ultraviolet absorbance which lead to a Patent invention.

In a third step the properties of BSA and LF were characterized by means of zeta potential, isoelectric point, size, aggregation and foam formation. Ultrafiltration and microfiltration membranes were also characterized in terms of zeta potential and adsorption capacity.

Viability of the separation of BSA-LF binary mixtures by means of electrodialysis with ultrafiltration membranes (EDUF) and diafiltration was carried out, followed by a study of the influence of the main operational conditions with the aim of improving the proposed separation processes. The obtained results, in terms of fluxes and selectivity, were compared with those previously reported in the literature. Additionally, the fouling was study through the changes in zeta potential of membranes and the Derjaguin, Landau, Verwey, and Overbeek (DLVO) theory, and the main mechanism of fouling was established.

Finally the main conclusions derived from the former studies and the future challenges that should be overcome are compiled in the last section of this thesis.

RESUMEN

Con el paso de los años, el uso de las proteínas de suero bovino como ingredientes alimentarios es cada vez mayor, debido principalmente a su equilibrada composición de aminoácidos y sus propiedades funcionales, incluyendo la capacidad de formar geles, su solubilidad y acción espumante y sus características emulsionantes. El suero está formado por una gran variedad de proteínas secretadas, que poseen una gran gama de propiedades químicas, físicas y funcionales. Entre todas las proteínas presentes en el suero, tienen especial relevancia la albúmina de suero bovino (BSA) y la lactoferrina bovina (LF). La primera tiene propiedades espumantes, gelificantes y nutracéuticas, la segunda posee características antinflamatorias, antimicrobianas y juega un papel significativo en el metabolismo del hierro. Estas propiedades hacen que su uso sea interesante en aplicaciones alimentarias y farmacéuticas. La separación de las proteínas a partir de sus mezclas originales se realiza generalmente a través de procesos costosos de purificación que pueden suponer hasta el 80 % de la totalidad del coste de producción. Durante 100 años las técnicas cromatográficas se han aplicado para la cuantificación y la producción industrial de las proteínas aisladas. Con esta técnica se obtienen purezas de más del 90 % pero tienen un alto coste asociado y rendimientos relativamente bajos. En comparación con los métodos cromatográficos, las separaciones con membrana son simples, eficientes energéticamente y fácilmente escalables desde el laboratorio a procesos industriales. A pesar del gran esfuerzo que se ha aplicado en el desarrollo de nuevos materiales, conformaciones y configuraciones, la aplicación industrial de esta tecnología no ha sido conseguida.

Esta tesis evalúa la cuantificación, caracterización y separación de dos biomoléculas de alto valor añadido: la albúmina de suero bovino (BSA) y la lactoferrina (LF). Los resultados principales obtenidos en esta tesis se presentan en cuatro capítulos.

En el primer Capítulo, se detalla la composición del medio natural en el que estas proteínas están presentes, el suero de leche. Después, un alcance del estado de las técnicas de medición, caracterización y la separación de mezclas binarias de BSA y LF fue llevado a cabo.

En el Capítulo dos, se desarrollan y evalúan dos métodos para la cuantificación individual de BSA/LF en mezclas binarias. En primer lugar, un método cromatográfico para mezclas en medios con baja concentración salina. En segundo lugar, un nuevo método de medición fue propuesto para la cuantificación de proteína individual y total en mezclas presentes en disoluciones salinas concentradas. Este método basado en absorción fluorescente y ultravioleta llevó a la presentación de una patente.

En el tercer Capítulo, se presentan los resultados de la caracterización de las proteínas, BSA y LF, a través de la medida de potencial zeta, tamaño, agregación y capacidad espumante. Las membranas de ultrafiltración y microfiltración fueron también caracterizadas mediante el potencial zeta y la capacidad de adsorción

En el Capítulo 4 se evaluó la viabilidad de la separación de mezclas de ambas proteínas mediante dos tecnologías, electrodiálisis con membranas de ultrafiltración y diafiltración, seguido del estudio de las principales variables de operación. Los resultados obtenidos fueron comparados en términos de flujo y selectividad con los valores reportados previamente en la literatura. Adicionalmente, el ensuciamiento fue estudiado a través de los cambios en el potencial zeta de las membranas y teoría Derjaguin, Landau, Verwey y Overbeek (DLVO), y el principal mecanismo de fouling fue determinado.

Por ultimo las conclusiones más relevantes y los retos a los que se deberá enfrentar el trabajo fututo están recogidos en la última sección de la tesis.

CONTENTS

1

MOTIVATION

Abstract

This thesis proposes innovative alternatives to the conventional separation process of two minor whey proteins with similar properties based on a combination of adequately modified charged membranes and optimum process conditions. To achieve this aim the study of the quantification method as well as the performance of surface characterization of proteins and membranes was needed. This preface chapter introduces an overview of the importance of whey protein and especially the targets bovine serum albumin and lactoferrin. The state of the art of the protein measurement, characterization and separation was reviewed. Finally, the scope and outline of the thesis are summarized.

1.1. MILK WHEY: CHARACTERISTICS AND COMPOSITION

Cheese is a foodstuff produced from curdled milk from a wide number of animals including cows, goats, sheep and water buffalos. Rennet is often used to make the milk to curdle conversion, although some cheeses are curdled with acids like lemon juice or vinegar. Whey is a by-product of these processes, which for years has been misused either as animal feed or it was disposed of as a waste. However, whey is of relative importance in the dairy industry due to the large volume of production and its nutritional composition. Its disposal as a waste is problematic due to several reasons: the high BOD_5, values in the range 35.000 - 55.000 mg O_2 L^1 [1] and the high volume of production, it has been estimated that, the world whey production is over 160 million tons per year [2] , that make its treatment cost prohibitive. The last reason is its composition formed by more than half of the solids present in the original whole milk, including whey proteins, lactose, minerals and water-soluble vitamins. Consequently, whey should be considered as a valuable by-product with several potential applications in the food and pharmaceutical industries [3].

Several types of whey can be found, depending on the method of precipitation that is employed to separate the casein. Sweet whey is obtained as a result of its precipitation by rennet. The production of soft, fresh and curd cheese relies on precipitation by lactic acid producing bacteria and acid whey types. Casein whey is the result of the production of casein that makes use of mineral acids as the means of precipitation. Sweet whey is the most commonly obtained whey [4].

Regarding the chemical composition of whey, it is formed by 94.0 per cent of water and 6.0 per cent of solids (around half of the dry total milk solids). Lactose is the main constituent, accounting for approximately 77.0 % of the total solids, followed by the proteins (approx. 12.0 %) and minerals (10.0 %). Fat only accounts 0.1% of the total solids [5]. The typical composition of the different types of liquid whey is given in Table 1.1.

Table 1.1. Typical composition of whey from different sources [5]**.**

Composition (%)	Sweet Whey	Acid Whey	Casein Whey
Total solids (%)	6.2	5.7	6.1
• **Lactose (%)**	69.0-76.0	65.0-69.0	64.0-68.0
• **Proteins (%)**	11.0-14.0	7.0-9.0	9.0-11.0
• **Fat (%)**	0.5-2.0	-	-
• **Ash (minerals) (%)**	6.0-9.0	9.0-12.0	10.0-13.0
• **pH**	6.0-6.8	4.2-5.0	4.0-4.8

Lactose

Lactose, the major component of whey (77.0 %), is probably the least valuable component and the most difficult to use. However, it is a very important source of energy and presenting several interesting functions. Some beneficial effects are attributed to lactose, like the stimulation of peristaltic activities in the digestive tract, the establishment of lightly acid reaction in the stomach, which inhibits the growth and expansion of pathogens, or the improvement of calcium and phosphor absorption [6]. Moreover, lactose also improves digestion of milk fat and other nutrients, carries a role for the development of the brain and nervous system through the galactose (the simple sugar found in lactose) and assures the optimal amount of magnesium [6]. Nevertheless there are some side effects as lactose intolerance; caused by the inability of the body to break down milk sugars. This disease affects to the 33.0 % of worldwide population (Data taken from National Digestive Diseases Information, USA Today. Date Verified: 23.7.2012).

Proteins

Due to their aminoacid composition (high content of essential aminoacids) whey proteins present higher biological value than casein or other proteins of animal origin, including egg proteins which have been considered for a long time as referent proteins [6]. Whey proteins (WP) are also rich in branched chain amino acids (leucine, isoleucine, and valine) (>20.0 %, w/w), which are thought to play a task as metabolic regulators in protein and glucose homeostasis (the maintenance of

metabolic equilibrium), and in lipid metabolism, and thus may play a function in weight control [7]. Moreover, WP is a rich and balanced source of sulfur amino acids (methionine, cysteine) that possess a critical anti-oxidants capacity, as precursors to the potent intracellular anti-oxidant glutathione, and in one-carbon metabolism [7]. Further information about whey proteins will be discussed in section 1.2.

Minerals

Whey is a good source of electrolytes including sodium and potassium, especially during diarrhea therapy. Some of them are present in solution and also partly bound to proteins. There are 20 minerals that are considered essential for humans and can be divided in two groups: macrominerals (Calcium, sodium, chloride, magnesium, phosphorus and potassium) and trace elements (Copper, nickel, manganese, iron, selenium, zinc, silicon, iodine, molybdenum, cobalt, boron, fluoride, chromium, arsenic and silicon [8,9]. Information about the electrolyte composition of whey is shown in Table 1.2.

Table 1.2. Chemical composition of Casein and Cheese (sweet-acid) whey.

Contents (mg L^{-1})	Casein whey	Sweet-Acid whey
Sodium	350±3.9	260±1.8
Potassium	1300±2.5	1300±1.6
Calcium	480±1.3	291±3.2
Magnesium	59±0.2	36±0.2
Chloride	1349±1.7	1167±1.5
Citrate	6750±1.7	2452±3.7
Zinc µg L^{-1}	280±0.2	210±0.2
Iron µg L^{-1}	25.7±0.1	23.8±0.0

Results are expressed as mean ± S.D, n=3. Source:[10] Goyal and Gandh (2009).

This mineral composition confers to the whey a high conductivity, about 5.0 S cm^{-1} [11]. The presence of mineral ions can alter the net charge on the protein molecules and hence the interaction forces and aggregation and therefore the different whey treatment processes.

Vitamins

At least the 50.0 % of each water-soluble vitamin present in milk is transferred to whey during the manufacturing process. The intervals of transmission are: 40.0 - 70.0 % for vitamin B12; 55.0 - 75.0 % for vitamin B6 and pantothenic acid; 70.0 - 80.0 % for riboflavin and biotin and 80.0 - 90.0 % for thiamine, nicotinic acid, folic acid and ascorbic acid [8].

Whey uses and recovery

Most of the work regarding the utilization of whey has been carried out worldwide in the production of Whey Protein Concentrates (WPC), isolates (WPI), hydrolyzates (WPH), lactose and lactic acid [10]. Many attempts have been done on utilization of whey in the formulation of different dairy products, particularly for its utilization in beverage in health based energy drink production industries [6,12–16].

Nevertheless, the three major forms in which whey protein products are available: WPC, WPI and WPH, have limited acceptance by the food processing industry because of the lack of consistency in the gross composition and functionality; whereas each individual whey protein has unique attributes for nutritional, biological and food ingredient applications; and moreover exhibits a better functionality than in their native protein mixtures [3].

1.2. MILK WHEY PROTEINS

Whey proteins exhibit a big nutraceutical and biological importance due to its essential amino acids profile and its easily digestibility. Moreover, they have become an important component for many food products due to their ability to confer functional characteristics that include foaming, emulsification, gelation and stabilization. For these reason, whey proteins fulfill all of the qualitative and quantitative requirements established by the Food and Agriculture Organization (FAO) and by the World Health Organization (WHO) [17]. The world whey (bovine, caprine or ovine) production is over 160 million tons per year [2], being bovine whey the major stream. The protein composition of bovine whey is shown in Table 1.3.

Table 1.3. Bovine whey protein composition [18]**.**

Protein	Concentration g L^{-1}	MW kDa	Isoelectric point (Ip)
β-Lactoglobulin (β-Lg)	2.7	18.4	5.2
α-Lactoalbumin (α-La)	1.2	14.2	4.5-4.8
Inmunoglobulins	0.6	150.0-100.0	5.5-8.3
Bovine serum albumin (BSA)	0.4	66.5	4.7-5.0
Lactoferrin (LF)	0.1	78.0	7.0-9.0
Lactoperoxidase	0.02	89.0	9.5

Serum proteins can be divided in major and minor proteins in terms of concentration. The first group is formed by β-Lactoglobulin and α-Lactalbumin with a concentration that ranges from 2.7 to 1.2 g L^{-1}. The second one is composed by Immunoglobulins, Bovine Serum Albumin, Lactoferrin and Lactoperoxidase and there are found in concentrations between 0.7 and 0.03g L^{-1} [19].

β-Lactoglobulin (β-Lg)

β-Lactoglobulin (β-Lg) is the major whey protein in the milk of ruminants and many other mammals, representing half of the whey proteins (Figure 1.1). This globular soluble protein presents a monomer form with a molecular mass of about 18.0 kDa at a pH of 3.0. At a pH of between 3.0 and 7.0 (range of stability), which includes the pH of cheese

whey, β-Lg exists in solution as a dimer with an effective molecular mass of about 36.0 kDa. It has an isoelectric point of 5.2 [20]. Each monomer is formed by 162 amino acids, with two disulphide bridges and one free cysteine [21]. β -Lg belongs to the lipocalin protein family, and it is one of the main milk allergens [22]. At pH above 8.6, with heating and/or in presence of high levels of Ca^{2+} ions, its irreversible denaturation takes place [23].

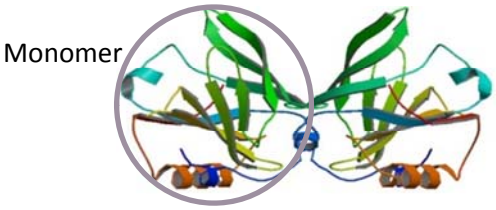

Figure 1.1. Bovine β-Lactoglobulin dimer crystal structure. (Protein Data Bank http://www.rcsb.org/pdb/home/home.do, 2014)

Many different variants of β-Lactoglobulin have been identified in the cow milk, being the most prevalent variants A and B, which differ at aminoacid position 64 (Asp/Gly) and 118 (Val/Ala) [21]. Although it is the most hydrophobic of whey proteins, it presents a high solubility in water due to the close position of non-polar components and the availability of polar ones [18].

It is an extensively studied protein with high ability to link in vitro to a wide range of hydrophobic substances, as retinol (Vitamin A) and long chain fatty acids but still its biological function is not well established. Some roles had been attributed to β-Lg, as the increase of fatty acids absorption [24], the modification of the kinetics of the enzymatic hydrolysis of the protein [25,26], the protection of sensitive ligands against oxidation [27] or other stresses, or the modification of the bioaccessibility of the ligands [28,29].

Regarding the food functional characteristics, β-Lg has excellent heat-set gelation characteristics [30]. The enrichment in this protein is used in ingredients in which water biding and texturing are required. Some examples are manufactured meats, reformed fish products and a variety of formulated foods. The nature of gels (translucent or opaque,

and elastic or inelastic) can be easily manipulated through control of chemical conditions (e.g. pH and ionic strength) during gelation, expanding the range of applications in which an ingredient enriched in this whey protein can be used [31]. Its excellent whippability, with a foam overrun capacity and heat stability equivalent to egg albumin (egg white), provides an alternative in some food applications. Thus, an ingredient enriched in β-Lg can be used as a cost-effective substitute for egg white in meringues and similar products [32].

α-Lactoalbumin (α-La)

α-Lactoalbumin (α-La) is a small, globular, acidic, cation binding milk protein (Figure 1.2), which plays an important role in lactose synthesis, it is used as a model Ca^{2+} binding protein or as molten globular protein and present important biological and functional properties (some forms of α-La can induce apoptosis in tumor cells [33]).

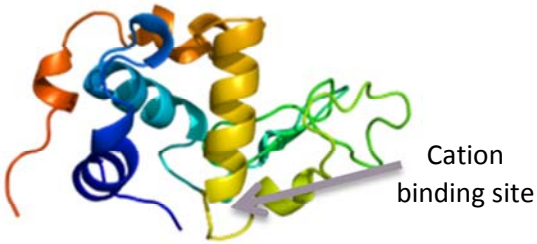

Figure 1.2. Bovine α-Lactoalbumin crystal structure. (Protein Data Bank http://www.rcsb.org/pdb/home/home.do, 2014)

It is a single polypeptide chain, made of 123 amino acid residues, forming a compact globular structure stabilized by four disulfide bonds. It has an isoelectric point of 4.6, a molecular mass of 14.2 KDa and present no free thiol groups [7]. α-La has a calcium ion linked which plays an essential role in the protein structure, stability and in its activity regulating the galactosyl transferase. Removal of the bound Ca^{2+} reduces the stability of the native tertiary structure, forming the so called *"molten globule structure"* (an intermediate denaturalized state) [18]. α-La is considered as the most heat-stable whey protein, but denaturation takes place regardless of whether the protein is at pH values below 4.0 or above 9.0, is heated above 50 °C, exposed to low

concentrations of guanidine hydrochloride, or subjected to Ca^{2+} removal from the native form. In solution, α-La undergoes intermolecular interactions leading to varying degrees of polymerization on both sides of its zone of insolubility. At acidic pH values, the protein performs a rapid reversible association and slow aggregation. Between pH 6.0 and 8.5 there is very little association, and above pH 9.5 there is expansion without aggregation [34]. α-La is commonly used as an additive in infant formula since in human milk was a high concentration (60.0 %) being the second major globular protein in the bovine milk (20.0 %), playing a role in the rapidly growing of neonate.

Immunoglobulins

Immunoglobulin (Ig) is an antibody or gamma-globulin (Figure 1.3). This general term is applied to a family of high molecular weight proteins that share common physico-chemical characteristics and antigenic properties [35]. There are five types of antibodies – IgA, IgD, IgE, IgG, and IgM, but only three of them are present in bovine milk whey: IgG, IgA, and IgM [36].

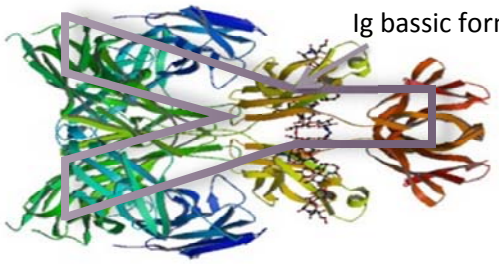

Figure 1.3. Bovine Immunoglobulin crystal structure. (Protein Data Bank http://www.rcsb.org/pdb/home/home.do, 2014)

All of these molecules present a similar basic structure being composed of 2 light chains with molecular weights of 20.0 – 25.0 kDa and two heavy chains, having molecular weights of 50.0 - 70.0 kDa. IgG antibodies, the major immune component of bovine whey, express multifunctional activities, including complement activation, bacterial opsonization and agglutination, and act by binding to specific sites on

the surfaces of most infectious agents or products, either inactivating them or reducing the infection.

IgG is a monomeric glycoprotein formed by two heavy (long) and two light (short) polypeptide chains that are linked by disulfide bonds. The polypeptide chains contain constant (Fc) and variable (Fab) regions of amino acid sequence, being the antigen-binding sites located in the Fab N-terminal region. Genes encoding the Fc domain are the primary factors characterizing Ig class. The subclasses IgG1 and IgG2 differ primarily in the Fc domain of their heavy chains [37].

IgM is present in serum, colostrum and milk. IgM looks like a polymer, being formed by five or four-chain subunits which are linked by inter-subunit disulfide bonds found on the Fc portion of their μ-heavy chains. This configuration provides IgM with ten, rather than two, potential antibody combining sites. IgM has an important role in the primary immune response, as an agglutinating antibody of the serum or in complement fixation. It its especially associated to the parasitic infections of Anaplasma [36].

As bovine α-La, there are commonly used as an additive in infant formula and other foods for trying to reduce viral and microbial infections, and to provide consumers with improved immune activity, although some researchers suggest that certain bovine Ig subclasses may display detrimental effects [37].

Bovine serum albumin (BSA)

Bovine serum albumin (BSA) is a globular protein (Figure 1.4) with a prolate ellipsoid shape that is not synthesized in the mammary gland, but appears instead in milk following passive leakage from the blood stream [36]. Fist isolated from human plasma, nowadays the BSA powder is obtained from bovine serum by Cohn fractionation or chromatographic techniques. The estimated worldwide production of BSA is about 300 tons per year [38].

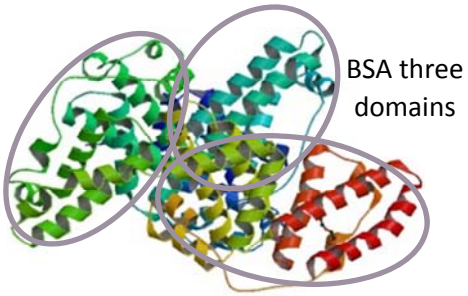

Figure 1.4. Bovine serum albumin crystal structure. (Protein Data Bank http://www.rcsb.org/pdb/home/home.do, 2014)

It contains 592 amino acid residues, which lead to a molecular weight of 66.5 kDa. In Table 1.4 the aminoacid composition of BSA is detailed.

Table 1.4. BSA aminoacid sequence [18]**.**

Aminoacid	Number	Aminoacid	Number
Valine (Val, V)	46	**Alanine (Ala, A)**	47
Leucine (Leu, L)	66	**Proline (Pro, P)**	28
Threonine (Thr, T)	36	**Glycine (Gly, G)**	16
Lysine (Lys, K)	59	**Serine (Ser, S)**	28
Tryptophan (Trp, W)	2	**Cysteine (Cys, C)**	34
Histidine (His, H) *	17	**Asparagine (Asn, N)**	14
Phenylalanine (Phe, F)	27	**Glutamine (Gln, Q)**	21
Isoleucine (Ile, I)	14	**Tyrosine (Tyr, Y)**	20
Arginine (Arg, R) *	26	**Aspartic acid (Asp, D)**	40
Methionine (Met, M)	4	**Glutamic acid (Glu, E)**	68

BSA Possesses 17 intermolecular disulphide bridges and one thiol group at residue 34 and can bind to free fatty acids and other lipids, as well as flavor compounds due to its size and structure. The three-dimensional conformation of BSA is composed of three homologous domains (I, II, III) specific for metals and fatty acids. Each domain is the product of two subdomains, which are predominantly helical [36]. Foster, 1977 [39] reported that BSA has several isomeric forms at different pH that correspond to different α-helix contents. The BSA conformers are classified as the following: E, extended; F, fast migration; N, normal dominant form at a neutral pH; B, basic form; and A, aged at an alkaline pH (Figure 1.5).

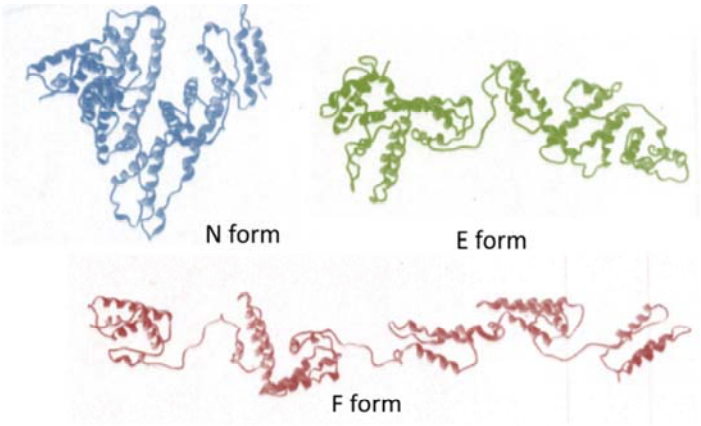

Figure 1.5. Bovine serum albumin isometric forms [40]**.**

BSA is readily soluble in water and requires high concentrations of neutral salts, such as ammonium sulfate, to induce precipitation [41]. It is also a source of essential amino acids, but there is very little available information regarding its potential therapeutic activity [36]. In spite of these, one important property that has been associated to BSA is the ability to inhibit tumor growth [42], it is known to participate in the synthesis of lipids [43] and to have antioxidant activity [44]. Moreover, there is a large of biochemical applications linked to BSA including ELISAs (Enzyme-Linked Immunosorbent Assay), immunoblots, and immunohistochemistry. It is also used as a nutrient in cell and microbial cultures and as model protein for concentration measurements (Bratford assay). In restriction digests, BSA is used to stabilize some enzymes during digestion of DNA and to prevent adhesion of the enzyme to reaction tubes, pipet tips, and other vessels [45]. It is also of interest in a number of food applications due to its foaming, gelling and ligand linking properties [41].

Lactoferrin (LF)

Lactoferrin (LF) is a monomeric, bilobal iron-blinding glycoprotein (Figure 1.6) with a molecular weight of about 80.0 kDa [46]. First identified in milk as the red milk protein due to its iron content, LF has attracted much interest over the past fifty years. It contains 685 amino

acid residues. In Table 1.5 the aminoacid composition of Lactoferrin is detailed.

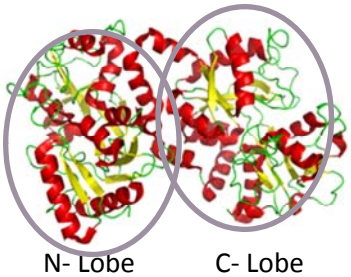

Figure 1.6. Bovine Lactoferrin crystal structure. (Protein Data Bank http://www.rcsb.org/pdb/home/home.do, 2014)

Table 1.5. LF aminoacid secuence [18]**.**

Aminoacid	Number	Aminoacid	Number
Valine (Val, V)	46	**Alanine (Ala, A)**	67
Leucina (Leu, L)	66	**Proline (Pro, P)**	29
Threonine (Thr, T)	36	**Glycine (Gly, G)**	49
Lysine (Lys, K)	54	**Serine (Ser, S)**	45
Tryptophan (Trp, W)	13	**Cysteine (Cys, C)**	34
Histidine (His, H) *	10	**Asparagine (Asn, N)**	29
Phenylalanine (Phe, F)	27	**Glutamine (Gln, Q)**	29
Isoleucine (Ile, I)	17	**Tyrosine (Tyr, Y)**	21
Arginine (Arg, R) *	37	**Aspartic acid (Asp, D)**	36
Methionine (Met, M)	4	**Glutamic acid (Glu, E)**	40

LF is considered to be an important host defense molecule and has a diverse range of physiological functions some related to its iron binding capacity as the absorption, antimicrobial activity or iron regulation in inflammation processes and many others not related like the anti-tumoral, the immunomodulatory and the procoagulant properties [47]. The most important capacities attributed to LF are shown in the Figure 1.7.

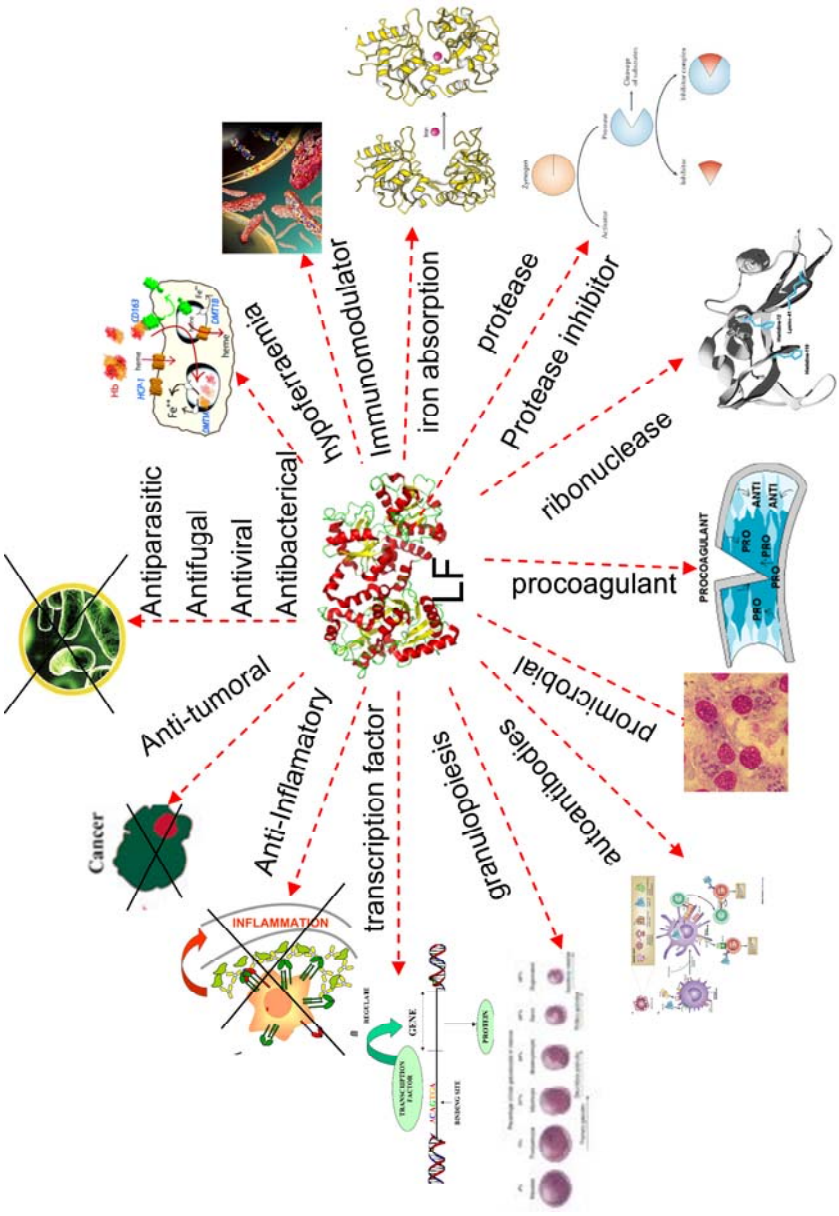

Figure 1.7. Roles of Lactoferrin reported in literature [18].

Some of these functions have been very well studied, like its antibacterial property, with more than two thousand papers [48–62]. In these works the ability of LF to inhibit the growth of a big variety of Gram positive and Gram-negative bacteria, among them: Escherichia coli, Salmonella typhimurium, Shigella dysenteriae, Listeria monocytogenes, Streptococcus mutants, Bacillus stearothermophilus and Bacillus subtilis, was established [63]. The function of the protein in the antimicrobial function has three steps: The first function attributed to LF was the activity that depended on its capacity to sequester iron, micronutrient of bacteria, which prevent their growth; the second role of LF is to modulate the motility and aggregation of pathogenic bacteria, increasing membrane permeability of lysozyme and other antibacterial molecules; the third one has been recently discovered, the proteolytic action that consists in the degradation of some microorganisms to reduce its pathogenicity [64]. Then, due to its large list of functions, LF may enter the composition of in a wide range of products from many different industries: food (infant formulas, health foods, preservatives and dairy products), pharma (prescription drug or Over-the-Counter (OTC)), cosmetics and hygiene products (skin and hair care, oral hygiene and chewing gun) and veterinary (preservatices) [65].

LF is found in cow and human milk as well as in other mucosal secretions as tears, synovial fluids, saliva or seminal plasma. The amount of this protein in this fluids has a huge range being the lowest for saliva (0.007 - 0.01 g L^{-1}) [66] and the biggest concentration by far, in human colostrum, the early milk, containing up to 7.0 g L^{-1} [67]. Nevertheless, for large scale production, native bovine lactoferrin is usually isolated from dairy products like bovine whey, with a concentration around 0.1 g L^{-1}. This low concentration as well as the presence of other proteins with similar molecular weight and properties made the isolation a technical challenge.

Due to LF cationic nature according to its amino acid composition, it can be purified by cation-exchange chromatography such as carboxymethyl (CM)-Sephadex [68,69] and this method is the most popular procedure for the purification in bLF-supplying companies with

a production of 60 tons annually worldwide [70].This method produces LF with purity of about 90.0 %, but with a high cost associated and relatively low throughputs [71].

1.3. STATE OF THE ART

1.3.1. PROTEIN QUANTIFICATION

One of the aims of this thesis is the development of a BSA-LF quantification method in binary mixtures. In this section, the related work reported in literature is described.

During a protein purification procedure, one of the most important aspect is to follow the recovery of the protein, by simply quantifying the desired component [72]. Several instrumental methods for protein concentration measurement can be found in the literature. They can be divided in i) total protein concentration and ii) individual protein concentration methods as it is shown in Table 1.6.

Table 1.6. Most used protein quantification methods.

Protein quantification methods	
Total	**Individual**
Absorbance- based methods	Enzyme-Linked Immunosorbent Assay (ELISA)
Kjeldahl	
Turbidimetric methods	Electrophoretic techniques
Nephelometric methods	Chromatographic techniques
Colorimetric methods	

Total Protein Concentration Methods

Regarding the total protein concentration methods, which follows the general concentration of the sample without identification of the species present; the absorbance based are the most commonly applied. Other measurements that used Kjeldahl, turbidimetric and nephelometric, or colorimetric methods are also applied. This methods use the BSA as a model protein, leading this assumption in some cases to a big measurement error.

*Absorbance- based method*s quantification leads on the use of the well-known Beer–Lambert law, which describes the linear relation between the concentration of the absorbing molecule, the absorbance coefficient of the absorbing molecule, optical path length, and

absorbance. 280.0 nm (aromatic rings emission) and 205.0 (peptide bonds emission) are the two major used wavelengths for protein determination The measurement at 205.0 nm is more difficult than at 280.0 nm, since the 205.0 nm peak is right on the shoulder of the protein peak. The assays require only a widely used spectrophotometer with a UV lamp. The properties of the surrounding medium of the molecule affect its absorption spectrum. Changes in temperature, pH, ionic strength, solvent purity and polarity, concentration of the molecule, and the interaction with another molecules are possible reasons for observed perturbations [73]. The use of BSA as a model protein for total protein concentration quantification, when the protein composition is unknown, may result in a wrong determination of the total amount, due to the differences of absorbance for the same concentration of the different proteins.

In the *Kjeldahl method* the sample is digested with a strong acid so that it releases nitrogen, which can be determined by a suitable titration technique. The amount of protein present is then calculated from the nitrogen concentration of the sample. It is usually considered to be the standard method of determining protein concentration. Because the Kjeldahl method does not measure the protein content directly a conversion factor (F) is needed to convert the measured nitrogen concentration to a protein concentration. A conversion factor of 6.25 (equivalent to 0.16 g nitrogen per gram of protein) is used for many applications, however, this is only an average value, and each protein has a different conversion factor depending on its amino-acid composition [74]. The use of BSA as a model protein for total protein concentration quantification results in a wrong determination of the total amount, due to the divergences in aminoacid composition of the different proteins.

The *turbidimetric and nephelometric techniques* are methods for determining the amount of cloudiness upon the transmission and scattering of light [75]. These techniques are also based on a model protein.

The most commonly used *colorimetric techniques* are Biuret method [76], the Lowry method [77], Bradford method [78] and the bicinchoninic acid (BCA) assay [79].

In the *Biuret method* by a simple addition of one component (a solution of copper sulfate ($CuSO_4$) and potassium hydroxide (KOH)) and after 20 min of incubation, the divalent copper ion in the reagent forms a complex with the amide groups of the protein and is reduced to a monovalent ion under alkaline conditions. The purple complex formed absorbs at 550.0 nm and the absorbance is directly proportional to the quantity of proteins [76] but different for each protein, leading to wrong measurements if the exact composition of the mixture is not known.

The principle behind the *Lowry method* lies in the reactivity of the peptide nitrogen with the copper (II) ions under alkaline conditions and the subsequent reduction of the Folin-Ciocalteay phosphomolybdicphosphotungstic acid to heteropolymolybdenum blue by the copper-catalyzed oxidation of aromatic acids within 30 min of incubation [80]. The Lowry method is sensitive to pH changes and therefore the pH of the assay solution should be maintained at 10.0 - 10.5. The main disadvantage of this method is the narrow pH range within which it is accurate. A variety of compounds will interfere with the Lowry procedure, including some amino acid derivatives, certain buffers, drugs, lipids, sugars, salts, nucleic acids, sulphydryl reagents, ammonium ions, zwitterionic buffers, nonionic buffers and thiol compounds. These substances should be removed or diluted before running Lowry assays. The complex formed absorbs at 600.0 nm and the absorbance is directly proportional to the quantity of proteins [77] but different for each protein, leading to wrong measurements if the exact composition of the mixture is not known.

The *Bradford assay* is a protein determination method that involves the binding of Coomassie Brilliant Blue G-250 dye to proteins [78]. Under acidic conditions, the dye is predominantly in the doubly protonated red cationic form. However, when the dye binds to protein, it is converted to a stable unprotonated blue form [81]. Certain

chemical-protein and chemical-dye interactions interfere with the assay [81]. Known sources of interference, such as some detergents, flavonoids, and basic protein buffers, stabilize the green neutral dye species by direct binding or by shifting the pH. The blue protein-dye form is detected at 595.0 nm in the assay using a spectrophotometer reader. The absorbance is directly proportional to the quantity of proteins but different for each protein, leading to wrong measurements if the exact composition of the mixture is not known.

The BCA [79] method combines the Biuret reaction with the colorimetric detection of the monovalent copper ion by bicinchoninic acid (BCA) with the intention of improving the sensitivity of the biuret method. After the reduction of the divalent copper ion, Cu^{2+} reacts with BCA and forms a complex with two BCA molecules. The complex is colored and absorbs at 562.0 nm. The absorbance increases linearly with increasing protein concentration, but different for each protein, leading to wrong measurements if the exact composition of the mixture is not known. The method tolerates contaminants, especially detergents, better than the Lowry method, as the BCA reagent does not precipitate as easily as the Folin-Ciocalteu reagent in the presence of both non-ionic and ionic detergents. The protein-to-protein variability is similar to the Lowry method [82].

Metsämuuronen et al, 2011 [83] performed a comparison between the most used methods for protein quantification: Lowry, far UV, Bradford and ninhydrin methods. They concluded that, despite the divergences in the protein absorption spectra, the UV 205.0 nm and the Lowry are the most recommended methods for analysis of total protein concentration in whey. The Lowry method results the most accurate methodology to be applied when disturbing substances are present or when the samples are heated or put through shear stress.

Individual Protein Concentration

Regarding individual protein concentration measurements, which follows identification of the species present in the sample as well as their quantification; the enzyme immunoassay, electrophoretic and chromatographic methods can be applied.

Traditionally, the *Enzyme-Linked Immunosorbent Assay (ELISA)* has been the major method used for targeted quantification of a protein, providing good sensitivity and throughput. ELISA is a biochemistry assay that uses a solid-phase enzyme immunoassay (EIA) to detect the presence of a substance, usually an antigen, in a liquid sample or wet sample. Antigens from the sample are attached to a surface. Then, a further specific antibody is applied over the surface so it can bind to the antigen. This antibody is linked to an enzyme, and, in the final step, a substance containing the enzyme's substrate is added. The subsequent reaction produces a detectable signal, most commonly a color change in the substrate. In the cases where ELISA assays or high quality antibodies already exist, the process of validating a biomarker candidate can be relatively straightforward. It has been reported in literature the use of ELISA for the quantification of BSA and LF in complex mixtures [84–89]. However, the ELISA approach is limited by the lack of availability of antibodies with high specificity [86].

On the *electrophoretic techniques* the separation methodology is based on the ion transport through a solution due to the electric field applied. If an electric field is applied to a protein solution, the migration rate during the electrophoresis depends on a variety of factors including the aggregate charge on its surface, size, shape, charge and strength of the applied electric field. Further, the pH of the electrophoresis buffer also influences protein migration since it affects the net charge on the protein surface. A typical electrophoretic run involves separation of samples on a gel support that is immersed in buffer with the gel sandwich spanning both electrodes and the proteins migrating as anions toward the cathode. Once the separation is achieved, the gel is stained by a variety of methods to visualize the separated proteins or processed

otherwise [90]. Among the electrophoretic techniques the capillary electrophoresis and the gel electrophoresis are the most commonly used techniques for serum protein determination [91–98], however, the accurate separation and determination of BSA and LF thought this technique is not already achieved.

Regarding the chromatographic techniques, the following specific techniques can be differentiated: ion-exchange chromatography, reversed-phase chromatography, size-exclusion chromatography and affinity chromatography.

Ion Exchange Chromatography and affinity chromatography are the most extended methods in use as in development. Several results that satisfactorily achieved the separation of LF from the other proteins mixture through this technique can be found in the literature [84,99–117]; nevertheless, this methodology has several disadvantages as low recovery and many elution steps. It is also very sensible to the work media, being the used of this technique, inappropriate in the case of high salty buffers.

Despite the efforts in chromatographic techniques research [118,119], no satisfactory results had been obtained regarding BSA and LF individual quantification in binary mixtures with size-exclusion chromatography or reversed-phase chromatography due to the proximity of their molecular weights and hydrophobicy.

To conclude, among all the techniques previously described in this section only Enzyme-Linked Immunosorbent Assay and Affinity or Ion-Exchange Chromatography had satisfactorily quantified individual BSA and LF from binary mixtures, but these methods are highly dependent of the solution medium. The research of a methodology method that can be applied in salty solutions is needed but the similarity in the measurable properties, the same emission wave length spectra (200.0 – 400.0), similar molecular weights (65.0 kDa BSA and 79.0 kDa LF), isoelectric points (BSA 4.5 and LF 7.0 – 9.0) or hydrophobicity (GRAVY Index: -0.4 BSA and -0.3 LF [113]), makes this protein mixture separation and quantification a technical challenge.

1.3.2. PROTEIN AND MEMBRANE CHARACTERIZATION

The separation of proteins from their original mixtures is carried out through costly downstream processes that can account for as much as 80.0 % of the total production cost [120]. There are many challenges that make protein separation a difficult task: (i) Proteins are composed of a large variety of amino acids and the difference in these amino acid sequences often leads to completely different properties and functions, ii) The different solution media (e.g., different pH values) may influence and change the activity of the same molecule, iii) When proteins are in their native environments, they always reside in a multi-component mixture where molecules with similar molecular weights (M_W) may coexist, iv) High value proteins may bind to other molecules, which complicate their separation by size exclusion methods (v) Protein solutions are colloidal and have transport properties related to the pH value of the solution, the proteins' M_W and the charge properties of the separation environment (e.g., solution, gel and membranes), etc. [121]. Thus, it seems to be infeasible to develop an all-embracing principle for protein separation based solely on single protein characteristics.

Among the factors that influence the separation of high added value food proteins, the electrostatic interactions, such as the zeta potential, are crucial for a better understanding of the process [41,122,123] Examples of the importance of such interactions are found in protein foams [124], the food industry [125], enzyme immobilization [126], food and pharmaceutical formulations [127] and other bioprocesses [128]. It is well established that protein transport through semipermeable ultrafiltration membranes (widely used for protein separation [129]) can be strongly affected by electrostatic interactions between the charged membrane and the charged protein [130]. Furthermore, due to the nature of protein interactions, protein aggregation may occur, leading to differences in size, shape and morphology. Therefore, it is important to understand the interactions, causes and analyses of such behavior to enable successful separations [131]. The study of the zeta potential has been applied so far to samples of a concentration up to 1.0 g L^{-1} of BSA and 0.4 g L^{-1} LF in electrolytic

solutions whit concentrations rages from 0.001 M to 0.1M [132–139], but it study has not been performed in buffer media, with the concentration of the protein or for the mixture of both proteins.

To maximize the effectiveness of the separation processes, an accurate description of the effect of physicochemical interactions between protein molecules is necessary [140]. Particle size measurements allow the correct selection of the membrane cut-off, as well as the proper prediction of protein aggregation and foaming, thus allowing for the correct selection of buffers, pH and temperatures for storage [141]. The description of the protein can be performed by zeta potential and particle size measurements through electrophoretic light scattering (ELS) and dynamic light scattering (DLS) techniques, respectively. Such measurements may be made in free solution and over a wide range of ionic strength and pH [142]. The size measurements found in literature [143–146] correspond to high dilated filtrated samples but there is a lack in the characterization on samples not treated that will give the behavior of proteins during the separation process. Moreover, there is a gap concerning the determination of zeta potential and size of proteins with similar characteristics found in the same natural media, such as bovine serum albumin (BSA) and bovine lactoferrin (LF). Membranes have been also deeply studied [147–150], but the influence of the specific medium of work made their characterization unavoidable.

Then, the precise determination in the separation mediums of protein and membrane zeta potential, protein electrophoretic mobility, isoelectric point, size, aggregation and membrane adsorption capacity is needed for the correct selection of the separation operational conditions.

1.3.3. PROTEIN SEPARATION

Due to the large number of potential applications of protein isolates, quite a large number chromatographic processes have been developed for the isolation of high-purity protein fractions [84,105,151–153]. Affinity chromatography is one of the most powerful techniques available for purifying biomolecules in large-scale production and is commonly applied in downstream processes [4,105,132,152,154–157]. Compared to resin-based chromatography, membrane separations are simple, energy efficient and readily scalable from the laboratory to industrial settings [121]. Despite the significant effort that has been applied toward developing new materials, conformations, and configurations, the industrial application of this technology has not yet been achieved. The low selectivity and/or flux, especially during the separation of similarly sized proteins, are issues that need further improvement before an industrial application can be viable. The model proteins mixtures more references in the literature are included in Table 1.7 where three different types of separation studies have been reported: i) those separation studies regarding proteins of similar size that can be found together in natural sources like β-lg and α-la; ii) those studies performed using similar size proteins than cannot be found together in literature as BSA and Ovalbumin (Egg) and finally iii) studies of different size protein mixtures.

Table 1.7. Relevant protein separation studies reported in literature.

NATURAL MIXTURES FROM SIMILAR SIZE PROTEINS				
Ref	**Proteins ($g\ L^{-1}$)**	**Technology**	**Flux ($g\ m^{-2}\ h^{-1}$)**	**Selectivity**
[158]	β-lg=6.1 α-la= 1.0 BSA= 0.2 Ig=0.1	UF	6.37 α-la 51.0 total $L\ m^{-2}\ h^{-1}$	α-la /β-lg =10.0
[159]	β-lg =3.0 α-la= 1.5	UF	0.7 α -la 10.1 total $L\ m^{-2}\ h^{-1}$	α-la /β-lg > 55
[160]	β-lg = 8.0 α-la=1.5 BSA=1.3	2 UF steps	Steps: 1º: 50.0 $L\ m^{-2}\ h^{-1}$ 2º: 50.0 $L\ m^{-2}\ h^{-1}$	α-la/ BSA = 74.0 α-la /β-lg = 21.0
[161]	β-lg, α-la WPI 5.0 ,10.0 and 20.0 % (w/w)	EA	Precipitation	Recovery of β-lg 44.0 % purity of 98.0 %
[162]	3.1 whey protein: β-lg and α-la real mixture	UF	26.4 α-la 64.0 total $L\ m^{-2}\ h^{-1}$	α-la /β-lg =45.0
[163]	β-lg =1.0 α-la=1.0	UF	93.0 $L\ m^{-2}\ h^{-1}$	α-la /β-lg =7.5
[164]	β-lg=0.2 α-la =0.1	EDUF	7.1 β-lg 28.6 $L\ m^{-2}\ h^{-1}$	α-la /β-lg=1.3
[165]	β-lg A=0.07 β-lg B=0.05 α-la= 0.03	P + UF-MF	Precipitation	Recovery of β-lg 80.2-97.3% purity of 97.2% Recovery of 60.7-80.4% α-la purity of 91.3%
[166]	HB and BSA	UF	---	HB/ BSA = 140.0
[157]	HB=1.0 BSA=1.0	IE ADS	8 BSA 10.0 total $L\ m^{-2}\ h^{-1}$	HB/ BSA = 40.0
[167]	HB=1.0 BSA=1.0	UF	25.8 HB	HB/ BSA = 70.0
[168]	HB= 0.1-0.5 BSA= 0.1-0.5	UF	240.0 total $L\ m^{-2}\ h^{-1}$	HB/BSA= 40.0
[169]	HB=1.0 BSA=1.0	EDUF	9.3 HB 31.1 L total $m^{-2}\ h^{-1}$	Total BSA
[170]	HB=1.7 BSA=1.6	UF	125892 BSA	HB/ BSA = 42.0

Table 1.7. Relevant protein separation studies reported in literature (cont).

Ref	Proteins ($g\ L^{-1}$)	Technology	Flux ($g\ m^{-2}\ h^{-1}$)	Selectivity
[171]	HB=0.113 BSA=0.113	UF	No data	HB/ BSA = 80.0
[10]	HB and BSA 40/1	M ADS	No data	HB/ BSA = 114.6
[132]	BSA=0.1 LF=0.1	UF	240.0 total $L\ m^{-2}\ h^{-1}$	αLF/BSA= 2.5
[172]	Acid Whey	UF	no data	90.0 % of LF in permeate for pH 5.0
[173]	β-lg and glycomacropeptide (GMP)	UF	$1.4{\cdot}10^{-4}$ total $L\ m^{-2}\ h^{-1}$	GMP/ β-lg =21.0
[135]	Synthetic and real Whey. 200.0 ml of whey +2.0 mg commercial LF.	EDUF	LF= 8.9 α-LA = 8.0 β-LG = 41.0 BSA = 2.0	LF/α-LA =1.1 LF/BSA= 4.5 LF/β-LG = 0.2
[174]	Mixture: 1.3 LF (normal or holo-LF)+ 1.3 WPI	EDUF	130.0 total $L\ m^{-2}\ h^{-1}$	$S_{LF/\beta\text{-}LG}$ =3.0–6.7 $S_{LF/\alpha\text{-}LA}$=9.0–62.2 (**)
NO NATURAL MIXTURES FROM SIMILAR SIZE PROTEINS				
Ref	**Proteins ($g\ L^{-1}$)**	**Technology**	**Flux ($g\ m^{-2}\ h^{-1}$)**	**Selectivity**
[175]	LYS egg= 2.0 MYO blood= 2.0 BSA= 5.0	NF	175 LYS	LYS/MYO=6.1 LYS/BSA=4.6
[176]	LYS egg=10.0 MYO blood=5	UF	26.5 Total $L\ m^{-2}\ h^{-1}$ 119.2	LYS/MYO= 12.1
[177]	LYS egg= 0.2 MYO blood= 0.2	UF	250.0 total	LYS/MYO= 2.5
[178]	LYS egg=10.0 MYO blood=5.0 BSA= 20.0	UF	39.8 LYS 26.5 total $L\ m^{-2}\ h^{-1}$	LYS/MYO= 9.0
[89]	BSA=3.0 FABDNA=3.0	UF	23.0 L total $m^{-2}\ h^{-1}$	BSA/FBDNA= 110.0
[179]	BSA=2 OVA egg=1.0	UF	No data	BSA/OVA=10.0
[130]	Cytochrome C=1.0 MYO blood= 1.0 α-la =1.0	UF	Individual transmision	--

Table 1.7. Relevant protein separation studies reported in literature (cont).

MIXTURES FROM DIFFERENT SIZE PROTEINS				
Ref	**Proteins ($g\ L^{-1}$)**	**Technology**	**Flux ($g\ m^{-2}\ h^{-1}$)**	**Selectivity**
[180]	HAS= 0.67 MYO blood=0.175	UF	2.6 12.1 total $L\ m^{-2}\ h^{-1}$	Total MYO
[181]	BSA =5.0 LYS egg =5.0	UF	3.2 total $L\ m^{-2}\ h^{-1}$	LYS/BSA=16.5
[182]	BSA =5.0 LYS egg =5.0	EUF	3.9 total $L\ m^{-2}\ h^{-1}$	LYS/BSA=38.0
[183]	BSA =5.0 MYO blood=5.0	EDUF	2.1 20.0 total $L\ m^{-2}\ h^{-1}$	Total BSA
[184]	BSA =0.08 MYO blood=0.02	UF	60.0 total $L\ m^{-2}\ h^{-1}$	MYO/BSA= 2.5
[185]	Cytocrome C BSA β Galactosidase	UF	0.02	No β Galactosidase in the permeate

(**) $S_{x/y}= Tr_x/Tr_y$ $Tr= (C_{Permeate}/C_{Feed})$ x100. UF: Ultrafiltration. EA: Electroadification. IE ADS: Ion exchange adsorption. P: Precipitation. M ADS: Membrane adsorption. EDUF: Electroultrafiltration.

As it is shown in Table 1.7, previous studies of the separation of similarly sized protein mixtures have examined the separation of i) β-lactoglobulin (β-lg) and α-lactalbumin (α-la) mixtures [158–165], where Chang and Zydney reported a flux of 10.1 L m^{-2} h^{-1} and a selectivity exceeding 55.0 for β-lg [161]; ii) lysozyme (LYS)/myoglobin (MYO) [175,178], where Yunos and Field reported a flux of 26.5 L m^{-2} h^{-1} and a selectivity of 12.1 for MYO [176]; and iii) bovine serum albumin (BSA)/hemoglobin (Hb) mixtures, where Cheng et al. reported a flux of 31.1 L m^{-2} h^{-1} and a total selectivity for BSA [121].

In addition to these well-studied mixtures, several examples of similarly sized protein mixtures (not found in nature) have been analyzed by other authors. These systems include iv) BSA/ ovalbumin by Rao and Zydney [179]; v) BSA/ Fab DNA by van Reis et al. [89]; or vi) cytochrome C / MYO / α-la by Rohani et al. [130]. The last example mixture displayed the best separation performance upon application of the modified Composite Regenerated Cellulosic (CRC) UF membranes with the addition of a zwitterionic ligand. The separation of different size proteins had been also studied [180–185] but these mixtures do not represent any technological challenge. On the other hand, the separation of high molecular weight proteins found in natural whey has deserved less attention [132,135]. The best results were obtained by Nyström et al. [132], who reported a flux of 240.0 L m^{-2} h^{-1} and a selectivity of 2.5 for BSA in a synthetic BSA/LF mixture in which each protein was present in an initial concentration of 0.1 g L^{-1}.

Milk whey is a mixture of a variety of secreted proteins. The mixture displays a wide range of chemical, physical, and functional properties [186]. Whey proteins have been satisfactorily separated into different fractions (casein and other major and minor proteins) [187,188] as well as the isolation of the major proteins, β-lg and α-la [158–163]; however, the separation of high-value minor proteins of similar size (BSA, LF, and immunoglobulin) remains a scientific challenge. BSA and LF have a high nutritional value because they contain essential amino acids and are easily digested. BSA is a 66.5 kDa protein with an isoelectric point (Ip) approaching 5.0 and has foaming and gelling

properties. Its concentration in milk is 0.4 g L^{-1}, on average. LF is a 78.0 kDa iron-binding protein with an Ip around 9.0. LF has important nutraceutical, anti-inflammatory, and antimicrobial properties, it plays an important role in iron metabolism [189], and it is present in a concentration of 0.1 g L^{-1} in milk. LF and BSA have comparable molecular weights (MWs). Both proteins tend to prevent foam formation at their isoelectric points by reducing the surface tensions [190], which makes their separation even more difficult.

1.4. THESIS SCOPE AND OUTLINE

The aim of this study is to develop an alternative separation process of BSA/LF mixtures using membrane technology. The performance of a suitable identification and quantification method as well as correct protein and membrane characterization is also needed.

Chapter 2 reports and describes the development and evaluation of two measurement methodologies that will be applied for BSA and LF individual quantification in salty and buffered binary mixtures. First a Chromatographic method based on ion-exchange column has been adapted for the measurement of non-high salty buffers, then, a new quantification method based on the couple fluorometric and UV-vis measurements was specifically developed for BSA and LF individual quantification in salty media.

Chapter 3 aims at the characterization of proteins in terms of zeta potential, isoelectric points and size. First of all a comparative analysis of different electrolytes, pH and concentrations of electrolyte or protein has been carried out. In a second stage, the influence of a surfactant presence was determined in terms of size. Furthermore the characterization of the surface zeta potential of the different membranes used in membrane separation processes was performed. Finally the protein adsorption onto membrane surface was determined.

Chapter 4 deals with the development of a separation process by means of the combination of adequately modified charged membranes and optimum process conditions to separate minor proteins present in milk whey. The combination of electrically enhanced and membrane separation process was also reported. Membrane fouling thought the Derjaguin, Landau, Verwey, and Overbeek (DLVO) theory was also evaluated.

Finally, Chapter 5 collects the general conclusions of this thesis and an overview of the challenges and prospects for future research.

1.5. REFERENCES

The references in this section were managed by the Mendeley reference software applying the Separation Science and Technology style.

[1] E. Tsakali, K. Petrotos, A.D. Allessandro, A review on whey composition and the methods used for its utilization for food and pharmaceutical products, in: 6th Int. Conf. Simul. Model. Food Bio-Industry. FOODSIM, Braganca, Portugal, 2010.
[2] OECD-FAO Agricultural Outlook 2008–2017. Highlights, Paris, 2013.
[3] C. Mollea, L. Marmo, F. Bosco, Valorisation of cheese whey, a by-product from the dairy industry, in: I. Muzzalupo (Ed.), Food Ind., 1st Ed, InTech, Rende, Italia, 2013.
[4] J.N. de Wit, Lecturer ' s Handbook on whey and whey products, 1st Ed, European Whey Products Association, Brusseles, Belgium, 2001.
[5] EWPA, Whey in animal nutrition: A valuable ingredient, Brusseles, Belgium, 2006.
[6] I. Jeli, R. Božani, L. Tratnik, Whey-based beverages- a new generation of diary products, Mljekarstvo. 58 (2008) 257–274.
[7] N.S.T.Ă. Stanciuc, G. Râpeanu, An overview of bovine α-lactalbumin structure and functionality, Food Technol. 34 (2010) 82–93.
[8] R.R. Zall, Whey and lactose processing, 1st Ed, Springer Netherlands, Dordrecht, Netherlands, 1992.
[9] P. Havea, H. Singh, L.K. Creamer, Heat-induced aggregation of whey proteins: comparison of cheese WPC with acid WPC and relevance of mineral composition, J. Agric. Food Chem. 50 (2002) 4674–4681.
[10] D.N. Goyal, N. and Gandh, Comparative analysis of Indian paneer and cheese whey for electrolyte whey drink, World J. Dairy Food Sci. 4 (2009) 70–72.
[11] L. Diblíková, L. Čurda, K. Homolová, Electrodialysis in whey desalting process, Desalin. Water Treat. 14 (2010) 208–213.
[12] K. Singh, A.K. and Singh, Utilization of whey for the production of instant energy beverage by using response surface methodology, J. Food Sci. Technol. 4 (2012) 103–111.
[13] J. Beucler, M. Drake, E.A. Foegeding, Design of a beverage from whey permeate, J. Food Sci. 70 (2006) S277–S285.
[14] M. Djurić, M. Carić, S. Milanović, M. Tekić, M. Panić, Development of whey-based beverages, Eur. Food Res. Technol. 219 (2004) 321–328.
[15] J.O. Hernandez-Mendoza, A., Robles, V.J., Angulo, H.S. de la Cruz, J. and Garcia, Preparation of a whey-based probiotic product with lactobacillus reuteri and bifidobacterium bifidum, Food Technol. Biotechnol. 45 (2007) 27–31.
[16] P.J. Huth, D.B. DiRienzo, G.D. Miller, Major scientific advances with dairy foods in nutrition and health, J. Dairy Sci. 89 (2006) 1207–21.
[17] C. Gauche, J.T.C. Vieira, P.J. Ogliari, M.T. Bordignon-Luiz, Crosslinking of milk whey proteins by transglutaminase, Process Biochem. 43 (2008) 788–794.

[18] M.C. Almecija, Obtención de Lactoferrina bovina mediante ultrafiltración de latosuero, Thesis work. Universidad de Granada, 2007.
[19] J.M. Steijns, a C. van Hooijdonk, Occurrence, structure, biochemical properties and technological characteristics of lactoferrin, Br. J. Nutr. 84 Suppl 1 (2000) S11–7.
[20] A.L. Zydney, Protein separations using membrane filtration: new opportunities for whey fractionation, Int. Dairy J. 8 (1998) 243–250.
[21] S. Brownlow, J.H.M. Cabral, R. Cooper, D.R. Flower, S.J. Yewdall, I. Polikarpov, et al., Bovine beta -lactoglobulin at 1 . 8 Å resolution lipocalin — still an enigmatic, Structure. 64 (1997) 481–495.
[22] J. Rytkönen, Effect of heat denaturation of bovine milk beta-lactoglobulin on its epithelial transport and allergenicity, Acta Universitatis Ouluensis: Medica. University of Oulu, 2006.
[23] P. Belitz, H.D., Grosch, W. and Schieberle, Food chemistry, 4th Revise, Springer, Stürtz, Germany, 2009.
[24] M.D. Pérez, P. Puyol, J.M. Ena, M. Calvo, Comparison of the ability to bind lipids of β-lactoglobulin and serum albumin of milk from ruminant and non-ruminant species, J. Dairy Res. 60 (2009) 55.
[25] P. Puyol, M.D. Perez, L. Mata, J. Ena, M. Calvo, Effect of retinol and fatty acid binding by bovine β-lactoglobulin on its resistance to trypsin digestion, Int. Dairy J. 3 (1993) 589–597.
[26] G. Mandalari, A.M. Mackie, N.M. Rigby, M.S.J. Wickham, E.N.C. Mills, Physiological phosphatidylcholine protects bovine beta-lactoglobulin from simulated gastrointestinal proteolysis, Mol. Nutr. Food Res. 53 Suppl 1 (2009) S131–9.
[27] S. Futterman, J. Heller, The enhancement of fluorescence and the decreased susceptibility to enzymatic oxidation of retinol complexed with bovine serum albumin, beta-lactoglobulin, and the retinol-binding protein of human plasma, J. Biol. Chem. 247 (1972) 5168–5172.
[28] P. Puyol, M. Dolores Perez, L. Sanchez, J.M. Ena, M. Calvo, Uptake and passage of β-lactoglobulin palmitic acid and retinol across the Caco-2 monolayer, Biochim. Biophys. Acta. 1236 (1995) 149–154.
[29] L. Riihimäki-lampén, Interactions of natural products with β-lactoglobulins , members of the lipocalin family, Thesis work. Faculty of Pharmacy; University of Helsinki, 2009.
[30] C. Holt, Molecular basis of whey protein food functionalities, Proc. Dairy Ingred. Sci. 55 (2000) 53–55.
[31] E. Dufour, P. Robert, D. Renard, G. Llamas, Investigation of β-Lactoglobulin Gelation in Water/Ethanol Solutions, Int. Dairy J. 8 (1998) 87–93.
[32] D.E.W. Chatterton, G. Smithers, P. Roupas, A. Brodkorb, Bioactivity of β-lactoglobulin and α-lactalbumin-Technological implications for processing, Int. Dairy J. 16 (2006) 1229–1240.
[33] E.A. Permyakov, L.J. Berliner, α-Lactalbumin: structure and function, FEBS Lett. 473 (2000) 269–274.

[34] J.I. Boye, I. Alli, A.A. Ismail, Use of differential scanning calorimetry and infrared spectroscopy in the study of thermal and structural stability of α-lactalbumin, J. Agric. Food Chem. 45 (1997) 1116–1125.
[35] K. Marshall, Therapeutic applications of whey protein, Altern. Med. Rev. 9 (2004) 136–156.
[36] J.E. Butler, Bovine immunoglobulins: A review, J. Dairy Sci. 52 (1969) 1895–1909.
[37] L.W. Gapper, D.E.J. Copestake, D.E. Otter, H.E. Indyk, Analysis of bovine immunoglobulin G in milk, colostrum and dietary supplements: a review, Anal. Bioanal. Chem. 389 (2007) 93–109.
[38] J. Bertolini, N. Goss, J. Curling, Production of plasma proteins for therapeutic use, 1st Ed, John Wiley & Sons, 2012.
[39] J.F. Foster, Albumin structure, function and uses, 1st Ed, Pergamon, Oxford, UK, 1977.
[40] D.C. Carter, J.X. Ho, Lipoproteins, apolipoproteins, and lipases, Adv. Protein Chem. 45 (1994) 153–203.
[41] V. Valiño, M.F. San Román, R. Ibañez, I. Ortiz, Improved separation of bovine serum albumin and lactoferrin mixtures using charged ultrafiltration membranes, Sep. Purif. Technol. 125 (2014) 163–169.
[42] I. Laursen, P. Briand, A.E. Lykkesfeldt, Serum albumin as a modulator on growth of the human breast cancer cell line, MCF-7, Anticancer Res. 10 (1990) 343–51.
[43] J.-K. Choi, Interactions of very long-chain saturated fatty acids with serum albumin, J. Lipid Res. 43 (2002) 1000–1010.
[44] L.M. Tong, S. Sasaki, D.J. McClements, E.A. Decker, Mechanisms of the antioxidant activity of a high molecular weight fraction of whey, J. Agric. Food Chem. 48 (2000) 1473–1478.
[45] A.K. Wright, M.R. Thompson, Hydrodynamic structure of bovine serum albumin determined by transient electric birefringence, Biophys. J. 15 (1975) 137–141.
[46] S. Farnaud, R.W. Evans, Lactoferrin—a multifunctional protein with antimicrobial properties, Mol. Immunol. 40 (2003) 395–405.
[47] P.L. Masson, J.F. Heremans, Lactoferrin in milk from different species, Comp. Biochem. Physiol. 39B (1971) 119–129.
[48] C. Conesa, M. Calvo, L. Sánchez, Recombinant human lactoferrin: a valuable protein for pharmaceutical products and functional foods, Biotechnol. Adv. 28 (2010) 831–8.
[49] A.D. Delillo, L.M. Quiros, J.F. Fierro, Relationship between antibacterial activity and cell surface binding of lactoferrin in species of genus, FEMS Microbiol. Lett. 150 (1997) 89–94.
[50] M.S. Diarra, D. Petitclerc, P. Lacasse, Effect of lactoferrin in combination with penicillin on the morphology and the physiology of Staphylococcus aureus isolated from bovine mastitis, J. Dairy Sci. 85 (2002) 1141–9.

[51] M.S. Diarra, D. Petitclerc, É. Deschênes, N. Lessard, G. Grondin, B.G. Talbot, et al., Lactoferrin against Staphylococcus aureus Mastitis, Vet. Immunol. Immunopathol. 95 (2003) 33–42.
[52] D.A. Dionysius, P.A. Grieve, J.M. Milne, Forms of lactoferrin: their antibacterial effect on enterotoxigenic Escherichia coli, J. Dairy Sci. 76 (1993) 2597–600.
[53] D.A. Dionysius, J.M. Milne, Antibacterial peptides of bovine lactoferrin: purification and characterization, J. Dairy Sci. 80 (1997) 667–74.
[54] M.E. Drago-Serrano, V. Rivera-Aguilar, A.A. Reséndiz-Albor, R. Campos-Rodríguez, Lactoferrin increases both resistance to Salmonella typhimurium infection and the production of antibodies in mice, Immunol. Lett. 134 (2010) 35–46.
[55] H.A. Elbarbary, A.M. Abdou, E.Y. Park, Y. Nakamura, H.A. Mohamed, K. Sato, Novel antibacterial lactoferrin peptides generated by rennet digestion and autofocusing technique, Int. Dairy J. 20 (2010) 646–651.
[56] H. Inoue, M. Sakai, Y. Kaida, K. Kaibara, Blood lactoferrin release induced by running exercise in normal volunteers: antibacterial activity, Clin. Chim. Acta. 341 (2004) 165–72.
[57] H. Jenssen, R.E.W. Hancock, Antimicrobial properties of lactoferrin, Biochimie. 91 (2009) 19–29.
[58] A.M. Mulder, P.A. Connellan, C.J. Oliver, C.A. Morris, L.M. Stevenson, Bovine lactoferrin supplementation supports immune and antioxidant status in healthy human males, Nutr. Res. 28 (2008) 583–9.
[59] M.A. Paulsson, U. Svensson, A.R. Kishore, A. Satyanarayan Naidu, Thermal behavior of bovine lactoferrin in water and its relation to bacterial interaction and antibacterial activity, J. Dairy Sci. 76 (1993) 3711–3720.
[60] H. Saito, H. Miyakawa, Y. Tamura, S. Shimamura, M. Tomita, Potent bactericidal activity of bovine lactoferrin hydrolysate produced by heat treatment at acidic pH, J. Dairy Sci. 74 (1991) 3724–30.
[61] M. Tomita, W. Bellamy, M. Takase, K. Yamauchi, H. Wakabayashi, K. Kawase, Potent antibacterial peptides generated by pepsin digestion of bovine lactoferrin, J. Dairy Sci. 74 (1991) 4137–42.
[62] J. Zhang, L. Li, Y. Cai, X. Xu, J. Chen, Y. Wu, et al., Expression of active recombinant human lactoferrin in the milk of transgenic goats, Protein Expr. Purif. 57 (2008) 127–35.
[63] R. Pakkanen, J. Aalto, Growth factors and antimicrobial factors of bovine colostrum, Int. Dairy J. 7 (1997) 285–297.
[64] P. Valenti, G. Antonini, Lactoferrin: an important host defence against microbial and viral attack, Cell. Mol. Life Sci. 62 (2005) 2576–87.
[65] B.A. Law, B. Reiter, The isolation and bacteriostatic properties of lactoferrin from bovine milk whey, J. Dairy Res. 44 (1977) 595–9.
[66] The world lactoferrin and lactoperoxidase market, UBIC Consult. (2011).

[67] A.R. Madureira, C.I. Pereira, A.M.P. Gomes, M.E. Pintado, F. Xavier Malcata, Bovine whey proteins – Overview on their main biological properties, Food Res. Int. 40 (2007) 1197–1211.
[68] S. Yoshida, Z. Wei, Y. Shinmura, N. Fukunaga, Separation of lactoferrin-a and -b from bovine colostrum, J. Dairy Sci. 83 (2000) 2211–5.
[69] M.M.E.-L. and M.B. Mahfouz, Lactoferrin in relation to biological functions and applications: a review, Int. J. Dairy Sci. 6 (2011) 79–111.
[70] M. Tomita, H. Wakabayashi, K. Shin, K. Yamauchi, T. Yaeshima, K. Iwatsuki, Twenty-five years of research on bovine lactoferrin applications, Biochimie. 91 (2009) 52–7.
[71] J.C.K. Chan, E.C.Y. Li-Chan, Production of lactoferricin and other cationic peptides from food grade bovine lactoferrin with various iron saturation levels, J. Agric. Food Chem. 55 (2007) 493–501.
[72] H. Schlitz, Protein purification: principles and practice, Biochem. Educ. 12 (1984) 143.
[73] S. Pihlasalo, Quantification of proteins and cells. Luminometric nonspecific particle-based methods, University of Turku, 2011.
[74] J.M. Bremner, Total nitrogen, 2nd Ed, American Society of Agronomy, Soil Science Society of America, Madison, USA, 1982.
[75] R.J. Henry, C. Sobel, M. Segalove, Turbidimetric determination of proteins with sulfosalicylic and trichloracetic acids, Proc. Soc. Exp. Biol. Med. 92 (1956) 748–51.
[76] A.G. Gornall, C.J. Bardawill, M. David, Determination of serum proteins by means of the biuret reaction, J. Biol. Chem. 177 (1949) 751–66.
[77] O.H. Lowry, N.J. Rosebrough, A.L. Farr, R.J. Randall, Protein measurement with the Folin phenol reagent., J. Biol. Chem. 193 (1951) 265–75.
[78] M.M. Bradford, A rapid and sensitive method for the quantitation of microgram quantities of protein utilizing the principle of protein-dye binding, Anal. Biochem. 72 (1976) 248–254.
[79] P.K. Smith, R.I. Krohn, G.T. Hermanson, A.K. Mallia, F.H. Gartner, M.D. Provenzano, et al., Measurement of protein using bicinchoninic acid, Anal. Biochem. 150 (1985) 76–85.
[80] M.J. Dunn, Protein determination of total protein concentration, 1st Ed, Protein Purification Methods, Oxford, UK, 1992.
[81] S.J. Compton, C.G. Jones, Mechanism of dye response and interference in the Bradford protein assay, Anal. Biochem. 151 (1985) 369–374.
[82] J.M. Walker, The protein protocols Handbook, 3rd Ed, Humana Press, New Jersey, USA, 2002.
[83] S. Metsämuuronen, M. Mänttäri, M. Nyström, Comparison of analysis methods for protein concentration and its use in UF fractionation of whey, Desalination. 283 (2011) 156–164.
[84] R. Hahn, P.M. Schulz, C. Schaupp, A. Jungbauer, Bovine whey fractionation based on cation-exchange chromatography, J. Chromatogr. A. 795 (1998) 277–287.

[85] H.E. Indyk, E.L. Filonzi, Determination of lactoferrin in bovine milk, colostrum and infant formulas by optical biosensor analysis, Int. Dairy J. 15 (2005) 429–438.
[86] S. Pan, R. Aebersold, R. Chen, J. Rush, D.R. Goodlett, M.W. Mcintosh, et al., Mass spectrometry based targeted protein quantification : methods and applications reviews, J. Proteome Res. 8 (2009) 787–797.
[87] N. Gasilova, A.-L. Gassner, H.H. Girault, Analysis of major milk whey proteins by immunoaffinity capillary electrophoresis coupled with MALDI-MS, Electrophoresis. 33 (2012) 2390–8.
[88] E.J. Dial, L.R. Hall, H. Serna, J.J. Romero, J.G. Fox, L.M. Lichtenberger, Antibiotic properties of bovine lactoferrin on Helicobacter pylori, Dig. Dis. Sci. 43 (1998) 2750–6.
[89] R. van Reis, J.M. Brake, J. Charkoudian, D.B. Burns, A.L. Zydney, High-performance tangential flow filtration using charged membranes, J. Memb. Sci. 159 (1999) 133–142.
[90] P.R. Srinivas, Protein electrophoresis : methods and protocols, 1st Ed, Humana Press, Oklahoma City, OK, USA, 2012.
[91] J.J. Basch, F.W. Douglas, L.G. Procino, V.H. Holsinger, H.M. Farrell, Quantitation of caseins and whey proteins of processed milks and whey protein concentrates, application of gel electrophoresis, and comparison with harland-ashworth procedure, J. Dairy Sci. 68 (1985) 23–31.
[92] N.M. Kinghorn, G.R. Paterson, D.E. Otter, Quantification of the major bovine whey proteins using capillary zone electrophoresis, J. Chromatogr. A. 723 (1996) 371–379.
[93] B. Vallejo-Cordoba, Rapid separation and quantification of major caseins and whey proteins of bovine milk by capillary electrophoresis, J. Capillary Electrophor. 4 (1997) 219–24.
[94] I. Recio, E. Molina, M. Ramos, M. de Frutos, Quantitative analysis of major whey proteins by capillary electrophoresis using uncoated capillaries, Electrophoresis. 16 (1995) 654–8.
[95] M. Strickland, M.E. Johnson, J.R. Broadbent, Qualitative and quantitative analysis of proteins and peptides in milk products by capillary electrophoresis, Electrophoresis. 22 (2001) 1510–7.
[96] J.-F. Fairise, P. Cayot, New ultrarapid method for the separation of milk proteins by capillary electrophoresis, J. Agric. Food Chem. 46 (1998) 2628–2633.
[97] J.M.L. Heck, C. Olieman, A. Schennink, H.J.F. van Valenberg, M.H.P.W. Visker, R.C.R. Meuldijk, et al., Estimation of variation in concentration, phosphorylation and genetic polymorphism of milk proteins using capillary zone electrophoresis, Int. Dairy J. 18 (2008) 548–555.
[98] S.G. Anema, The use of “lab-on-a-chip” microfluidic SDS electrophoresis technology for the separation and quantification of milk proteins, Int. Dairy J. 19 (2009) 198–204.
[99] A.A. Foley, G.W. Bates, The purification of lactoferrin from human whey by batch extraction, Anal. Biochem. 162 (1987) 296–300.

[100] S. Yoshida, Isolation of lactoperoxidase and lactoferrins from bovine milk acid whey by carboxymethyl cation exchange chromatography, J. Dairy Sci. 74 (1991) 1439–1444.
[101] L. Zhang, N.T., Nakano, T., Ozimek, Isolation of lactoferrin from bovine colostrum by SP-Sepharose cation-exchange chromatography, Milchwissenschaft. 57 (2002) 614–617.
[102] S. Doultani, K.N. Turhan, M.R. Etzel, Fractionation of proteins from whey using cation exchange chromatography, Process Biochem. 39 (2004) 1737–1743.
[103] A. Heebøll-Nielsen, S.F.L. Justesen, O.R.T. Thomas, Fractionation of whey proteins with high-capacity superparamagnetic ion-exchangers, J. Biotechnol. 113 (2004) 247–62.
[104] X. Ye, S. Yoshida, T.B. Ng, Isolation of lactoperoxidase, lactoferrin, α-lactalbumin, β-lactoglobulin B and β-lactoglobulin A from bovine rennet whey using ion exchange chromatography, Int. J. Biochem. Cell Biol. 32 (2000) 1143–1150.
[105] J. Andersson, B. Mattiasson, Simulated moving bed technology with a simplified approach for protein purification. Separation of lactoperoxidase and lactoferrin from whey protein concentrate, J. Chromatogr. A. 1107 (2006) 88–95.
[106] C.J. Fee, A. Chand, Capture of lactoferrin and lactoperoxidase from raw whole milk by cation exchange chromatography, Sep. Purif. Technol. 48 (2006) 143–149.
[107] K. Plate, S. Beutel, H. Buchholz, W. Demmer, S. Fischer-Frühholz, O. Reif, et al., Isolation of bovine lactoferrin, lactoperoxidase and enzymatically prepared lactoferricin from proteolytic digestion of bovine lactoferrin using adsorptive membrane chromatography, J. Chromatogr. A. 1117 (2006) 81–6.
[108] V. Adam, O. Zitka, P. Dolezal, L. Zeman, A. Horna, J. Hubalek, et al., Lactoferrin isolation using monolithic column coupled with spectrometric or micro-amperometric detector, Sensors. 8 (1995) 464–487.
[109] C. Conesa, L. Sánchez, C. Rota, M.-D. Pérez, M. Calvo, S. Farnaud, et al., Isolation of lactoferrin from milk of different species: calorimetric and antimicrobial studies, Comp. Biochem. Physiol. 150 (2008) 131–9.
[110] B.Y. Fong, C.S. Norris, K.P. Palmano, Fractionation of bovine whey proteins and characterisation by proteomic techniques, Int. Dairy J. 18 (2008) 23–46.
[111] M. Wu, Y. Xu, Isolation and purification of lactoferrin and immunoglobulin G from bovine colostrum with serial cation-anion exchange chromatography, Biotechnol. Bioprocess Eng. 14 (2009) 155–160.
[112] S.M. Saufi, C.J. Fee, Recovery of lactoferrin from whey using cross-flow cation exchange mixed matrix membrane chromatography, Sep. Purif. Technol. 77 (2011) 68–75.
[113] M.J. Santos, J.A. Teixeira, L.R. Rodrigues, Fractionation and recovery of whey proteins by hydrophobic interaction chromatography, J. Chromatogr. B. 879 (2011) 475–9.

[114] H. Kawakami, H. Shinmoto, S. Dosako, Y. Sogo, One-step isolation of lactoferrin using immobilized monoclonal antibodies, J. Dairy Sci. 70 (1987) 752–9.
[115] D.Q. Lin, Separation of lactoferrin from whey by expanded bed adsorption with mixed-mode adsorbent, Thesis work. Zhejiang University, 2009.
[116] L. Chen, C. Guo, Y. Guan, H. Liu, Isolation of lactoferrin from acid whey by magnetic affinity separation, Sep. Purif. Technol. 56 (2007) 168–174.
[117] F.J. Wolman, D.G. Maglio, M. Grasselli, O. Cascone, One-step lactoferrin purification from bovine whey and colostrum by affinity membrane chromatography, J. Memb. Sci. 288 (2007) 132–138.
[118] S.A. Al-Mashikhi, S. Nakai, Isolation of bovine immunoglobulins and lactoferrin from whey proteins by gel filtration techniques., J. Dairy Sci. 70 (1987) 2486–92.
[119] X. Felipe, A.J. Law, Preparative-scale fractionation of bovine, caprine and ovine whey proteins by bel permeation chromatography, J. Dairy Res. 64 (1997) 459–64.
[120] C. Schmitt, C. Bovay, A.-M. Vuilliomenet, M. Rouvet, L. Bovetto, R. Barbar, et al., Multiscale characterization of individualized beta-lactoglobulin microgels formed upon heat treatment under narrow pH range conditions, Langmuir. 25 (2009) 7899–909.
[121] T.R. Gaborski, J.L. Snyder, C.C. Striemer, D.Z. Fang, M. Hoffman, P.M. Fauchet, et al., High-performance separation of nanoparticles with ultrathin porous nanocrystalline silicon membranes, ACS Nano. 4 (2010) 6973–81.
[122] A.E. Wiącek, E. Chibowski, Zeta potential and droplet size of n-tetradecane/ethanol (protein) emulsions, Colloids Surfaces B Biointerfaces. 25 (2002) 55–67.
[123] Y. Ding, Y. Tian, Z. Li, H. Wang, L. Chen, Interaction energy evaluation of the role of solution chemistry and organic foulant composition on polysaccharide fouling of microfiltration membrane bioreactors, Chem. Eng. Sci. 104 (2013) 1028–1035.
[124] J.P. Davis, E.A. Foegeding, F.K. Hansen, Electrostatic effects on the yield stress of whey protein isolate foams, Colloids Surf. B. Biointerfaces. 34 (2004) 13–23.
[125] A. Ye, Complexation between milk proteins and polysaccharides via electrostatic interaction: principles and applications – a review, Int. J. Food Sci. Technol. 43 (2008) 406–415.
[126] J.D. Marion, D.N. Van, J.E. Bell, J.K. Bell, Measuring the effect of ligand binding on the interface stability of multimeric proteins using dynamic light scattering, Anal. Biochem. 407 (2010) 278–80.
[127] R. Beleca, M. Abbod, W. Balachandran, P.R. Miller, Investigation of electrostatic properties of pharmaceutical powders using phase doppler anemometry, IEEE Trans. Ind. Appl. 46 (2010) 1181–1187.
[128] M. Moniruzzaman, K. Nakashima, N. Kamiya, M. Goto, Recent advances of enzymatic reactions in ionic liquids, Biochem. Eng. J. 48 (2010) 295–314.

[129] A. Saxena, B.P. Tripathi, M. Kumar, V.K. Shahi, Membrane-based techniques for the separation and purification of proteins: an overview, Adv. Colloid Interface Sci. 145 (2009) 1–22.
[130] M.M. Rohani, A.L. Zydney, Effect of surface charge distribution on protein transport through semipermeable ultrafiltration membranes, J. Memb. Sci. 337 (2009) 324–331.
[131] H.-C. Mahler, W. Friess, U. Grauschopf, S. Kiese, Protein aggregation: pathways, induction factors and analysis., J. Pharm. Sci. 98 (2009) 2909–2934.
[132] M. Nyström, P. Aimar, S. Luque, M. Kulovaara, S. Metsämuuronen, Fractionation of model proteins using their physiochemical properties, Colloids Surfaces A Physicochem. Eng. Asp. 138 (1998) 185–205.
[133] F. Zhang, M.W.A. Skoda, R.M.J. Jacobs, R.A. Martin, C.M. Martin, F. Schreiber, Protein interactions studied by SAXS: effect of ionic strength and protein concentration for BSA in aqueous solutions, J. Phys. Chem. B. 111 (2007) 251–9.
[134] A. Salis, M. Boström, L. Medda, F. Cugia, B. Barse, D.F. Parsons, et al., Measurements and theoretical interpretation of points of zero charge/potential of BSA protein, Langmuir. 27 (2011) 11597–604.
[135] N. Ndiaye, Y. Pouliot, L. Saucier, L. Beaulieu, L. Bazinet, Electroseparation of bovine lactoferrin from model and whey solutions, Sep. Purif. Technol. 74 (2010) 93–99.
[136] S. Salgin, U. Salgin, S. Bahadir, Zeta potentials and isoelectric points of biomolecules: the effects of ion types and ionic strengths, Int. J. Electrochem. Sci. 7 (2012) 12404–12414.
[137] I. Mela, E. Aumaitre, A.-M. Williamson, G.E. Yakubov, Charge reversal by salt-induced aggregation in aqueous lactoferrin solutions, Colloids Surf. B. Biointerfaces. 78 (2010) 53–60.
[138] Y. Mukai, E. Iritani, T. Murase, Effect of protein charge on cake properties in dead-end ultrafiltration of protein solutions, J. Memb. Sci. 137 (1997) 271–275.
[139] M.G. Carneiro-da-Cunha, M.A. Cerqueira, B.W.S. Souza, J.A. Teixeira, A.A. Vicente, Influence of concentration, ionic strength and pH on zeta potential and mean hydrodynamic diameter of edible polysaccharide solutions envisaged for multinanolayered films production, Carbohydr. Polym. 85 (2011) 522–528.
[140] N.S. Pujar, A.L. Zydney, Electrostatic and electrokinetic interactions during protein transport through narrow pore membranes, Ind. Eng. Chem. Res. 33 (1994) 2473–2482.
[141] W.R. Bowen, P.M. Williams, The osmotic pressure of electrostatically stabilized colloidal dispersions, J. Colloid Interface Sci. 184 (1996) 241–250.
[142] A. Hawe, W.L. Hulse, W. Jiskoot, R.T. Forbes, Taylor dispersion analysis compared to dynamic light scattering for the size analysis of therapeutic peptides and proteins and their aggregates, Pharm. Res. 28 (2011) 2302–2310.

[143] M.F. Drenski, M.L. Brader, R.W. Alston, W.F. Reed, Monitoring protein aggregation kinetics with simultaneous multiple sample light scattering, Anal. Biochem. 437 (2013) 185–97.
[144] Y.-I. Lim, S.B. Jørgensen, I.-H. Kim, Computer-aided model analysis for ionic strength-dependent effective charge of protein in ion-exchange chromatography, Biochem. Eng. J. 25 (2005) 125–140.
[145] K. Shiba, T. Niidome, E. Katoh, H. Xiang, L. Han, T. Mori, et al., Polydispersity as a parameter for indicating the thermal stability of proteins by dynamic light scattering, Int. J. Japan Soc. Anal. Chem. 26 (2010) 659–63.
[146] H. Ye, Simultaneous determination of protein aggregation, degradation, and absolute molecular weight by size exclusion chromatography-multiangle laser light scattering, Anal. Biochem. 356 (2006) 76–85.
[147] J. Yang, Characterization of porous membranes by zeta-potential under an ac electric field: analytical treatment of time-dependent electroosmostic flow, J. Memb. Sci. 225 (2003) 155–164.
[148] M.H. Oo, S.L. Ong, Implication of zeta potential at different salinities on boron removal by RO membranes, J. Memb. Sci. 352 (2010) 1–6.
[149] K.S. Kim, K.H. Lee, K. Cho, C.E. Park, Surface modification of polysulfone ultrafiltration membrane by oxygen plasma treatment, J. Memb. Sci. 199 (2002) 135–145.
[150] M. Kumar, M. Ulbricht, Novel antifouling positively charged hybrid ultrafiltration membranes for protein separation based on blends of carboxylated carbon nanotubes and aminated poly(arylene ether sulfone), J. Memb. Sci. 448 (2013) 62–73.
[151] Advances in Chromatographic Techniques for Therapeutic Drug Monitoring, CRC Press, 2009.
[152] S. a Al-Mashikhi, E. Li-Chan, S. Nakai, Separation of immunoglobulins and lactoferrin from cheese whey by chelating chromatography, J. Dairy Sci. 71 (1988) 1747–55.
[153] P. Bican, The application of the high-performance ion-exchange chromatography for the analysis of bovine milk proteins, Experientia. 41 (1985) 958–60.
[154] G.M. Ghiggeri, G. Candiano, G. Delfino, C. Queirolo, Highly selective one-step chromatography of serum and urinary albumin on immobilized Cibacron Blue F3GA. Studies on normal and glycosyl albumin, Clin. Chim. Acta. 145 (1985) 205–11.
[155] W.R. Bezwoda, N. Mansoor, Isolation and characterisation of lactoferrin separated from human whey by adsorption chromatography using Cibacron Blue F3G-A linked affinity adsorbent, Clin. Chim. Acta. 157 (1986) 89–93.
[156] M.M.H. El-Sayed, H. a Chase, Trends in whey protein fractionation, Biotechnol. Lett. 33 (2011) 1501–11.
[157] M.-E. Avramescu, Z. Borneman, M. Wessling, Mixed-matrix membrane adsorbers for protein separation., J. Chromatogr. A. 1006 (2003) 171–83.

[158] D. Lucas, M. Rabiller-Baudry, L. Millesime, B. Chaufer, G. Daufin, Extraction of α-lactalbumin from whey protein concentrate with modified inorganic membranes, J. Memb. Sci. 148 (1998) 1–12.
[159] B. Cheang, A.L. Zydney, Separation of alpha-lactalbumin and beta-lactoglobulin using membrane ultrafiltration, Biotechnol. Bioeng. 83 (2003) 201–9.
[160] B. Cheang, A.L. Zydney, A two-stage ultrafiltration process for fractionation of whey protein isolate, J. Memb. Sci. 231 (2004) 159–167.
[161] B. Bazinet, L., Ippersiel, D., and Mahdavi, Fractionation of whey proteins by bipolar membrane electroacidification, Innov. Food Sci. Emerg. Technol. 5 (2004) 17–25.
[162] S. Metsämuuronen, M. Nyström, Evaluation of six flat sheet ultrafiltration membranes for fractionation of whey proteins, Desalination. 200 (2006) 290–291.
[163] S. Cowan, S. Ritchie, Modified polyethersulfone (PES) ultrafiltration membranes for enhanced filtration of whey proteins, Sep. Sci. Technol. 42 (2007) 2405–2418.
[164] S. Galier, H.R. Balmann, The electrophoretic membrane contactor: A mass-transfer-based methodology applied to the separation of whey proteins, Sep. Purif. Technol. 77 (2011) 237–244.
[165] J. Toro-Sierra, A. Tolkach, U. Kulozik, Fractionation of α-lactalbumin and β-lactoglobulin from whey protein isolate using selective thermal sggregation, an optimized membrane separation procedure and resolubilization techniques at pilot plant scale, Food Bioprocess Technol. 6 (2011) 1032–1043.
[166] R.H. van Eijndhoven, S. Saksena, A.L. Zydney, Protein fractionation using electrostatic interactions in membranel filtration, Biotechnol. Bioeng. 48 (1995) 406–14.
[167] J. Ku, P. Stroeve, Protein diffusion in charged nanotubes : “On - Off ” behavior of molecular transport, Langmuir. 20 (2004) 2030–2032.
[168] S.-H. Lin, C.-L. Hung, R.-S. Juang, Effect of operating parameters on the separation of proteins in aqueous solutions by dead-end ultrafiltration, Desalination. 234 (2008) 116–125.
[169] J. Cheng, Y. Li, T.S. Chung, S.-B. Chen, W.B. Krantz, High-performance protein separation by ion exchange membrane partitioned free-flow isoelectric focusing system, Chem. Eng. Sci. 63 (2008) 2241–2251.
[170] H.U. Osmanbeyoglu, T.B. Hur, H.K. Kim, Thin alumina nanoporous membranes for similar size biomolecule separation, J. Memb. Sci. 343 (2009) 1–6.
[171] L. Li, G. Yan, J. Wu, Modification of polysulfone membranes via surface-initiated atom transfer radical polymerization and their antifouling properties, J. Appl. Polym. Sci. 11 (2008) 1942–1946.
[172] M.C. Almécija, R. Ibáñez, A. Guadix, E.M. Guadix, Influence of pH in the recovery of lactoferrin from whey with ceramic membranes, Desalination. 200 (2006) 475–476.

[173] S. Bhushan, M.R. Etzel, Charged ultrafiltration membranes increase the selectivity of whey protein separations, J. Food Sci. 74 (2009) E131–9.
[174] G. Brisson, M. Britten, Y. Pouliot, Electrically-enhanced crossflow microfiltration for separation of lactoferrin from whey protein mixtures, J. Memb. Sci. 297 (2007) 206–216.
[175] P.-S. Cheow, E.Z.C. Ting, M.Q. Tan, C.-S. Toh, Transport and separation of proteins across platinum-coated nanoporous alumina membranes, Electrochim. Acta. 53 (2008) 4669–4673.
[176] K.F. Md Yunos, R.W. Field, Rejection amplification in the ultrafiltration of binary protein mixtures using sandwich configurations, Chem. Eng. Process. Process Intensif. 47 (2008) 1053–1060.
[177] C. Müller, G. Agarwal, T. Melin, T. Wintgens, Study of ultrafiltration of a single and binary protein solution in a thin spiral channel module, J. Memb. Sci. 227 (2003) 51–69.
[178] R.W. Field, K.F. Md Yunos, Z. Cui, Separation of proteins using sandwich membranes, Desalination. 245 (2009) 597–605.
[179] S. Rao, A.L. Zydney, High resolution protein separations using affinity ultrafiltration with small charged ligands, J. Memb. Sci. 280 (2006) 781–789.
[180] D. Zhou, C.O. Too, G.G. Wallace, A.M. Hodges, A.W.H. Mau, Protein transport and separation using polypyrrole coated, platinised polyvinylidene fluoride membranes, React. Funct. Polym. 45 (2000) 217–226.
[181] A. Saxena, B.P. Tripathi, V.K. Shahi, An improved process for separation of proteins using modified chitosan-silica cross-linked charged ultrafilter membranes under coupled driving forces: isoelectric separation of proteins, J. Colloid Interface Sci. 319 (2008) 252–62.
[182] A. Saxena, M. Kumar, B.P. Tripathi, V.K. Shahi, Organic–inorganic hybrid charged membranes for proteins separation: Isoelectric separation of proteins under coupled driving forces, Sep. Purif. Technol. 70 (2010) 280–290.
[183] J.-H. Cheng, T.S. Chung, S.H. Neo, Investigation of mass transfer in the ion-exchange-membrane-partitioned free-flow IEF system for protein separation, Electrophoresis. 30 (2009) 2600–12.
[184] P.D. Peeva, T. Knoche, T. Pieper, M. Ulbricht, Cross-flow ultrafiltration of protein solutions through unmodified and surface functionalized polyethersulfone membranes – effect of process conditions on separation performance, Sep. Purif. Technol. 92 (2012) 83–92.
[185] P. Roy, T. Dey, K. Lee, D. Kim, B. Fabry, P. Schmuki, Size-selective separation of macromolecules by nanochannel titania membrane with self-cleaning (declogging) ability, J. Am. Chem. Soc. 132 (2010) 7893–5.
[186] J. Baró, L. Jiménez, L.J., Martínez-Pérez, A. and Bouza, Péptidos y proteínas de la leche con propiedades funcionales, Ars Pharm. 42 (2001) 135–145.
[187] M.P. Mier, R. Ibañez, I. Ortiz, Influence of process variables on the production of bovine milk casein by electrodialysis with bipolar membranes, Biochem. Eng. J. 40 (2008) 304–311.

[188] L. Voswinkel, U. Kulozik, Fractionation of whey proteins by means of membrane adsorption chromatography, Procedia Food Sci. 1 (2011) 900–907.
[189] G. Brisson, M. Britten, Y. Pouliot, Effect of iron saturation on the recovery of lactoferrin in rennet whey coming from heat-treated skim milk, J. Dairy Sci. 90 (2007) 2655–64.
[190] J. Noel, A. Prokop, R.D. Tanner, Foam fractionation of a dilute solution of bovine lactoferrin, Appl. Biochem. Biotechnol. 98-100 (2002) 395–402.

2

DEVELOPMENT OF A QUANTITATIVE BSA-LF MEASUREMENT METHOD

Abstract

Accurate individual quantification of proteins in complex mixtures is still a challenge when proteins present relative similar characteristics, like Bovine Serum Albumin (BSA) and Lactoferrin (LF). In this chapter the main results regarding the development of quantitative BSA-LF measurement are presented. Frist, an individual quantification in no electrolytic binary mixtures has been achieved by means of the High Performance Liquid Chromatography (HPLC) method based on ion-exchange chromatography adapted for this specific application, validated in a wide range of protein concentration and with a detection limit lower than 0.01 g L^{-1}. Secondly, a new method based on Fluorescence and Ultraviolet techniques able to quantify individual BSA and LF in electrolytic solutions in a range of protein concentration up to 1.0 g L^{-1} is presented. This method is under patent process Ref: P201400165.

2.1 INTRODUCTION

Protein quantification is an important step for handling protein samples for isolation, and it is needed to carry out the assessment of a separation process. In this sense, accurate, precise, sensitive and rapid analytical determinations are essential. The most commonly used total and individual protein assay methods are described in the previous section.

Total Protein quantification is aimed to determine the general concentration of proteins in the sample without any specific identification. Among all the available techniques, the adsorbed based and colorimetric techniques are the most accurate and commonly applied. Regarding the *Individual Protein* quantification, which aim is to identify and quantify each individual protein present in the sample, the use of Enzyme Immunoassay, Electrophoretic techniques and chromatographic techniques are of common use.

Nevertheless, the conventional technologies regarding the BSA and LF individual quantification in binary mixtures have been proved to be inefficient due to the similar characteristics of both proteins, thus, requiring the research and development of specific analytical methods [1–4].

2.2 QUANTIFICATION OF BSA-LF IN BINARY MIXTURES BY HIGH PERFORMANCE LIQUID CHROMATOGRAPHY

The principle of *chromatographic fractionation* is based on the interaction of the proteins with the solid support (stationary phase) and the mobile-phase. The different chromatographic techniques studied in this work are:

- The *Reverse-Phase Chromatography (RPC)* separation of proteins is based on their relative hydrophobicities. In spite of the highly selectivity of this technique, the requirement of use of organic solvents, which in some cases denatured proteins, make this process not recommended for all applications, particularly if the retention of the protein activity (non-denaturalized) is necessary [5].
- *Size-Exclusion Chromatography* (gel filtration) (SEC) takes advantage of the differences in the velocity of travelling through the column between larger proteins and small ones. The larger molecules travel faster through the cross-linked polymer in the chromatography column, since the large proteins do not fit into the pores of the polymer, whereas smaller proteins do (travelling through the chromatography column via their less direct route). A difference of 10.0 % difference in molecular mass is needed to have a good resolution [6].
- *Ion-Exchange Chromatography* (IEX) refers to the separation of proteins based on the charge. Columns can be either for anion exchange or cation exchange. Elution of the target protein(s) is done by changing the pH or the salt amount in the column, which results in a change or neutralization of the charged functional groups of each protein or the displacement of protein by a smaller ion [7].

In this study measurements were performed using individual and mixtures standards of the native BSA (Catalog A-6003 Sigma Chemical, Spain) and native LF (NutriScience Innovations, USA). BSA is readily soluble in water and requires high concentrations of neutral salts, such as ammonium sulfate, to induce precipitation. Bovine LF is highly soluble in water (2.0 %, 20°C) and has an Fe^{3+} content of 3.0 mg/100 g protein. The isoelectric point of BSA is close to 4.9, its molecular weight is 66.5 kDa, and the protein shape is a prolate ellipsoid with dimensions of 14.0 x 3.8 x 3.8 nm [8]. LF has an isoelectric point around 9.0, a molecular weight of 78 kDa, and a globular shape with dimensions of 4.0 x 5.1 x 7.1 nm, as determined using the lattice cell parameter data [9,10].

Protein standards of BSA, LF and their mixture in the range of concentrations of 0.01 - 3.0 g L^{-1} were prepared by adding the protein powder to the desired buffer solution, pH 5.0 (sodium acetate/acetic acid Analytical grade, Merk), pH 7.0 (sodium phosphate/dipotassium phosphate, Analytical grade, Merk); pH 9.0 (borax/hydrochloric acid (Fluka, Spain)) or different electrolyte solutions (KCl, NaCl or $CaCl_2$ Analytical grade, Merk). Shaking was avoided to prevent foam formation, which can seriously interfere with analytical procedure. Protein standards were used within the subsequent 24 h. to minimize the likelihood of protein aggregation. NaOH and HCL 0.1 M (Analytical grade, Merk) were employed to rise or reduce the pH of the electrolytic protein solutions.

The chromatographic analyses were performed using High-performance liquid chromatography (HPLC). The equipment used was HPLC Waters 2690 Separation Module (Waters) with the spectroscopic detector Waters 996 diode-array with a wavelength range of 210.0 - 400.0 mm (UV, Waters) (Figure 2.1). The software employed was Millelium (Waters).

Figure 2.1. High-performance liquid chromatography system Waters 2690 Separation Module.

Six different kinds of chromatographic columns were evaluated in the chromatographic tuning process. In all cases, the applied methods were provided by the different columns suppliers. The main characteristics of the columns are described in Table 2.1.

Table 2.1. Chromatographic columns used in the tuning process.

Chromatographic technique	Column	Size	Application	Stationary phase	Common Eluent
Reverse-Phase	**XBridge BEH300 C4 (Waters)**	3.5µm 2.1 x 50mm.	Protein and peptide separation	300Å packed material support	A: 99.9% H_2O, 0.1% TFA B: 28.56% H_2O, 71.4% ACN, 0.075% TFA
Reverse-Phase	**Zorbax 300SB-C3 (Agillent)**	3.5µm 4.6 x 150mm	Protein and peptide separation	Organosilane bonded to 300Å Zorbax Silica support	A: 95.0% H_2O, 5% ACN, 0.1% TFA B: 5.0% H_2O, 95% ACN, 0.07% TFA
Reverse-Phase	**Jupiter C18 (Phenomenex)**	5µm 4.6 x 150mm	Protein and peptide separation	Fully Porous Silica support	A: 99.9% H_2O, 0.1% TFA B: 99.9% ACN, 0.1% TFA
Size exclusion	**Superose 12 10/300 GL (GE Healthcare)**	11µm 10 x 300mm	Protein and peptide separation (1-300 kDa)	Composite of cross-linked agarose	A: 0.05 M Phosphate, 0.15 M NaCl, pH 7.0
Size exclusion	**Superdex Peptide 10/300 GL (GE Healthcare)**	13µm, 10 x 300mm	Protein and peptide separation (0.1-7 kDa)	Spherical composite of cross-linked agarose and dextran	A: 0.05 M Phosphate, 0.15 M NaCl, pH 7.0
Ion exchange	**Cimac™ -SO3 (BiaSeparations)**	bed volume: 0.106 mL 52 x 50 mm	Protein and peptide separation	SO_3^-: strong cation exchanger	A: 0.2 M Phosphate pH 7.0 B: 0.2 M Phosphate, 1.5 M NaCl pH 7.0

TFA: Trifluoroaceticacid; ACN: Acetonitrile

A systematic methodology, described in Figure 2.2, was applied to evaluate the performance of the columns and analytical conditions presented in Table 2.1 for the individual quantification of BSA and LF in binary mixtures. The basic method is formed by the use of Ultrapure (UP) water and 0.1 % TFA (A) and 71.4 % Acetonitrile (AcN) with 0.075 % TFA (B) as mobile phases. The column is first equilibrated with 0.25 mL min^{-1} in a proportion of 28.0 / 72.0 of phases A and B. Then, a gradient from 28.0 % to 100.0 % of B in 20 minutes is applied to the individual and mixture standards measurement. The injection volume applied is 20.0 µL, the flux 0.25 mL min^{-1} and column temperature used is 40ºC.

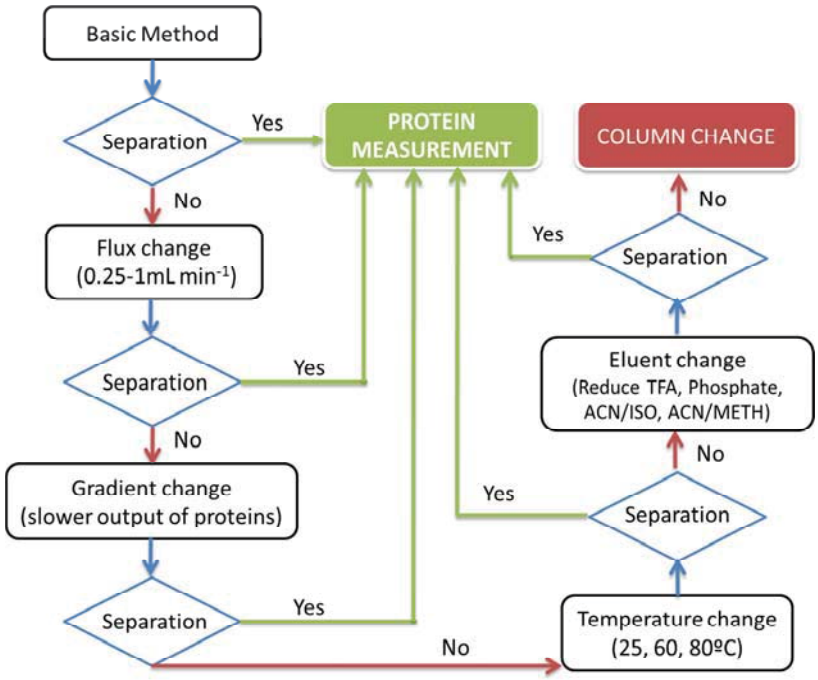

ISO: Isopropanol; METH: Methanol

Figure 2.2. Systematic methodology applied for BSA and LF quantification by HPLC.

Additionally to the described changes in Figure 2.2, the use of other detectors (Infrared) and the combination of several previously described changes were applied in the chromatographic tuning process.

Size-Exclusion chromatography

Two protein separation columns based on gel permeation were used: **Superose 12 10/300 GL** and **Superdex Peptide 10/300 GL**. First, individual standards of 1.0 g L^{-1} of BSA and LF in 2.0 g L^{-1} of KCl were injected in the columns. The mobile phase conditions were 0.05M phosphate + 0.15 M NaCl at a constant flow of 0.5 mL min^{-1}, the injection volume was 20.0 µL, no temperature was applied and the analysis last 60 min. Figure 2.3 shows chromatograms obtained under these conditions.

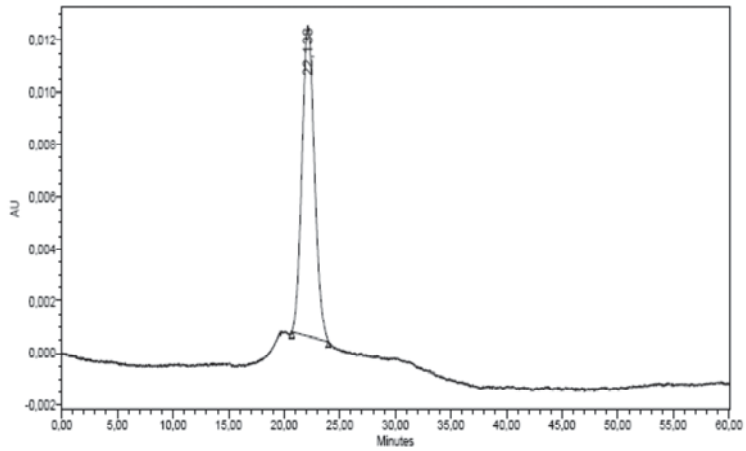

a)

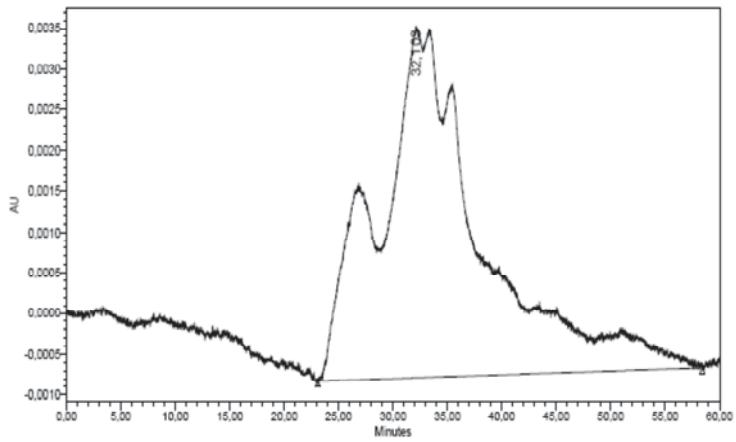

b)

Figure 2.3. HPLC Chromatograms obtained using the size exclusion columns a) BSA protein b) LF protein.

In Figure 2.3a the chromatogram of 1.0 g L^{-1} BSA in 2.0 g L^{-1} KCl is shown. The elution of the protein was from 20 to 25 minutes. Figure 2.3b depicts the chromatogram of 1.0 g L^{-1} LF in 2.0 g L^{-1} KCl. A very low resolution is obtained and the range of elution is from 24 to 58 minutes, falling the beginning in the range of BSA. The low resolution of the chromatograms and the elution of protein at the same time prevented the further exploration of this technique.

Reverse-Phase Chromatography

The systematic methodology previously described was applied to individual standards of 1.0 g L^{-1} of BSA and LF in buffer sodium acetate/acetic acid using the reverse-phase based **XBridge BEH300 C4 Column** (Waters). Both standards presented a proper resolution and despite the elution time was close the study of this column to mixture standards of equal BSA and LF concentration (3.0 g L^{-1}; 2.0 g L^{-1}; 1.0 g L^{-1}; 0.75 g L^{-1}; 0.5 g L^{-1}; 0.25 g L^{-1}; 0.1 g L^{-1} and 0.01 g L^{-1}) was performed with this column. Examples of the chromatograms obtained with this method for protein mixtures are shown in Figure 2.4.

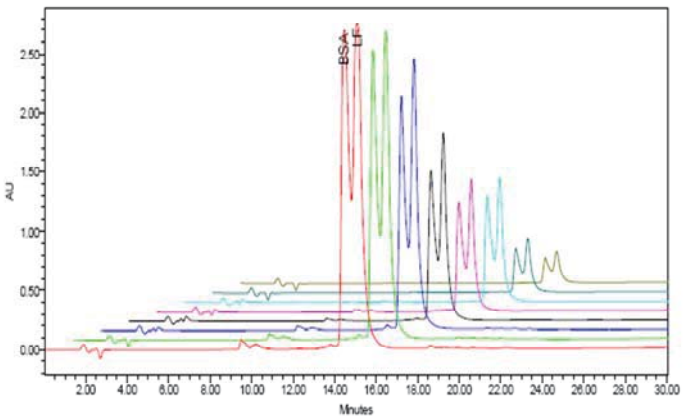

Figure 2.4. HPLC Chromatograms obtained with XBridge BEH300 C4 column (Waters).

Figure 2.4 describes the typical chromatogram obtained when a calibration of BSA/LF mixtures, which ranges from 3.0 to 0.01 g L^{-1} in

sodium acetate/acetic acid buffer pH 5.0, is measured. The BSA and LF peaks elute in the same range of time, preventing proper measurement if one was qualitatively greater than the other. The separation must be improved if the quantification of BSA and LF with proportions far from the 50.0 % mixture is needed.

The systematic methodology described in Figure 2.2 was followed in order to improve the separation with no positive results. Then, the column was changed. Two reverse-phase trial columns, **Zorbax 300SB-C3** 150mm x 4.6mm x 3.5µm from Agilent and **Jupiter C18** 150mm x 4.6mm x 5µm from Phenomenex, were probed. No improvement was found when applying these chromatographic columns so both were dismissed.

Ion-Exchange Chromatography

After deep research about the state of the art [11–32] the **Cimac™ -SO_3 column (BiaSeparations)** was selected due to the accurate quantification of LF found in the literature [21]. Following Adam et al. [21] results, the method applied in this study was the following: phosphate/dipotassium phosphate buffer solution pH 7.25 (A) and a phosphate/dipotassium phosphate buffer solution pH 7.25 with 1.5M NaCl (B) as mobile phase. The column was first equilibrated with fresh mobile phase A flowing at a flow rate of 0.75 mL min^{-1}. After injection of the sample, buffer A was pumped for 20 minutes to separate proteins with isoelectric point below 7.25 in the outlet of the ion exchange monolithic column. After 15 minutes the elution solution (B) was flowing with a flow rate of 0.25 ml min^{-1}. After 30 minutes the analysis was stopped and the chromatogram was processed at 280.0 nm with Millenium software (Waters). Mixture samples of BSA and LF with different proportions of both in the mixture were analyzed (4.0 g L^{-1} BSA + 1.0 g L^{-1} LF; 3.0 g L^{-1} BSA + 0.5 g L^{-1} LF; 2.0 g L^{-1} BSA + 0.5 g L^{-1} LF; 1.0 g L^{-1} BSA + 0.25 g L^{-1} LF; 0.4 g L^{-1} BSA + 0.1 g L^{-1} LF; 0.75 g L^{-1} BSA + 0.25 g L^{-1} LF; 0.5 g L^{-1} BSA + 0.25 g L^{-1} LF; 0.04 g L^{-1} BSA + 0.01 g L^{-1} LF). Chromatograms of the separation of mixture standards are shown as an example in Figure 2.5.

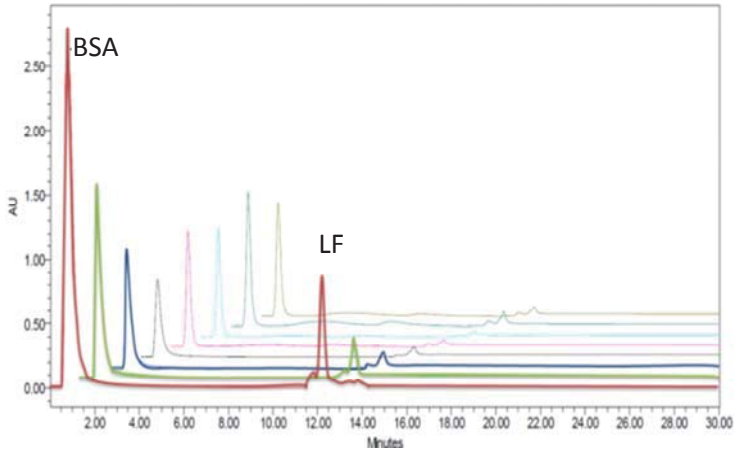

Figure 2.5. HPLC Chromatograms obtained with the column Cimac ™ - SO_3^- for BSA/Mixtures of 4.0-0.01g L^{-1} in sodium acetate/acetic acid buffer.

As it is shown in Figure 2.5, the correct separation of BSA and LF is achieved in the chromatograms with high resolution in a wide range of concentrations (0.01 - 4.0 L^{-1}) in the sodium acetate/acetic acid buffer as well as in the borax/hydrochloric acid buffer of pH 9.0.

Once the correct separation of both proteins was achieved a calibration was performed in the range 0.01 - 4.0 g L^{-1}. The obtained calibration curves are depicted in Figure 2.6.

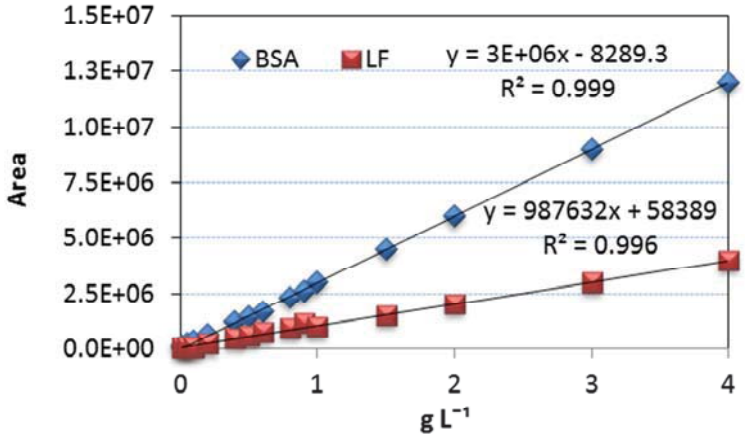

Figure 2.6. Calibration curves for BSA and LF in the range of 0.01-4 g L^{-1}using the ion exchange column Cimac ™ - SO_3^-.

As it is shown in Figure 2.6 this analytical technique allows the qualitative and quantitative determination of BSA and LF in buffer solutions in a wide range of protein concentration with a detection limit lower than 0.01 g L^{-1}.

Whey, in its natural form, present a high conductivity of about 5.0 S cm^{-1} [33]. For this reason, the presence of salts in the medium was study by means of 0.5 g L^{-1} of LF in KCl, in the range of concentration from 1.0 to 5.0 g L^{-1}, as it is shown in Figure 2.7.

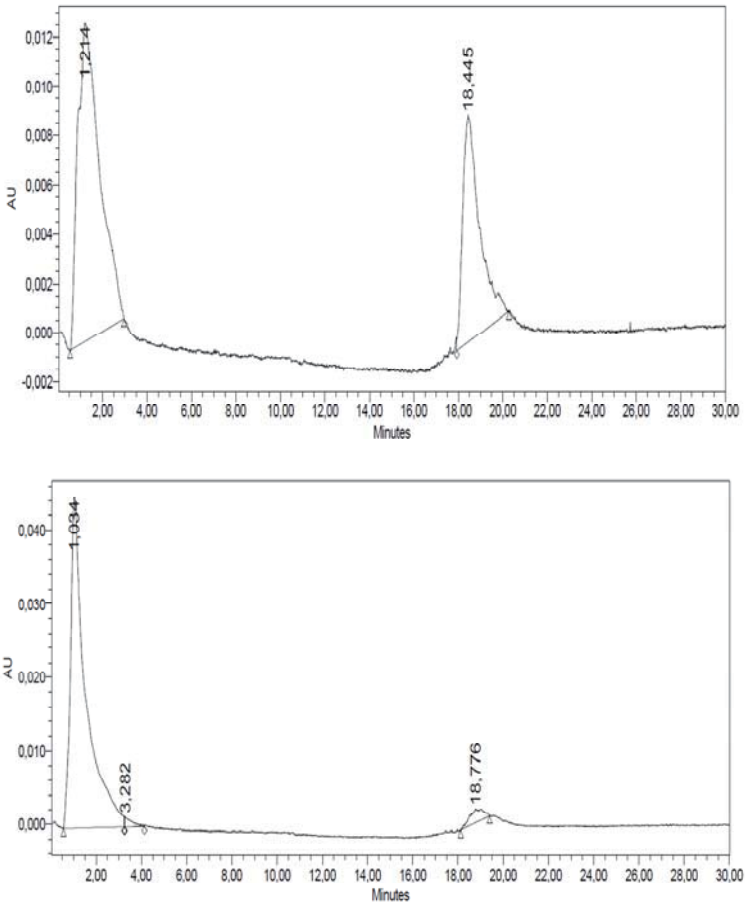

Figure 2.7. LF Chromatograms using the ion exchange column Cimac ™ - SO_3^-, a) 0.5 g L^{-1} LF in H_2O and b) 0.5 g L^{-1} LF in 1.0 g L^{-1} KCl.

As it is shown in Figure 2.7a, the LF in water presents a peak at 18.44 minutes that allows its quantification in mixtures. On the other hand, with 1.0 g L^{-1} KCl the first peak is increased, but the intensity signal at 18.77 minutes (Figure 2.7b) decreases dramatically. Moreover, the presence of salts in the electrolyte solutions avoids the proper retention of LF in the column and then the correct measurement with this method.

2.3 QUANTIFICATION OF BSA-LF IN BINARY MIXTURES BY FLOURESCENCE-ULTRAVIOLET COMBINED METHOD

The need of the qualitative and quantitative determination of BSA and LF in electrolytic solutions promoted the development of a new measurement method based on Fluorescence and Ultraviolet absorbance. The spark of this work was born in the Institut Européen des Membranes in Montpellier, during the research period under the supervision of Dr. Philippe Sistat and finally was performed in collaboration with the Dr. Rafael Valiente Barroso, Department of Applied Physics of the University of Cantabria.

Absorption and "instantaneous" re-emission of radiant energy from a molecule or atom accompanied by a change in wavelength as well as direction, is known as *Fluorescence*. Despite the Fluorescence is not consider as a protein quantification method, its use in protein structures or function studies is widely applied [34]. When a quantum of light is absorbed by a protein, the protein is raised to an excited state by absorption of ultraviolet, visible, or near infrared radiation. The excited protein then decays back to the ground state, or to a lower-lying excited electronic state, by emission of light. The emitted light is detected [35]. In proteins, the three aromatic amino acids—phenylalanine, tyrosine, and tryptophan—are all fluorescent. These three amino acids are relatively rare in proteins. Tryptophan, which is the dominant intrinsic fluorophore, is generally present at about 1.0 % in proteins, being 0.3 % in BSA and 1.9 % in LF (Section 1.2) [36].Two basic types of spectra can be produced by a fluorescence spectrometer. In a fluorescence spectrum, or emission spectrum, the wavelength of the exciting radiation is held constant (at a wavelength at which the analyte absorbs) and the spectral distribution of the emitted radiation is measured. In an excitation spectrum, the fluorescence signal, at a fixed emission wavelength, is measured as the wavelength of the exciting radiation is varied [37]. In this work the *Emission Scan* was the selected procedure. The same proteins and buffers described in section 2.2 were used.

The Flourometric measurements were performed using a FLSP920 fluorescence spectrometer (Edinburgh Inst.) with single photon counting. Quartz cuvettes were employed in all the measurements (Figure 2.8a). The absorbance-based analyses were performed using a high performance UV-Visible-NIR spectrophotometer, Cary 6000i UV-Vis-NIR (Agilent) with a photometric performance in the 175.0 -1800.0 nm range. Quartz cuvettes were employed in all the measurements, (Figure 2.8b). Additionally, the free software Fityk was used to adjust the absorbance profiles.

a)

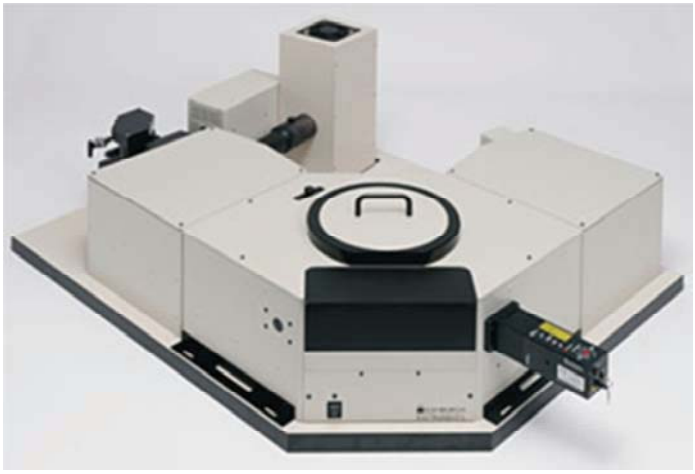

b)

Figure 2.8. a) FLSP920 Fluorescence spectrometer (Edinburgh Inst.), b) High performance UV-Visible-NIR spectrophotometer Cary 6000i UV-Vis-NIR (Agilent).

As a first step, using a fluorescence spectrometer (FLSP920, Edinburgh Inst.) the measurement was conducted with individual standards of 1.0 g L^{-1} of both proteins in KCl without setting the pH, using an excitation wavelength (λ) of 277.0 nm (maximum emission wavelength) and an emission scan from 280.0 - 450.0 nm, obtaining absorption spectra of both proteins as showed in Figure 2.9.

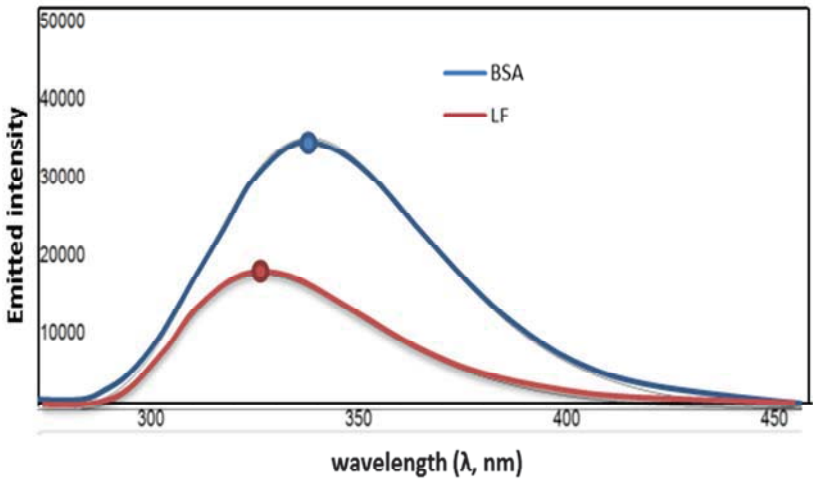

Figure 2.9. Fluorometric absorption spectra of BSA and LF proteins individual standards.

Figure 2.9 depicts the BSA and LF Fluorometric spectra adjusted to a Logarithm Normal (LogN) by the Fityk software. Both proteins emit in the same wavelength range, however, they present different Fluorescence profiles trends and different maximum position (dots in Figure 2.9, also called “center”, nm).

A feature of intrinsic protein fluorescence is the high sensitivity of tryptophan (fluorescent) to its local environment. Changes in the emission spectra of tryptophan often occur in response to conformational transitions, substrate binding, or denaturation, mainly due to change in protein concentration or solutions conditions. For this reason, a study of the protein emitted intensity height and maximum position (center, nm) with concentration and pH was performed. No linear relationship between protein concentration and height was

shown. On the other hand, the protein's emitted intensity position showed a defined pattern with protein concentration and solution pH. The obtained results are presented in Table 2.2.

Table 2.2. BSA and LF center position as a function of concentration and pH.

	Center position (λ, nm)									
	Unfixed		pH 3.0		pH 5.0		pH 7.0		pH 9.0	
g L^{-1}	BSA	LF	BSA	LF	BSA	LF	BSA	LF	BSA	LF
0.01	337.1	338.7	324.6	337.7	338.8	329.5	339.2	328.4	329.0	328.4
0.1	324.6	340.5	324.2	337.9	337.2	325.7	337.3	326.1	337.8	325.8
0.3	338.5	325.7	324.6	337.9	338.9	326.0	338.2	326.3	337.4	326.2
0.5	334.9	325.9	324.4	336.9	337.7	326.3	338.3	326.3	337.4	326.5
0.8	335.2	340.3	324.2	337.8	338.5	326.3	339.4	326.5	336.9	326.4
1.0	338.4	341.1	324.3	337.8	338.7	326.2	338.2	326.5	337.8	326.6
S.D.	5.2	7.5	**0.2**	**0.4**	0.7	1.4	0.8	0.9	3.4	0.9

As it is shown in Table 2.2, the position (center) of BSA and LF has their lowest standard deviation (S.D) from the mean value at pH 3.0. Thus, if the pH is fixed to 3.0, the position of the center of the Fluorometric spectra is constant with the variation of the concentration for each protein. This difference in the center position allows the differentiation between proteins.

When mixtures of both proteins were analyzed in the working range of concentration of 0.01-1.0 g L^{-1}, an almost linear relationship with the percentage of each protein and the position of the center was found (Figure 2.10) with a measurement error lower than the 9.0 % for the worst scenario and an average error of 2.5 %.

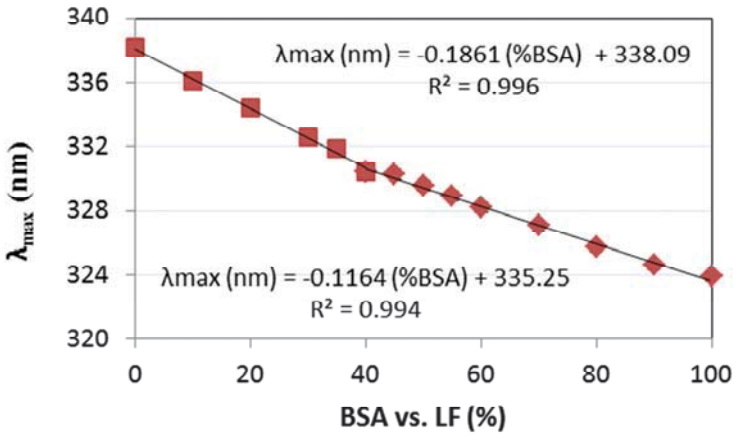

Figure 2.10. Calibration curve, position vs. % of BSA in the mixture.

As is depicted in Figure 2.10, two calibration curves were obtained:

$$\lambda_{max}\,(nm) = -\,0.1861\,(\%BSA) + 338.09 \quad (\%BSA) = 0 - 40 \qquad (2.1)$$

$$\lambda_{max}\,(nm) = -\,0.1164\,(\%BSA) + 335.25 \quad (\%BSA) = 40 - 100 \qquad (2.2)$$

With this calibration by measuring the position (center) of an unknown sample, the relative percentage of BSA from LF can be read in the calibration curve. Despite this technique has been previously applied to the determination of hydrocarbons and some living cells [38–42], its use in protein determination without the addition of a fluorophore had not been previously performed. Thus, this work presents the first demonstration that it is possible to determine the relative percentage of BSA and LF in binary mixtures in electrolytic media.

To quantify the individual concentration protein from the relative percentage obtained in the previous step, the measurement of total protein concentration in the sample problem is needed.

The most commonly used methods to determine the total protein concentration (direct measurement at 280.0 nm, Bradford method (595.0 nm), difference at two wavelengths (235.0 and 280.0 nm) and Lowry method (595.0 nm) were applied for individual and mixtures of protein standards in the range of total concentration of 0.01-1.0 g L^{-1}.

The calibration curves obtained applying these methods are shown in Figures 2.11-2.14.

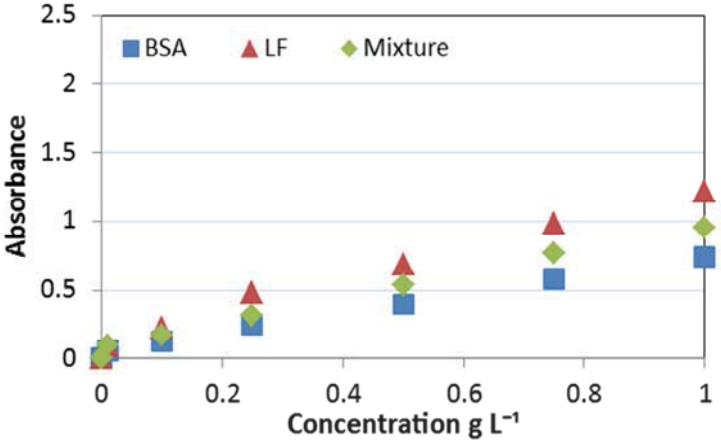

Figure 2.11. Calibration curves of BSA, LF proteins and their mixtures. Direct measurement method at 280.0 nm.

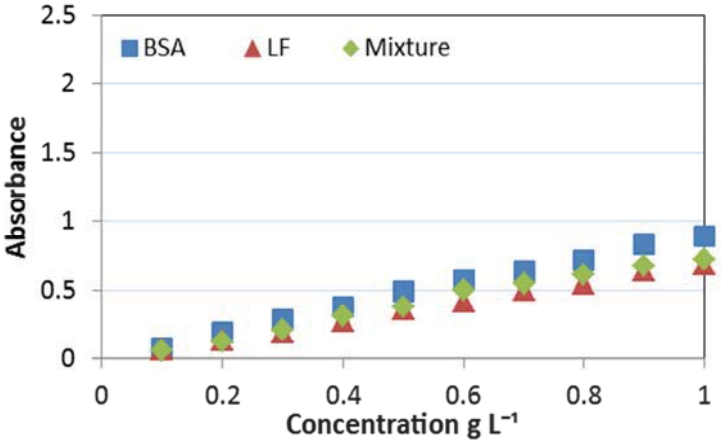

Figure 2.12. Calibration curves of BSA, LF proteins and their mixtures. Bradford method at 595.0 nm.

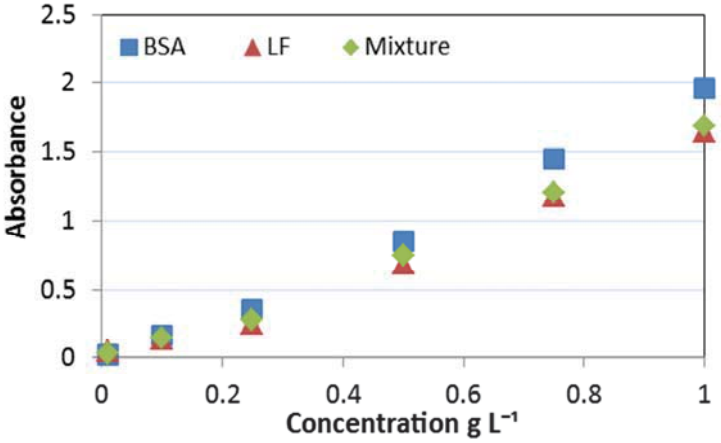

Figure 2.13. Calibration curves of BSA, LF protein and their mixtures. Absorbance difference between 235.0 and 280.0 nm.

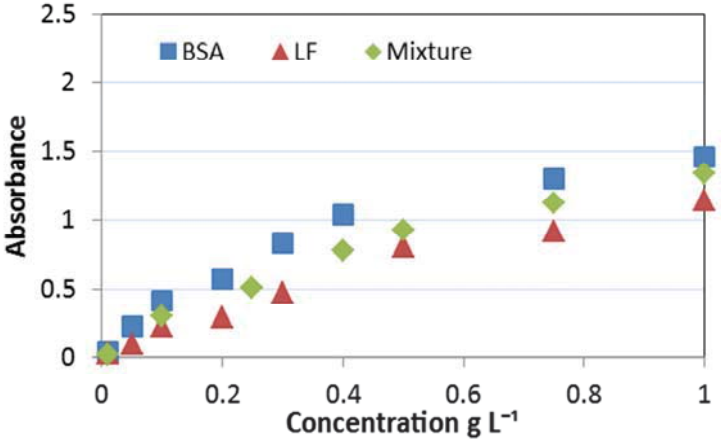

Figure 2.14. Calibration curves of BSA, LF proteins and their mixtures. Lowry method at 595.0 nm.

As is shown in Figure 2.11 different absorbance values are obtained for the same total protein concentration depending on the composition. These divergences avoid the proper quantification of proteins if the composition is not known. The same behavior is found using Bradford method, Figure 2.12.

The same conclusions were reached using the absorbance difference between 235.0 and 280.0 nm and Lowry method at 595.0 nm, Figures 2.13-2.14. The unsatisfactory results obtained with conventional total concentration measurement methods encouraged the development of a specific method for the total concentration of BSA-LF mixtures in electrolytic media.

Specific method for total concentration of BSA-LF mixtures

Taking advantage of the adequate performance of Fluorescence in the individual BSA/LF protein quantification, this technique was evaluated for the quantification total protein in electrolytic media.

Absorption curves were determined with the spectrophotometer UV-vis at different concentrations (0.01-1.0 g L^{-1}) for the individual standards in 2.0 g L^{-1} KCl in the wavelength range of 180.0 - 400.0 nm. In a first step, the solution pH was fixed at 3.0 (lowest standard deviation of the position center in the individual protein measurement).

Figure 2.15 depicts, as an example, the absorbance profiles for the measurement of 1.0 g L^{-1} of BSA in 2.0 g L^{-1} of KCl (Figure 2.15a) and of 1.0 g L^{-1} of LF in 2.0 g L^{-1} of KCl (Figure 2.15b). In order to mathematically describe the protein fluorescence spectrum, several Gaussians are applied. A Gaussian is mathematically defined by three parameters: center, height and full width at half maximum (hwhm). The absorbance profiles showed in Figure 2.15 have been modeled by means of the Fityk software

In the same way, the absorbance profiles for the measurement of mixtures 0.5 g L^{-1} of BSA and 0.5 g L^{-1} of LF in 2.0 g L^{-1} of KCl and the corresponding Gaussian have been plotted in Figure 2.16.

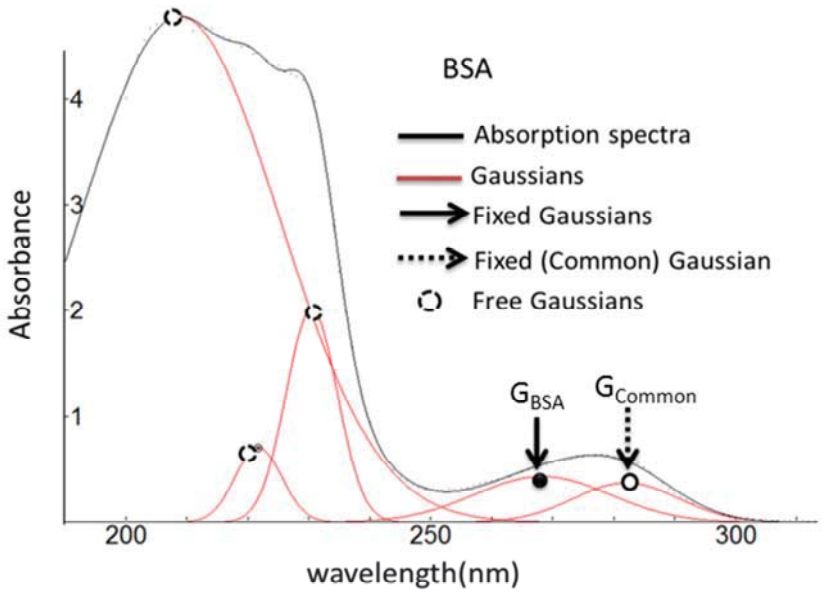

a)

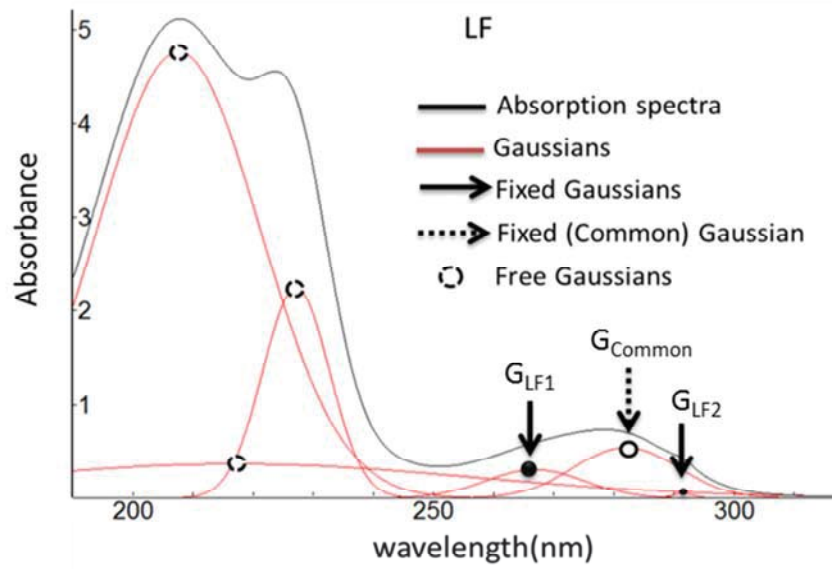

b)

Figure 2.15. Absorption spectra in UV-vis and corresponding Gaussians for individual standards of a) BSA protein and b) LF protein.

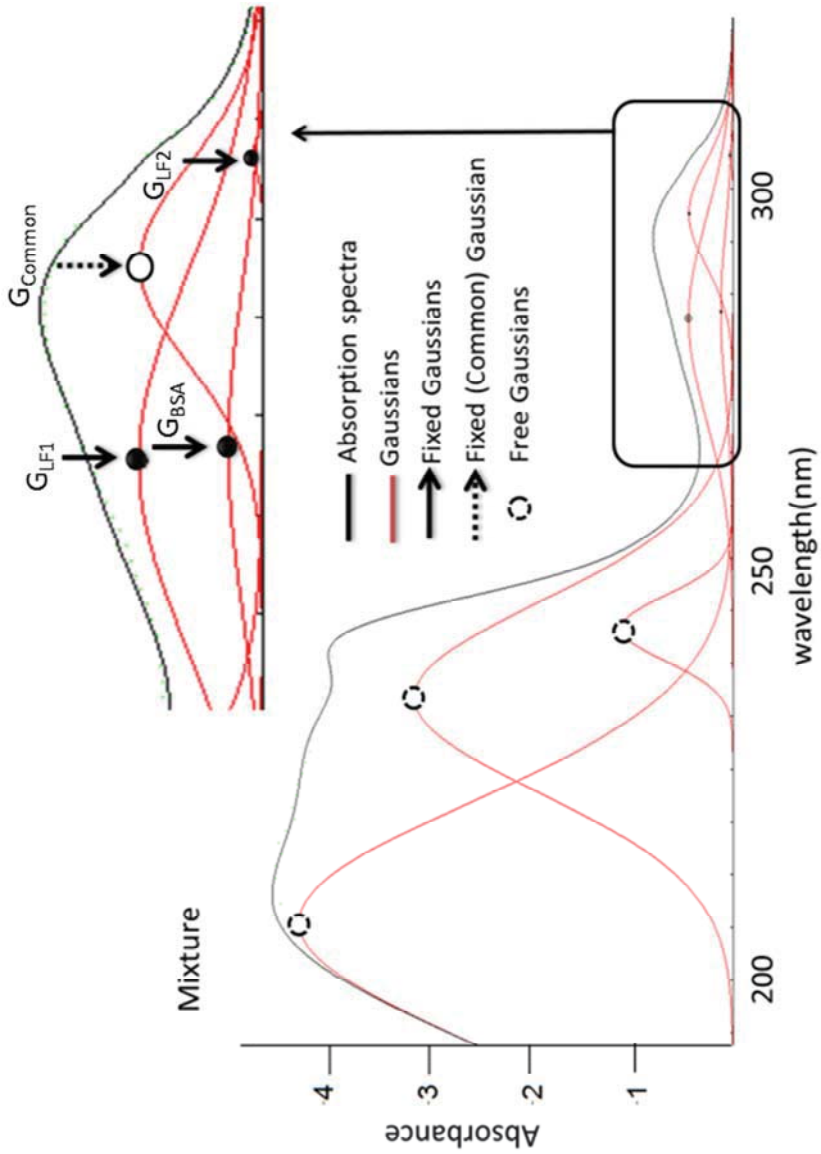

Figure 2.16. Absorption spectra in UV-vis for a mixture standard of BSA and LF proteins.

As it can be observed in Figure 2.15, for the correct description of a BSA and LF absorption curve, the contribution of five or six Gaussians is needed, respectively. Changes in BSA concentration implies that the center and full width at half maximum (hwhm) of three of the five Gaussian need to define the absorption spectra are concentration dependent, while two (G_{BSA} and the G_{Common}, red line) of them keep constant (fixed Gaussian) in the concentration range considered in this study (0.01-1.0 g L^{-1}). Changes in LF concentration implies that the center and full width at half maximum (hwhm) of three of the six Gaussian need to define the absorption spectra are concentration dependent, while three of them(G_{LF1}, G_{LF2} and G Common) keep constant (fixed Gaussian) in the concentration range considered in this study (0.01-1.0 g L^{-1}). One of the fixed Gaussian is the same of both proteins (G_{Common}). In the case of the protein mixtures, Figure 2.16, it can be observed that the intensity spectrum is described by the contribution of the seven Gaussians, three free Gaussians and four fixed Gaussians. These fixed Gaussians correspond to G_{BSA}, G_{LF1}, G_{LF2} and G_{Common}.

Table 2.3 presents the center and full width at half maximum (hwhm) values for the fixed Gaussians of the BSA, LF and mixture spectra in the concentration range considered in this study.

Table 2.3. Parameters of fixed Gaussians of the BSA, LF and mixture spectra in the concentration range considered in this study.

Absorption Curves	Conditions g L^{-1}	Gaussian	Center	Full width at half maximum (hwhm)
BSA protein	0.01-1.0	G_{BSA}	268.21	13.23
		G_{Common}	281.98	10.25
LF protein	0.01-1.0	G_{LF1}	266.78	9.87
		G_{LF2}	291.43	2.22
		G_{Common}	281.98	10.25
Mixture	0.01-1.0	G_{BSA}	268.21	13.23
		G_{LF1}	266.78	9.87
		G_{LF2}	291.43	2.22
		G_{Common}	281.98	10.25

The relationship between the height of the common Gaussian, which is known to be related to the intensity of light absorbed, and the concentration was measured. For this aim the calibration of individual standards as well as mixture standards with different proportion of BSA in the mixture (10.0 - 90.0 %) in the range of total concentration from 0.01 to 1.0 g L^{-1} was carried out. The different heights of the common Gaussian were noted and represented versus the total concentration for the different percentages of BSA in the sample in Figure 2.17 with a measurement error lower than 14.0 %.

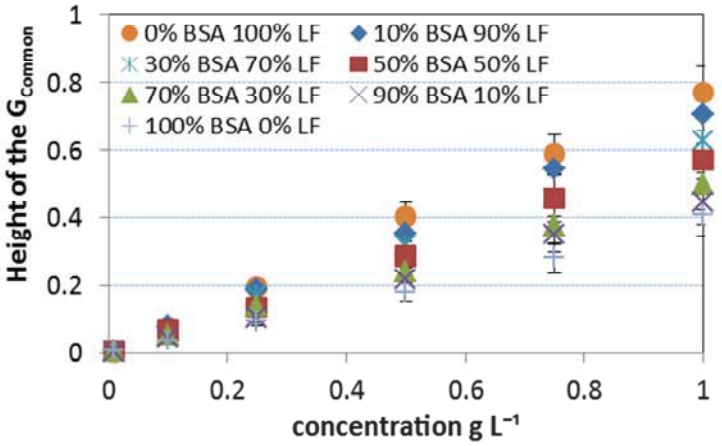

Figure 2.17. Heights of common Gaussian vs. total protein concentration calibration curves.

As it is shown in Figure 2.17, the height of the common Gaussian increases with the proportion of LF in the mixture and the total protein concentration. From the linear regression of the curves the general equation 2.3 was obtained for the different percentages of BSA:

$$H_{Common\ Gaussian} = \varepsilon * [BSA+LF](g\ L^{-1}) \quad (2.3)$$

Being ε the slope of the regression curve (absorbency). With the absorbency values obtained from the regression of the curves described in Figure 2.17, the curve absorbency vs. percentage of BSA in the mixture is drawn in Figure 2.18, through the equation:

$$\varepsilon = 0.0036\ (\%BSA) + 0.758 \quad (2.4)$$

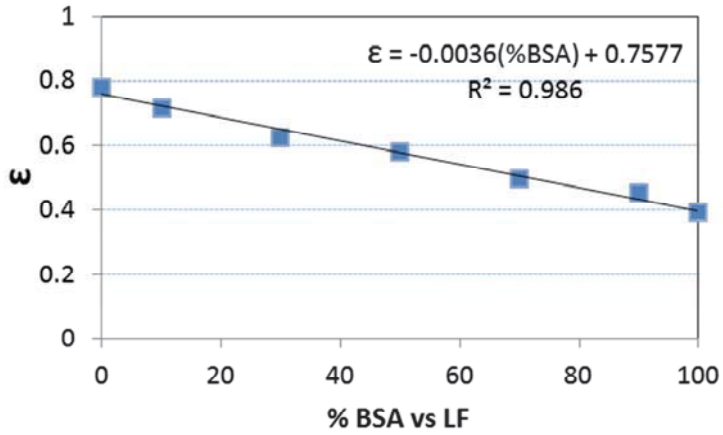

Figure 2.18. Absorbency vs percentage of BSA protein in the mixture.

In this way, if the relative percentage of BSA obtained from the Fluorometric calibration is introduced in equation 2.4, the absorbency of the mixture can be determined by means of equation 2.3. Appling this method errors an average error of 5.2 % has been obtained.

The Fluorescence UV-vis method developed in this research is fully described in Figure 2.19, indicating the specific steps needed to quantify individually BSA and LF proteins in electrolyte media.

The results obtained in this section are in patent process Ref: **P201400165** (Presented on 28/02/2014 and favorably informed on 02/06/2014 Ref numer: **2464440-A1**).

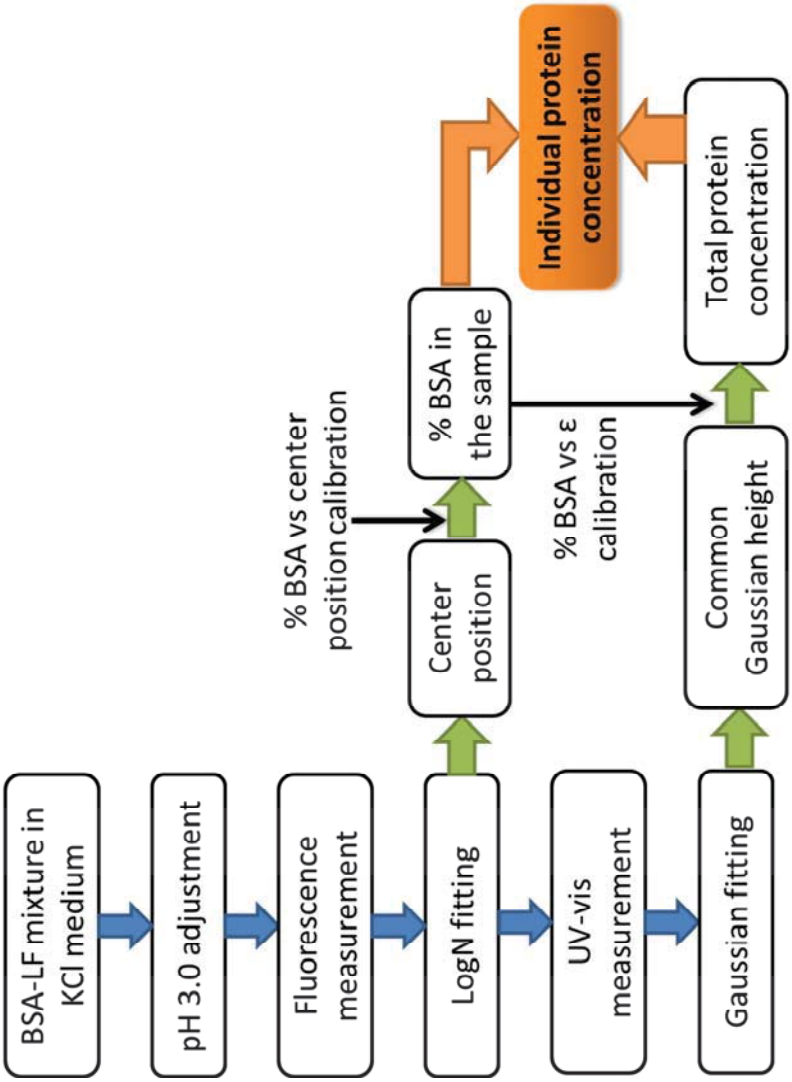

Figure 2.19. Methodology procedure of a problem sample measurement.

Summary

In this chapter, the development of analytical techniques for the quantification of BSA- LF in binary mixtures in the range of 0.01 to 4.0 g L^{-1} has been carried out.

A HPLC method based on ***ion-exchange Chromatography*** has been adapted for the qualitative and quantitative determination of BSA and LF in mixtures *using a* ***Cimac™-SO_3^-*** column and sodium phosphate/dipotassium phosphate buffer as mobile phase. This method allows the qualitative and quantitative individual determination of BSA and LF in buffer solutions in a wide range of protein concentration with a detection limit lower than 0.01 g L^{-1}.

The need of the qualitative and quantitative determination of BSA and LF in electrolytic solutions promoted the development of a specific measurement based on Fluorescence and Ultraviolet techniques. The method implies two steps. In a first step the relative percentage of BSA in the sample is obtained by Fluorometric determination and in a second step, the total protein concentration is obtained by UV-vis measurements. The fitting of the Fluorescence and UV-vis spectra by the Fityk software is needed to determine the parameters that will be applied in the calibration curves describe in the equations 2.1-2.4. This method allows the qualitative and quantitative individual determination of BSA and LF in electrolytic solutions in a range of protein concentration up to 1.0 g L^{-1}.

2.4 REFERENCES

The references in this section were managed by the Mendeley reference software applying the Separation Science and Technology style.

[1] N.M. Kinghorn, G.R. Paterson, D.E. Otter, Quantification of the major bovine whey proteins using capillary zone electrophoresis, J. Chromatogr. A. 723 (1996) 371–379.
[2] I. Recio, E. Molina, M. Ramos, M. de Frutos, Quantitative analysis of major whey proteins by capillary electrophoresis using uncoated capillaries, Electrophoresis. 16 (1995) 654–8.
[3] J.M.L. Heck, C. Olieman, A. Schennink, H.J.F. van Valenberg, M.H.P.W. Visker, R.C.R. Meuldijk, et al., Estimation of variation in concentration, phosphorylation and genetic polymorphism of milk proteins using capillary zone electrophoresis, Int. Dairy J. 18 (2008) 548–555.
[4] S.G. Anema, The use of "lab-on-a-chip" microfluidic SDS electrophoresis technology for the separation and quantification of milk proteins, Int. Dairy J. 19 (2009) 198–204.
[5] A.P. Biotech, Protein purification: Handbook, 2nd Ed, Amersham Pharmacia Biotech Inc., New Jersey, USA., 1999.
[6] D.A. Skoog, F.J. Holler, S.R. Crouch, Principles of instrumental analysis, 6th Ed, Cengage Learning, Belmont, CA, USA, 2007.
[7] G.L. Zubay, D.E. Atkinson, Biochemistry, 4th Ed, WCB/McGraw-Hill, Macmillan, USA, 1997.
[8] J. Ku, P. Stroeve, Protein diffusion in charged nanotubes : "On - Off " behavior of molecular transport, Langmuir. 20 (2004) 2030–2032.
[9] S.A. Moore, B.F. Anderson, C.R. Groom, M. Haridas, E.N. Baker, Three-dimensional structure of diferric bovine lactoferrin at 2.8 A resolution, J. Mol. Biol. 274 (1997) 222–36.
[10] P.G. Thakurta, D. Choudhury, R. Dasgupta, J.K. Dattagupta, Tertiary structural changes associated with iron binding and release in hen serum transferrin: a crystallographic and spectroscopic study, Biochem. Biophys. Res. Commun. 316 (2004) 1124–31.
[11] A.A. Foley, G.W. Bates, The purification of lactoferrin from human whey by batch extraction, Anal. Biochem. 162 (1987) 296–300.
[12] R. Hahn, P.M. Schulz, C. Schaupp, A. Jungbauer, Bovine whey fractionation based on cation-exchange chromatography, J. Chromatogr. A. 795 (1998) 277–287.
[13] S. Yoshida, Isolation of lactoperoxidase and lactoferrins from bovine milk acid whey by carboxymethyl cation exchange chromatography, J. Dairy Sci. 74 (1991) 1439–1444.
[14] L. Zhang, N.T., Nakano, T., Ozimek, Isolation of lactoferrin from bovine colostrum by SP-Sepharose cation-exchange chromatography, Milchwissenschaft. 57 (2002) 614–617.

[15] S. Doultani, K.N. Turhan, M.R. Etzel, Fractionation of proteins from whey using cation exchange chromatography, Process Biochem. 39 (2004) 1737–1743.
[16] A. Heebøll-Nielsen, S.F.L. Justesen, O.R.T. Thomas, Fractionation of whey proteins with high-capacity superparamagnetic ion-exchangers, J. Biotechnol. 113 (2004) 247–62.
[17] X. Ye, S. Yoshida, T.B. Ng, Isolation of lactoperoxidase, lactoferrin, α-lactalbumin, β-lactoglobulin B and β-lactoglobulin A from bovine rennet whey using ion exchange chromatography, Int. J. Biochem. Cell Biol. 32 (2000) 1143–1150.
[18] J. Andersson, B. Mattiasson, Simulated moving bed technology with a simplified approach for protein purification. Separation of lactoperoxidase and lactoferrin from whey protein concentrate, J. Chromatogr. A. 1107 (2006) 88–95.
[19] C.J. Fee, A. Chand, Capture of lactoferrin and lactoperoxidase from raw whole milk by cation exchange chromatography, Sep. Purif. Technol. 48 (2006) 143–149.
[20] K. Plate, S. Beutel, H. Buchholz, W. Demmer, S. Fischer-Frühholz, O. Reif, et al., Isolation of bovine lactoferrin, lactoperoxidase and enzymatically prepared lactoferricin from proteolytic digestion of bovine lactoferrin using adsorptive membrane chromatography, J. Chromatogr. A. 1117 (2006) 81–6.
[21] V. Adam, O. Zitka, P. Dolezal, L. Zeman, A. Horna, J. Hubalek, et al., Lactoferrin isolation using monolithic column coupled with spectrometric or micro-amperometric detector, Sensors. 8 (1995) 464–487.
[22] C. Conesa, L. Sánchez, C. Rota, M.-D. Pérez, M. Calvo, S. Farnaud, et al., Isolation of lactoferrin from milk of different species: calorimetric and antimicrobial studies, Comp. Biochem. Physiol. 150 (2008) 131–9.
[23] B.Y. Fong, C.S. Norris, K.P. Palmano, Fractionation of bovine whey proteins and characterisation by proteomic techniques, Int. Dairy J. 18 (2008) 23–46.
[24] M. Wu, Y. Xu, Isolation and purification of lactoferrin and immunoglobulin G from bovine colostrum with serial cation-anion exchange chromatography, Biotechnol. Bioprocess Eng. 14 (2009) 155–160.
[25] S.M. Saufi, C.J. Fee, Recovery of lactoferrin from whey using cross-flow cation exchange mixed matrix membrane chromatography, Sep. Purif. Technol. 77 (2011) 68–75.
[26] M.J. Santos, J.A. Teixeira, L.R. Rodrigues, Fractionation and recovery of whey proteins by hydrophobic interaction chromatography, J. Chromatogr. B. 879 (2011) 475–9.
[27] H. Kawakami, H. Shinmoto, S. Dosako, Y. Sogo, One-step isolation of lactoferrin using immobilized monoclonal antibodies, J. Dairy Sci. 70 (1987) 752–9.
[28] D.Q. Lin, Separation of lactoferrin from whey by expanded bed adsorption with mixed-mode adsorbent, Thesis work. Zhejiang University, 2009.
[29] L. Chen, C. Guo, Y. Guan, H. Liu, Isolation of lactoferrin from acid whey by magnetic affinity separation, Sep. Purif. Technol. 56 (2007) 168–174.

[30] F.J. Wolman, D.G. Maglio, M. Grasselli, O. Cascone, One-step lactoferrin purification from bovine whey and colostrum by affinity membrane chromatography, J. Memb. Sci. 288 (2007) 132–138.
[31] X. Felipe, A.J. Law, Preparative-scale fractionation of bovine, caprine and ovine whey proteins by bel permeation chromatography, J. Dairy Res. 64 (1997) 459–64.
[32] S.A. Al-Mashikhi, S. Nakai, Isolation of bovine immunoglobulins and lactoferrin from whey proteins by gel filtration techniques., J. Dairy Sci. 70 (1987) 2486–92.
[33] L. Diblíková, L. Čurda, K. Homolová, Electrodialysis in whey desalting process, Desalin. Water Treat. 14 (2010) 208–213.
[34] J.R. Lakowicz, Topics in fluorescence spectroscopy, 6th Ed, KIuwer Academic Publishers, New York, USA, 2000.
[35] R.C. Smith, K.S. Baker, P. Dustan, Fluorometric techniques for the measurement of oceanic chlorophyll in the support of remote sensing, San Diego, USA, 1981.
[36] J.R. Lakowicz, Principles of fluorescence spectroscopy, 3th Ed, Springer, New York, USA, 2009.
[37] E.L. Wehry, Molecular fluorescence and phosphorescence spectrometry, in: F.A. Settle (Ed.), Handb. Istrumental Tech. Anal. Chem., 1st Ed, Prentice Hall PTR, New Jersey, USA, 1997: pp. 507–539.
[38] M.W. Renfro, S.D. Pack, G.B. King, N.M. Laurendeau, A pulse-pileup correction procedure for rapid measurements of hydroxyl concentrations using picosecond time-resolved laser-induced fluorescence, Appl. Phys. B Lasers Opt. 69 (1999) 137–146.
[39] A. Choudhuri, Laser induced fluorescence measurements of radical concentrations in hydrogenâ hydrocarbon hybrid gas fuel flames, Int. J. Hydrogen Energy. 25 (2000) 1119–1127.
[40] O. Abdallah, O., Fluorescence spectroscopy by detection of glucose concentrations in DMEM-solutions and its perspectives for non-invasive measurement, in: BIODEVICES 2011, 4th Int. Conf. Biomed. Electron. Devices. Proc., 2011.
[41] C.J. Lorenzen, A method for the continuous measurement of in vivo chlorophyll concentration, Deep Sea Res. Oceanogr. Abstr. 13 (1966) 223–227.
[42] S. Ohkuma, B. Poole, Fluorescence probe measurement of the intralysosomal pH in living cells and the perturbation of pH by various agents, Proc. Natl. Acad. Sci. 75 (1978) 3327–3331.

3

PROTEIN AND MEMBRANE CHARACTERIZATION

Abstract

The aim of this chapter is to accurately measure fundamental surface properties, e.g., zeta potential, isoelectric point and protein size that can lead to the determination of the optimal separation conditions of Bovine serum albumin and Lactoferrin, two high added value food proteins whose similarity in weight makes their separation a scientific and technical challenge.

Taking advantage of the Electrophoretic light scattering (zeta potential) and Dynamic light scattering (size), a systematic study of these proteins' surface properties was performed under different conditions: i) $3.0 < pH < 10.0$, ii) electrolyte type: KCl, NaCl and $CaCl_2$ and concentration (0.01 - 0.1 M KCl; Buffer pH 7.0 0.05 - 0.15 M), and iii) protein concentration in the range of 0.04 – 4.0 g L^{-1} for BSA and 0.01 – 1.0 g L^{-1} for LF. Additionally, the values of zeta potential of five membranes were tested, two Polysulfone membranes and three Composited Regenerated Cellulosic membranes (CRC) by the Streaming potential using a 0.01 M NaCl as electrolyte.

3.1 STRUCTURAL CHANGES OF THE PROTEINS

Whey proteins have been increasingly used as food ingredients, mainly due to their well-balanced amino acid formulation and their functional properties, including the ability to form gels, their solubility and their foaming and emulsifying characteristics [1]. But these properties, that sometimes are desirable, can lead to changes in configuration and denaturation during handling steps.

BSA and LF are emulsifiers widely used as functional ingredients for the formation and stabilization of foodstuffs due to its foam capacity [2]. Foam highest concentration typically occurs when the solution pH happens to be the isoelectric point of the protein. At its isoelectric point the protein is more hydrophobic due to the lack of net charge. An hydrophobic protein tends to concentrate at the gas–liquid interface of the liquid phase [3]. If the protein concentration is increased at this surface, the decrease in the surface tension of the solution generally takes place. Then, the highest concentration of foam is found when the pH approaches the isoelectric point at the lowest surface tension [3]. Despite the extendedly used of this property, it is also a potential source of damage (denaturation) in the processing of protein solutions [4]. It is of special concern in processes where the foam formation is promoted as fermentation, air-lift bio-reactors, and turbulent mixing and foam fractionation [4]. Although foam control systems are widely used in industry (Sugar production, Food processing, Dairy products, Fermentation, Food washing, etc.) preventing the foam formation is preferable if this can be achieved without any adverse effects on the productivity of the process (some antifoaming agents can denature proteins) [5].

BSA has been reported to have a big foaming capacity, greater than other commonly foaming agents as Egg albumin [4,6–11]. No numerical data has been found about the foam power of LF but its ability to produce foams has been previously reported [12].

Besides foam formation, some other phenomena can take place during the protein handling:

Protein denaturation is produced if any modification in secondary, tertiary or quaternary conformation not accompanied by the rupture of peptides of the primary structure, takes place. The final conformation after denaturation can correspond to a totally (random coil) or partially unfolded polypeptide structure [13]. On the other hand, the changes occurring at molecular level, (e.g. dimerization) characterized by weak bonds at specific interaction sites, are known as *protein association*. If the protein-protein interactions are unspecific and result in the formation of large complexes, with higher molecular weights, the appropriate terms are *aggregation, polymerization, precipitation, coagulation and flocculation* [14]. Finally, *Gelation* is an orderly aggregation of native and/or (partially) denatured proteins where a well-ordered matrix, forming a three dimensional network by balanced the protein-protein and the protein-solvent interactions, is able to hold a significant amount of water [14].

These modifications can be induced through exposure to temperature increase or decrease (e.g., freezing), mechanical stresses such as shear strain, surface adsorption or foaming, pH shift, high protein or salt concentration among others [13].

The heat treatment is well-known to have a pronounced effect on the structures and functional properties of proteins. In globular proteins is associated with the destruction of some of the forces that stabilize native conformations, such as hydrogen bonds and hydrophobic interactions [15]. Bovine serum albumin (BSA) and Lactoferrin (LF) are denatured at relative low temperature, being the melting points, TM, of both proteins were around 65°C [14,16,17].

The effects of pressure and temperature on equilibria or kinetics are antagonistic in molecular terms, as follows from the principle of microscopic ordering, an increase in pressure at constant temperature leads to an ordering of molecules or a decrease in the entropy of the system [18]. Such changes may result in denaturation and aggregation of

proteins and thus may bring about textural changes, nevertheless BSA and LF are known to have excellent stability to high pressure [14].

In areas of large charge density (far from the isoelectric point of the protein), the intramolecular repulsion may be great enough to cause unfolding of the protein. This will have an effect similar to that of mild heat treatment on the protein structure. In some cases the unfolding may be extensive enough to expose hydrophobic groups and cause irreversible aggregation. Until this occurs such unfolding will be largely reversible [19].

Salt concentration influences protein stability through electrostatic mechanisms (contributing through the ionic force) as well as through Hofmeister effects. The effect of salts on protein solubility (Hofmeister effect) in aqueous solutions is a function of the ionic species present; being a salt concentration of 0.15 mol L^{-1} enough to change the structure of the water and conformation of the proteins. However, this will depend on the content and type of salt present in the medium (divalent salts have more ionic strength than monovalent salts with the same molar concentration) [20].

The relationship between protein concentration and aggregation is not deeply study, nevertheless higher concentrations are known to yield to high molecular weight aggregates [21].

3.1.1 CHARGE ON PROTEINS AND MEMBRANES

When two phases are placed in contact a difference in potential between them is generally developed. The sign and magnitude of such potentials affect process and quality control, and product specification [22]. In Figure 3.1 the schematic description of the charge developed by a molecule in an electrolytic medium is described.

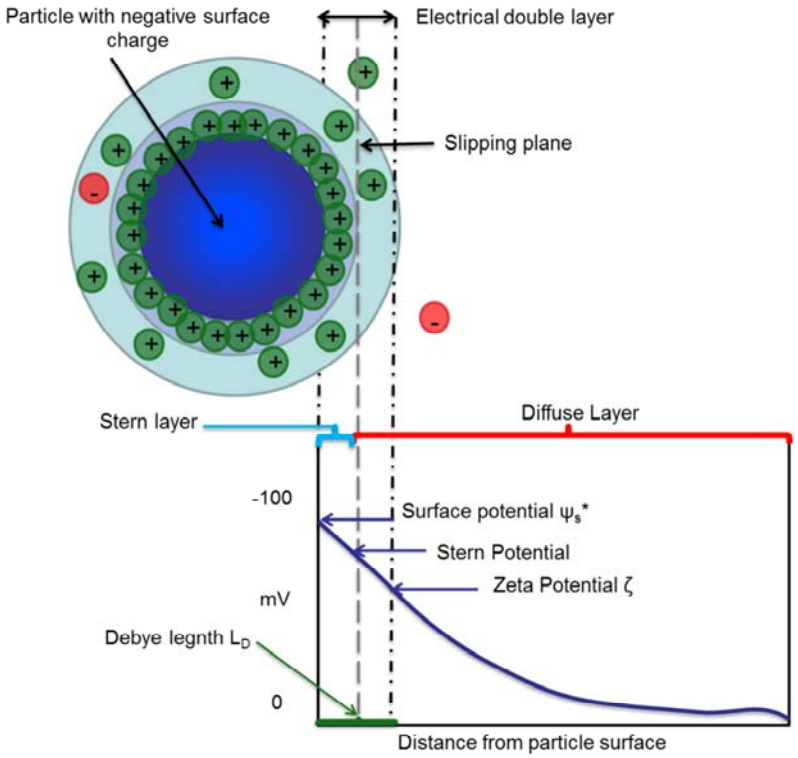

Figure 3.1. Schematic picture of the particle (protein) charge in an electrolytic medium.

When a protein is introduced in an electrolytic medium (Figure 3.1), an increase in the concentration of counter ions close to the surface takes place. Thus, an electrical layer is formed around each particle. The liquid layer surrounding the particle exists as two parts; an inner region, called the Stern layer (Stern potential), where the ions are strongly bound, and an outer or diffuse region (diffuse layer) where they are less firmly attached. Within the diffuse layer there is a notional

boundary inside which the ions and particles form a stable entity. When a particle moves (e.g. due to gravity), ions within the boundary move with it, but any ions beyond the boundary do not travel with the particle: this boundary is called the surface of hydrodynamic shear or slipping plane [23]. Both layers form an electrical double layer also called Debye length. The zeta potential (ζ-potential) is the charge associated with the plane of the Debye length, which includes the intrinsic charge of the protein as well as the charge of the double layer.

The importance of the ζ-potential to so many applications in science and engineering has led to the development of a number of techniques for measuring this quantity, based on one of the three electrokinetic effects: electrophoresis (the motion of particles induced in an applied electric field), electroosmosis (solid remain stationary and the charges in the adjoining liquid are moved by the applied electric field), and streaming potential (solid remain stationary and the charges in the adjoining liquid are moved by the pressure gradient) [24].

Protein Zeta Potential

When the electrophoresis method is applied, the ζ-potential is determined by placing fine particles in an electric field and measuring their mobility, μ_E, using a suitable microscopic technique. The electrophoretic velocity (v_E) observed in such an experiment is equal to the applied field (E) multiplied by the electrophoretic mobility (μ_E cm s^{-1} V^{-1}):

$$v_E = \mu_E E \tag{3.1}$$

The electrophoretic mobility is related to the zeta potential ζ by the Smoluchowski equation:

$$\mu_E = \frac{\varepsilon \zeta}{\eta} \tag{3.2}$$

In this expression ε is the dielectric constant of the dispersion medium (78.5), η is the dynamic viscosity of the dispersion medium (Pa s), and ζ is zeta potential (V). Soon after the publication by Debye and

Hückel of the theory of the behavior of the strong electrolytes, Hückel (1924) reevaluated the Smoluchowski equation obtaining:

$$\mu_E = \frac{2\varepsilon\zeta}{3\eta} \tag{3.3}$$

Henry [25] analyzed in 1931 the difference between the equations 3.2 and 3.3 taking into account the electric field in the neighborhood of the particle: Smoluchowski had assumed the field to be uniform and everywhere parallel to the particle surface and Hückel had disregarded the deformation of the applied field by the presence of the particle. These assumptions are justifiable in the extreme situations of $\kappa a >> 1$ and $\kappa a << 1$, where a is the particle radius and $1/\kappa$ is the thickness of the double layer. In this sense, Henry described the intermediate situation, it is, when the external field was superimposed on the local field around the particle, the mobility can be written [26]:

$$\mu_E = \frac{2\varepsilon\zeta f(\kappa a)}{3\eta} \tag{3.4}$$

The thickness of the double layer, κ (m), can be calculated as a function of the ionic strength of the suspending medium:

$$\kappa = \sqrt{\left(\frac{F^2}{\varepsilon_0\,\varepsilon RT}\right)\sum z_i^{\,2}\,C_i} \tag{3.5}$$

Where F is Faraday's constant (96500 C mol^{-1}), R is the gas constant (8.314 J mol^{-1} K^{-1}), T the absolute temperature (K), z the valence and C_i the concentration of each ion (mol m^{-3}).

Membrane Zeta Potential

To measure the surface charge of larger particles, which do not form stable suspensions or indeed flat substrates, such as membranes, the streaming potential (Figure 3.2) is used. This theory instead of applying an electric field to cause liquid to move through a capillary porous plug, force the liquid through under a pressure gradient. The excess charges near the wall are carried along by the liquid and their

accumulation down-stream causes the build-up of an electric field which drives an electric current back (by ion conduction through the liquid) against the direction of the liquid flow. A steady state is quickly established, and the measured potential difference across the capillary or plug is called the steaming potential [27].

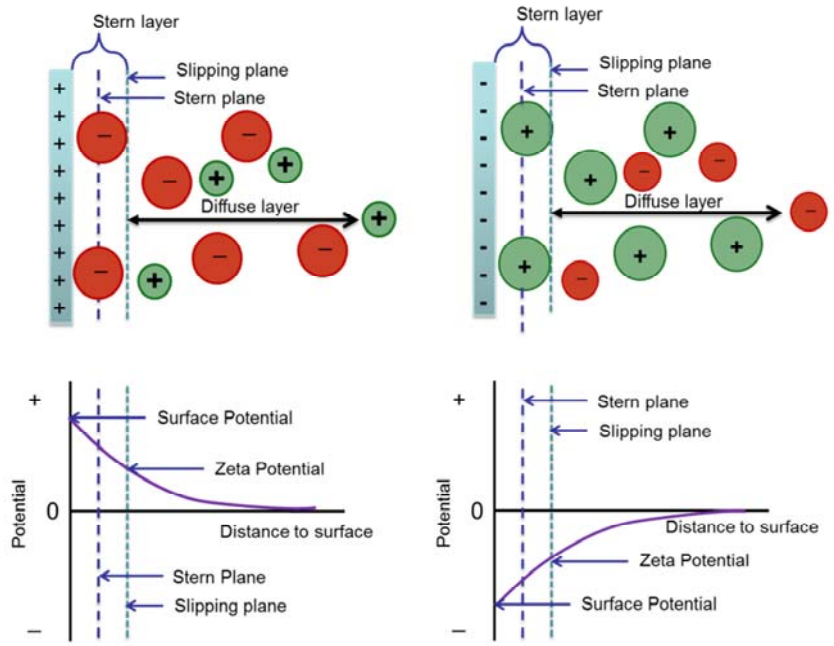

Figure 3.2. Schematic picture of a positive and negative surface (membrane) charge according to the streaming potential principle [28]**.**

The apparent zeta potential of the membrane (ζ) was evaluated by the streaming potential from the slope of the voltage as a function of applied pressure from the Helmoltz-Smoluchowski equation [29]:

$$\frac{dE_z}{dP} = \left(\frac{\varepsilon_0 \varepsilon \zeta}{\mu \Lambda} \right) \qquad (3.6)$$

Where E_z is the transmembrane voltage (Vm^{-1}), P is the pressure (Pa), ζ is zeta potential (V), μ is the viscosity (Pa s) and Λ represents the solution conductivity ($\Omega^{-1}\ m^{-1}$).

3.1.2 CHARGE REGULATION MODEL

Net charge is defined as the sum over all charged groups that are covalently or tightly associated with a particle [30]. This parameter easily calculable, is useful to determine theoretical isoelectric points.

The net protein charge can be calculated as a function of the solution pH and the ionic strength using a modified form of the charge regulation model (CRM) developed by Tanford et al. [31] and Scatchard et al. [32] that accounts for the protonation / deprotonation of the amino acids due to a shift in the local hydrogen ion concentration [33]. The extent of ionization of a given amino acid is a function of the local H^+ concentration, which can be represented for a carboxylic acid as:

$$R\text{ - }COOH \xleftrightarrow{K^{int}} R - COO^- + H^+ \tag{3.7}$$

On a real protein, charges are located creating local variations in charge density and counterions clustering at the charged group. Despite its obvious simplifications, it has been demonstrated that the simplified charged regulation model can explain qualitatively many trends in protein solution [33].

The net protein charge ($Z_{protein}$) is evaluated from the difference in the number of protonated amino acids (Z_{H^+}) and the number of bound anions (Z_{ion^-}):

$$Z_{protein} = Z_{H^+} + Z_{ion^-} \tag{3.8}$$

Z_{H^+} calculation

Proteins are made up of a number of different types of amino acids. Only certain amino acids take part in the ionization reactions which will generate a charged on protein surface. These groups are called the “titratable amino acids” or the “charged amino acid residues” [34]. The positive charge of the protein is calculated taking into account the local concentration of protons ions near the surface and the corresponding equilibrium reaction of the acids:

$$Z_{H+} = z_{max-} - \sum_i \frac{n_i K_i^{int}}{K_i^{int} + \left[H_b^+\right] \exp\left(-e\psi_s^*/kT\right)} \quad (3.9)$$

In equation 3.9 the local concentration protons ions is expressed as the bulk hydrogen ion concentration, $[H_b^+]$ (mol m^{-3}), ψ_s* electrostatic potential (V), e is the electron charge (1.602×10^{-19} C), k is the Boltzmann constant (1.38×10^{-23} J K^{-1}), T is the temperature (K) and n_i and K^{int} the number and intrinsic equilibrium constants for each titratable amino acid (i). The values of these parameters are given in Table 3.1 for BSA and for LF. The total number of positively charged amino acid residues at very low pH, z_{max}, e.g. where all the available sites are protonated, is z_{max} = 96.0 for BSA [35] and z_{max} = 82.0 for LF [34]. The exponential term in equation 3.9 is the Boltzmann factor and accounts for the partitioning of the hydrogen ions into the region immediately adjacent to the protein surface due to electrostatic interactions.

A direct relationship between the surface potential (ψ_s*) and the net surface charge density (σ_s^*) can be obtained using the overall electroneutrality condition of the system:

$$\sigma_s^* = \frac{\varepsilon_0 \varepsilon \psi_s^* (1 + \kappa r_s)}{r_s} \quad (3.10)$$

Being the surface charge density, σ_s^*, directly related to the number of charged groups on the protein surface as:

$$\sigma_s^* = \frac{e Z_{protein}}{4\Pi r_s^2} \quad (3.11)$$

Where r_s is the effective radius of the (spherical) BSA or LF (m) and κ is the inverse of the Debye length (m^{-1}) (equation 3.5) and $Z_{protein}$ is the net protein charge evaluated from equation 3.8.

The equations 3.9 and 3.10 consider a single globular protein surrounded by an aqueous solution of anions and cations. The protein is modeled as a homogeneous dielectric sphere of radius 35.0 Å for the

BSA [35] and 30.0 Å for the LF [34], the electrostatic potential (ψ_s*) on the model protein surface is averaged over the spherical surface.

Table 3.1. Type and number of titratable amino acids on BSA and LF.

BSA [35]			**LF** [34]		
Type (i)	**Number (n_i)**	**pK^{int}**	**Type (i)**	**Number (n_i)**	**pK^{int}**
a-Carboxyl	1	3.75	**Aspartic acid**	30	4.70
b, g-Carboxyl	99	4.02	**Glutamic acid**	34	4.70
Imidazole	16	6.90	**Histidine**	3	6.50
a-Amino	1	7.75	**Lysine**	39	10.20
e-Amino	57	9.80	**Tyrosine**	10	9.95
Phenolic	19	10.35	**Arginine**	30	12.00
Guanidine	22	12.00			
Z_{max} = 96			Z_{max} = 82		

Z_{ion^-} calculation

In the same way the number of bound ions is calculated according to equation 3.12 [36]:

$$Z_{ion^-} = \sum_j \frac{m_j K_j \gamma [Ion^-] \exp(-e\psi_s^*/kT)}{1 + K_j \gamma [Ion^-] \exp(-e\psi_s^*/kT)} \qquad (3.12)$$

Chloride salts are the most common electrolytes used in separation processes. The parameters number (m_j) and intrinsic equilibrium constants (K_j) for the three distinct Cl^- binding sites are m_1= 1; m_2=8; m_3=18 and K_1=2400 M^{-1}; K_2=100 M^{-1}; K_3=3.3 M^{-1} [29]. k is the Boltzmann constant and γ is the activity coefficient of the ion (dimensionless) that was evaluated as:

$$-\log\gamma = \frac{0.5\sqrt{[Ion^-]/2}}{\left(1 + 2\sqrt{[Ion^-]/2}\right)} \qquad (3.13)$$

The theoretical net protein charge in a given solution was evaluated by simultaneously solving equations from 3.8 to 3.13.

3.1.3 PROTEIN MOLECULAR SIZE

An important part of characterizing any protein molecule is the determination of its size and shape. The hydrodynamic diameter (d) of a protein can be calculated by dynamic light scattering (DLS). This procedure takes advantage of the fact that, if the scattering particle is moving when the light proton hits it, the re-radiated light will have a slightly different frequency when viewed by a stationary observer. For this reason it is called quasi-elastic scattering. The frequency is slightly increased or decreased depending on whether the particle is moving towards or away from the observer. This is called the *"Doppler broadening"* effect and it can be measured accurately, providing a means of determining the diffusion coefficient of the particles (D_{app}) and consequently a mean hydrodynamic diameter (d) can be calculated using the Stokes-Einstein equation [37]:

$$D_{app} = \frac{k\ T}{3\Pi\eta\ d} \tag{3.14}$$

where k is the Boltzmann constant, T is the absolute temperature, η is the sample dynamic viscosity and D_{app} is the diffusion coefficient ($m^2\ s^{-1}$).

Theoretical size determination

The radius of a spherical protein can be determined from the diffusion coefficient (e.g. the Stokes radius). However, biological molecules are always hydrated and solvation effectively increases the hydrodynamic volume of a molecule, and therefore its frictional coefficient. If f_0 is defined as the frictional coefficient expected for an un-hydrated molecule and f the frictional coefficient for a fully hydrated system, then:

$$\frac{f}{f_0} = \left(\frac{V_2 + \partial V_1}{v} \right) \tag{3.15}$$

The numerator is the total hydrodynamic volume, (v_2+δv_1) including hydration (δv_1) and the denominator is the volume of an un-hydrated molecule (v), and. f/f0 is the frictional ratio which would be 1.0 if an ideal sphere is measured. Deviations from this value indicate increasing asymmetry or hydration of the molecule [38]. This parameter takes the value of 1.3 for BSA (Sigma technical specifications) and 1.4 for LF [39]. The partial specific volume (v), In the equation 3.15, is the volume change in the solution when w_2 grams of solute are added (it expresses essentially the volume of solution occupied per gram of un-hydrated solute, e.g. protein) [25]. The partial specific volume (v) is 0.73 $cm^3\ g^{-1}$ for BSA [40] and 0.72 $cm^3\ g^{-1}$ for LF [39]

To obtain theoretical protein size data the equation 3.16 proposed by Compton in 1991 was used [40]. Compton, 1991 [40] described the Stoke's radius of the protein (r) in terms of the more useful, but in fact the more approximate, protein mass, through the equation and considering the hydration of protein:

$$r = \left(\frac{3M_w v}{4\Pi N} \right)^{1/3} \left(\frac{f}{f_0} \right) \qquad (3.16)$$

where M_w is the molecular weight of each protein (BSA=65.0 kDa and LF=78.0 kDa) and N is Avogadro's number (6.022 10^{23} mol^{-1}).

In this chapter BSA and LF protein will be characterized in terms of zeta potential, isoelectric point, molecular size and aggregation. Additionally, the surface characterization of membranes that will be used in the viability study of the BSA/LF separation processes (Chapter 4) is included.

3.2 MATERIALS AND METHODS

3.2.1 MATERIALS

Proteins and Buffers

In this study measurements were performed using individual and mixtures standards of the native BSA (Catalog A-6003 Sigma Chemical, Spain) and native LF (NutriScience Innovations, USA). BSA is readily soluble in water and requires high concentrations of neutral salts, such as ammonium sulfate, to induce precipitation. Bovine LF is highly soluble in water (2.0 %, 20°C) and has an Fe^{3+} content of 3.0 mg/100 g protein. The isoelectric point of BSA is close to 4.9, its molecular weight is 66.5 kDa, and the protein shape is a prolate ellipsoid with dimensions of 14.0 x 3.8 x 3.8 nm [41]. LF has an isoelectric point around 9.0, a molecular weight of 78 kDa, and a globular shape with dimensions of 4.0 x 5.1 x 7.1 nm, as determined using the lattice cell parameter data [42,43].

Protein standards of BSA, LF and their mixture in the range of concentrations of 0.1 - 4.0 g L^{-1} were prepared by adding the protein powder to the desired buffer solution, pH 5.0 (sodium acetate/acetic acid Analytical grade, Merk), pH 7.0 (sodium phosphate/dipotassium phosphate, Analytical grade, Merk); pH 9.0 (borax/hydrochloric acid (Fluka, Spain)) or different electrolyte solutions (KCl, NaCl or $CaCl_2$ Analytical grade, Merk). Shaking was avoided to prevent foam formation, which can seriously interfere with analytical procedure. Protein standards were used within the subsequent 24 h. to minimize the likelihood of protein aggregation. NaOH and HCl 0.1 M (Analytical grade, Merk) were employed to rise or reduce the pH of the electrolytic protein solutions.

3.2.2 ELECTROKINETIC ANALYTICAL TECHNIQUES

Zeta Potential measurements

The protein zeta potential was measured by electrophoretic light scattering (ELS) using a Zetasizer Nano ZS is shown in Figure 3.3a (Malvern Instruments, U.K.) and zeta potential folded capillary cell (Malvern) in Figure 3.3b. Experimental work was performed at the laboratory of the Department of Chemical Engineering, University of Burgos.

a) 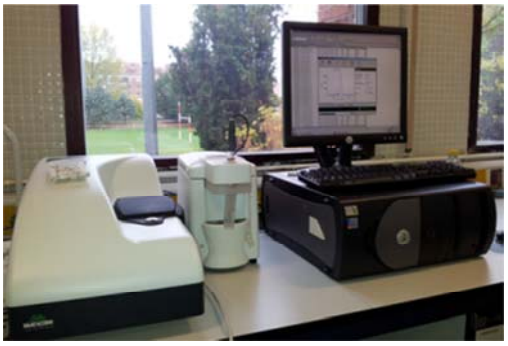 b) 

Figure 3.3. a) Zetasizer Nano ZS (Malvern) and b) zeta potential folded capillary cell (Malvern).

The zeta potential in Zetasizer Nano ZS was determined using the M3-PALS technique, a combination of laser Doppler velocimetry (LDV) and phase analysis light scattering (PALS), for particles in the size range from 0.4 nm to 100.0 µm. In this technique, an electrical field is applied across a pair of electrodes placed at both ends of a DTS1061 disposable folded capillary cell (Figure 3.3b) containing the particle dispersion. Charged particles are attracted to the oppositely charged electrode, and their velocity was measured and expressed per unit of field strength as the electrophoretic mobility, μ_E. Then, the zeta potential was calculated using Henry equation 3.4 assuming that the double layer thickness is larger than the particle size [27] and using the Hückel approximation ($\kappa a < 1$) in its calculation, where $f(\kappa a) = 1$. Six zeta potential measurements of 11 runs each were performed for every sample.

Protein size measurements

Protein size was determined by dynamic light scattering (DLS) using the aforementioned Zetasizer Nano ZS. The apparatus is equipped with a He-Ne laser emitting at 633.0 nm and with a 4.0 mW power source. The instrument uses a backscattering configuration where detection is done at a scattering angle of 173º using an avalanche photodiode. The protein dispersions (1.0 mL) were poured into DTS0012 square disposable polystyrene cuvettes, and measurements were performed at 298 K. Depending on the sample turbidity, the path length of the light was set automatically by the apparatus. From the polynomial fit of the logarithm of the correlation function using the cumulants method, the translational diffusion coefficient of the particle (D_{app}) was calculated using the Stokes-Einstein equation 3.14. In this equation, the hydrodynamic diameter (d) was calculated by assuming that the diffusing particles were monodisperse spheres. Three measurements of 20 runs each were performed for each sample.

The molecular size is obtained from the correlation function by using appropriate algorithms. Two different approaches can be taken into account, (1) the *"cumulants analysis"* that fits a single exponential to the correlation function to obtain the mean size (z-average diameter) and an estimation of the width of the distribution (polydispersity index, PDI), or (2) so called "*CONTIN analysis"* which fits a multiple exponential to the correlation function to obtain the distribution of particle sizes.

The size distribution obtained is expressed as the relative intensity of light scattered by particles in various size groups, known as an intensity size distribution. If the distribution by intensity is a single fairly smooth peak (PDI < 0.2), then there is little point in doing the conversion to a volume distribution using the Mie theory. If the optical parameters are correct, this will just provide a slightly different shaped peak. However, if the plot shows a substantial tail, or more than one peak (PDI > 0.2), then Mie theory can make use of the input parameter of the sample refractive index to convert the intensity distribution to a volume distribution. This will then give a more realistic view of the relative importance of the tail or the rest of the peaks present in the

analysis. In general terms it will be seen that: d(intensity) > d(volume) > d(number) [44].

A very simple way to describe the difference between intensity, volume and number distributions is to consider 2 populations of spherical particles of diameter 5.0 nm and 50.0 nm present in equal numbers (Figure 3.4). If a number distribution of these 2 particle populations is plotted, a plot consisting of 2 peaks (positioned at 5.0 and 50.0 nm) of a 1 to 1 ratio would be obtained. If this number distribution was converted into volume, then the 2 peaks would change to a 1:1000 ratio (because the volume of a sphere is equal to $4/3\pi\ (d/2)^3$. If this was further converted into an intensity distribution, a 1:1000000 ratio between the 2 peaks would be obtained (because the intensity of scattering is proportional to d^6 (from Rayleighs approximation) [45].

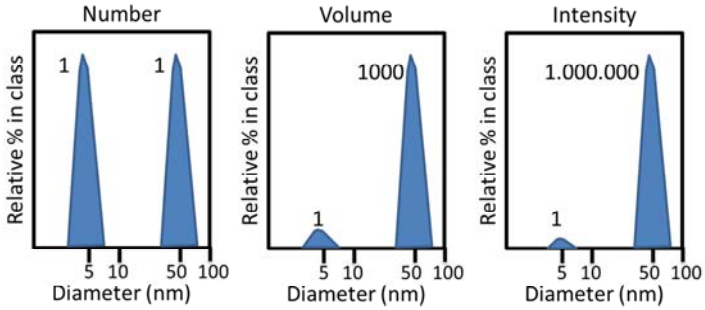

Figure 3.4. Number, volume and intensity distributions of a bimodal mixture of 5.0 and 50.0 nm lattices present in equal number.

When the sample is dispersed, the PdI value is not an accurate parameter to describe it. The % Pd (width peak*100/mean peak) is more suitable. The limits of this parameter are: lower than 28.0 %, monodisperse sample (narrow distribution), higher than this value, polydisperse (broad distribution) [45].

The membranes used in this thesis, were characterized by means of zeta potential (ζ) using the SurPASS electrokinetic analyzer UAnton (Anton Paar, Barcelona; Spain) (Figure 3.5).

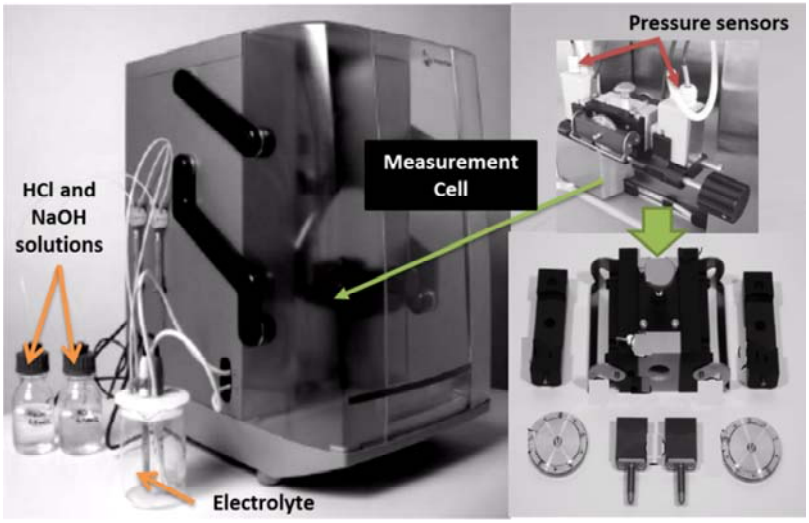

Figure 3.5. SurPASS electrokinetic analyzer UAnton (Anton Paar).

Before each measurement, the membranes were stabilized in the same buffers solutions that will be applied in the separation process. According to the equipment technical specifications, a solution of 10.0 mM NaCl (reagent grade, Sigma, Spain) was applied as electrolyte and the change of zeta potential with pH was determined. The pH in which the zeta potential is zero, determines the isoelectric point of the membrane. The electrokinetic analyzer uses the Helmholtz-Smoluchowski equation 3.6 for the zeta potential measurements, applying the streaming potential method.

A different methodology for the characterization of the membrane charge at the surface is the determination of the surface density (σ_P) of the membrane (C m^{-2}) whose relationship with ζ is given by equation 3.17:

$$\sigma_P = 4c_o F.\kappa^{-1}\sinh\left(\frac{F\zeta}{2RT}\right) \qquad (3.17)$$

where C_o is the salt concentration (mol m^{-3}), F is the Faraday's constant (C mol^{-1}), κ^{-1} is the thickness of the electrical double layer (m), ζ is the zeta potential (V), R is the gas constant (J $mol^{-1}K^{-1}$) and T is the absolute temperature (K).

Membrane adsorption capacity

Individual experiments containing 4.0 g L^{-1} BSA and 1.0 g L^{-1} LF as well as the mixture of both proteins were prepared at pH 5.0 (sodium acetate/acetic acid) –or pH 9.0 (borax/hydrochloric acid) buffers in order to develop the three adsorption scenarios. The membrane was introduced into test tubes containing the protein solutions (40.0 mL) and then the test tubes were gently shaken (20.0 rpm) at 25ºC. The protein concentration in the test tubes was measured with time (0-24 h.) using a UV-Vis spectrometer (Shimadzu UV-1800) via the absorbance at 280.0 nm. By comparing the initial and the later concentrations the adsorbed amount of protein can be determined.

3.3 PROTEIN CHARACTERIZATION: ZETA POTENTIAL AND SIZE

3.3.1 FOAM STABILITY

Foam formation is a non-desirable phenomenon in the experimental work of this thesis. In order to mitigate or, if possible, avoid foam formation during the measurement, characterization and separation steps, the study of the influence of the temperature of storage in the stability of foam was performed. In this study the time and temperature needed for foam to disappear have been established according to Zawala et al [7] by means of foam height measurements with time. Experiments were performed using mixtures of both proteins (4.0 g L^{-1} BSA + 1.0 g L^{-1} LF) in buffer solutions. The solution was vigorously agitated and the height of the foam was measured with time at room (20 ± 2ºC) and fridge (4ºC) temperature conditions. The end of the experiment was established when the foam completely disappeared. Figure 3.6 shows a capture of the naturally formed protein foam. The reduction of the height of the foam with time for the temperatures considered is shown in the Figure 3.7.

Figure 3.6. Foam formed by BSA-LF mixtures.

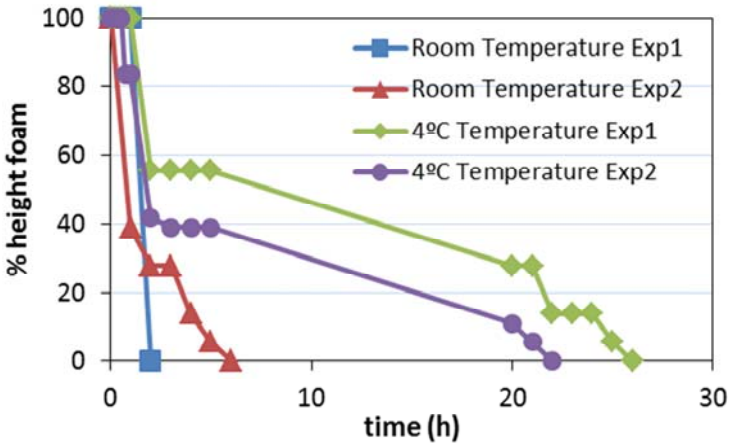

Figure 3.7. Influence of the temperature on the stability of the foam formed in BSA-LF mixtures.

As it is shown in Figure 3.7 the stability of foam is higher at lower temperatures. Under the conditions used in the study, 6 h. are needed to eliminate foam at room temperature while up to 26 h. are needed when 4ºC are studied. According to these results, the BSA-LF mixtures are kept at room temperature until foam is not seen by human eyes to avoid measurement errors.

3.3.2 PROTEIN ZETA POTENTIAL

Protein charge plays an important role in the performance of separation processes, being of special relevance when charged membranes are involved. In this work the zeta potential of BSA and LF solutions was measured under different operational conditions relevant to the separation process.

First the influence of the electrolyte type was measured with 0.01 M solutions of KCl, NaCl and $CaCl_2$ and 3 buffers: sodium acetate/acetic acid pH 5.0 (corresponding to BSA Ip), sodium phosphate/dipotassium phosphate pH 7.0 (Ip BSA < pH < Ip LF) and borax-hydrochloric acid buffer pH 9.0 (corresponding to LF Ip).

Secondly the influence of the concentration (0.01-0.1 M) was studied for KCl and buffer sodium phosphate/dipotassium phosphate, pH 7.0. Thirdly the influence of the protein concentration by diluting 1/10 and 1/100 the initial concentration (4.0 g L^{-1} BSA and 1.0 g L^{-1} LF) was studied. Finally the comparison with the electric points obtained by the charge regulation model was performed.

Influence of the electrolyte type

The influence of the electrolyte type, using 0.01 M solutions of KCl, NaCl and $CaCl_2$, on the zeta potential of 4.0 g L^{-1} of BSA and 1.0 g L^{-1} of LF solutions was determined. Figure 3.8 plots the change in the zeta potential for both proteins with pH; experimental data are plotted together with error bars obtained from replication of the measurements and show that the relative error is less than 13.0 % in all cases.

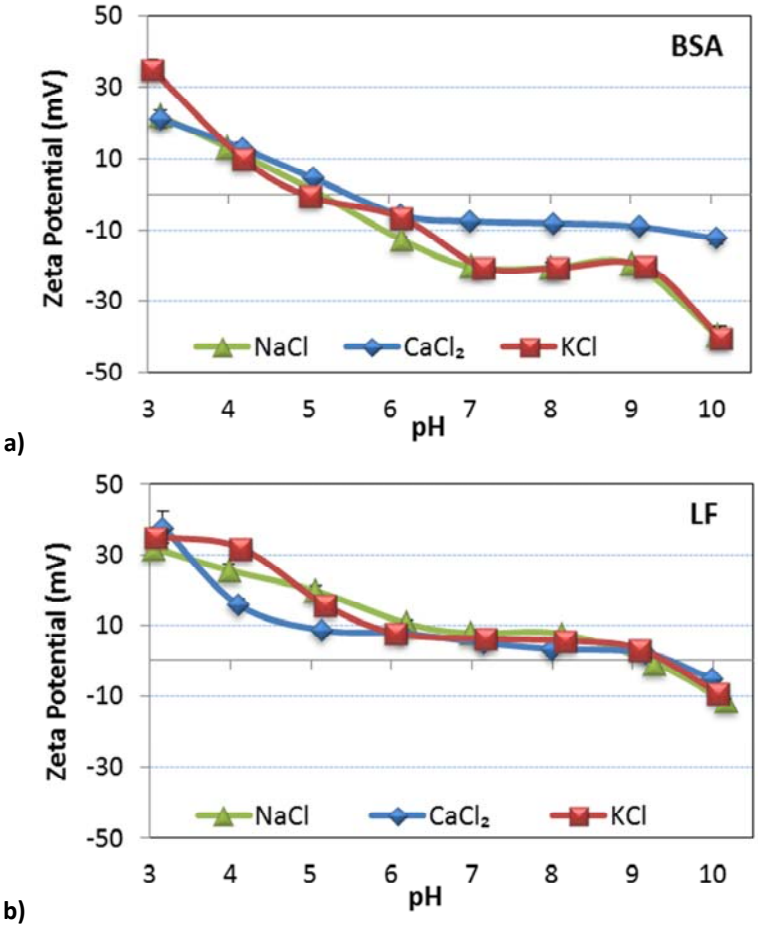

Figure 3.8. Change in zeta potential with pH for different electrolytes (0.01M): a) BSA protein and b) LF protein.

The Ip of both proteins falls inside the studied pH range. When the pH is lower than the Ip, the biomolecules present positive zeta potential values that decrease with increasing pH (Figure 3.8). This behavior can be theoretically described by the dependency of the zeta potential on the ionic strength that results by combining equations 3.4 and 3.5. Thus, it is expected that 1:2 type electrolytes, which exert a greater contribution to the ionic strength for the same concentration level than 1:1 type electrolytes, will lead to lower zeta potential values than the latter due to the compression of the electrical double layer thickness. The calculated values of this Debye layer (equation 3.5) are

96.17 nm for KCl and NaCl and 60.82 nm for $CaCl_2$. With regard to the influence of the electrolyte type, Figure 3.8a confirms that the difference in the zeta potential values of BSA when using different electrolytes (1:1 and 1:2) appeared to be significant at pHs above the isoelectric point, whereas in the case of LF this difference is found at pHs below the isoelectric point (Figure 3.8b).

Additionally, the values of zeta potential obtained with the buffer media are shown in Figure 3.9 where they are compared to those obtained with KCl solutions at the same pH.

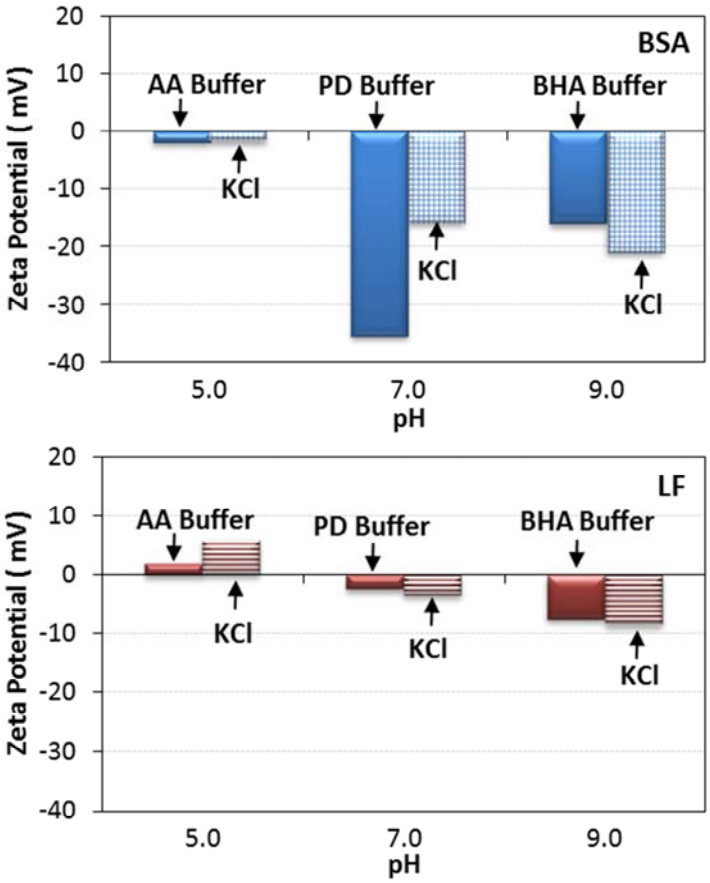

Figure 3.9. Electrophoretic mobility in media buffers and KCl solutions vs. pH: a) BSA protein, b) LF protein. AA buffer: sodium acetate/acetic acid, PD buffer: sodium phosphate/dipotassium phosphate and BHA buffer: borax/hydrochloric acid.

As it is depicted in Figure 3.9a, BSA zeta potential has negative values whatever the pH used. The highest zeta potential is obtained in sodium phosphate/dipotassium phosphate buffer at pH 7.0. This zeta potential has a value around -35.0 mV. Figure 3.9b shows that LF presents positive zeta potential at pH 5.0 while pH 7.0 and 9.0 are associated to negative zeta potential. Similar values (~ -8.0 mV) are found working with borax/hydrochloric acid buffer and KCl solutions at pH 9.0. This value in (in absolute) is the highest obtained.

Influence of the electrolyte concentration

Food proteins can be found in different media with different salt concentrations. The analysis of the influence of the electrolyte concentration in 4.0 g L^{-1} of BSA and 1.0 g L^{-1} of LF was carried out using KCl (the most commonly applied electrolytic solution in protein separation) in the concentration range of 0.01-0.1 M and the pH range of 3.0-10.0. Figure 3.10 shows the change in zeta potential for both proteins under the studied conditions with a measurement error lower than 15.0 %.

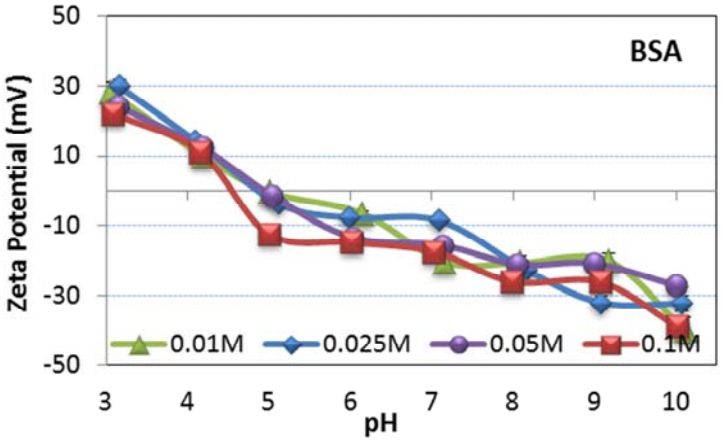

a)

Figure 3.10. Change in zeta potential with pH for different ionic strengths: a) BSA protein

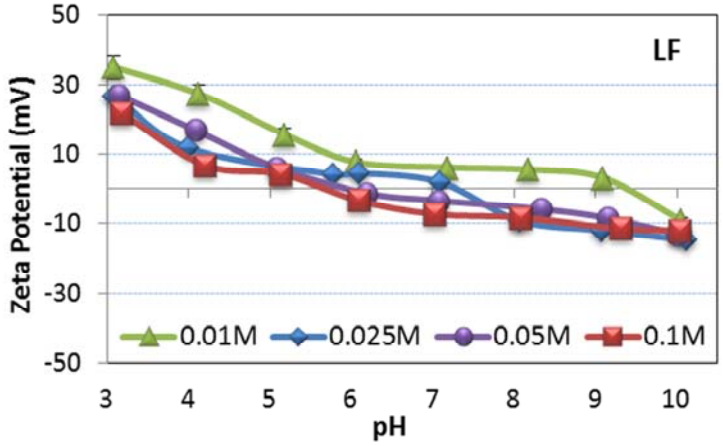

b)

Figure 3.10. Change in zeta potential with pH for different ionic strengths: b) LF protein.

As it is shown in Figure 3.10, both proteins show a similar behavior. The zeta potential values varied from 30.0 mV to -40.0 mV for BSA and from 35.0 mV to -15.0 mV for LF. The isoelectric point of BSA was the same for the 0.01-0.05 M KCl solutions (4.90-4.96) and was slightly lower value for the highest studied concentration of 0.1 M (4.65) (Figure 3.10a). Similar trends have been reported previously [46]. In the case of LF, the effect of the electrolyte concentration on the zeta potential was more significant, with Ip values ranging from 9.33 (0.01 M) to 5.66 (0.1 M) (Figure 3.10b). This is consistent with the large range of isoelectric points that have been reported so far for this protein; 8.0 – 9.0 for 0.01 M NaCl [47]; 7.2 for 0.025 M KCl [48]; 5.6 for 0.15 M NaCl [49]. It is well known that when the electrolyte concentration is increased, the surface charge is comprensated at a lower distance from the particle surface and thus, the surface potential drops faster and the diffuse layer is thinner. Consequently, the measured zeta potential should decrease with increasing electrolyte concentration [49]. This effect can be increased by the high PDI values obtained in the size determination study for the LF.

Influence of protein concentration

Any separation/purification process results in a change in the protein concentration of the involved solutions. Therefore, the influence of this variable on the zeta potential in the range of 0.04 – 4.0 g L^{-1} for BSA and 0.01 – 1.0 g L^{-1} for LF was analyzed. Figure 3.11 depicts the change in zeta potential for BSA and LF as a function of pH for different protein concentrations in 0.025 M KCl, which is the concentration more commonly applied in protein separation process as it gives a good conductivity without depletion in protein electrophoretic mobility.

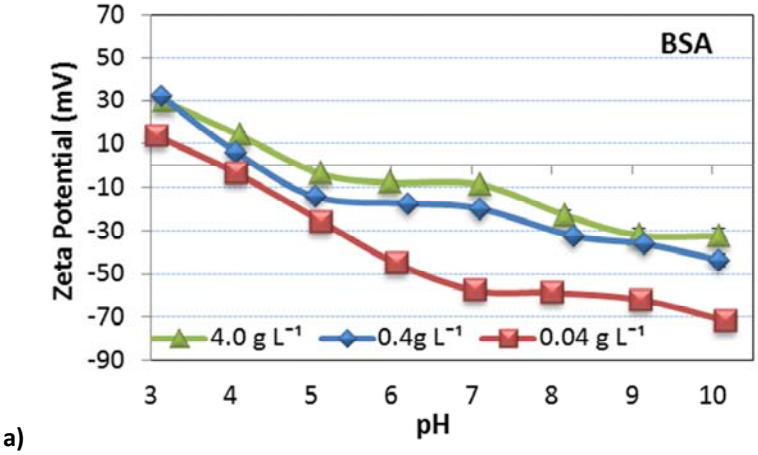

a)

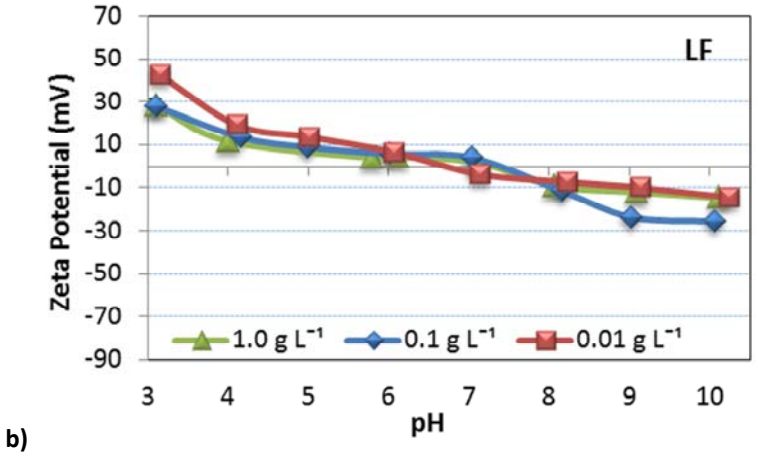

b)

Figure 3.11. Change in zeta potential with pH for different protein concentrations using 0.025 M KCl: a) BSA protein and b) LF protein.

As showed in Figure 3.11a, the decrease in protein concentration in the case of BSA was translated into an increase in the absolute value of the zeta potential and a decrease in the isoelectric point, which changed from 4.90 to 3.87 in the studied range of protein concentrations. This behavior is consistent with the decrease of electrophoretic mobility when increasing the concentration reported by Ho et al., 2000 [50]. However, in the case of LF, the decrease in the protein concentration (Figure 3.11b) did not lead to significant changes in the zeta potential behavior. This could be explained with the high PDI values obtained in the size determination study for the LF.

Figure 3.12 depicts the change in zeta potential for BSA-LF mixtures as a function of pH for different protein concentrations in 0.025 M KCl.

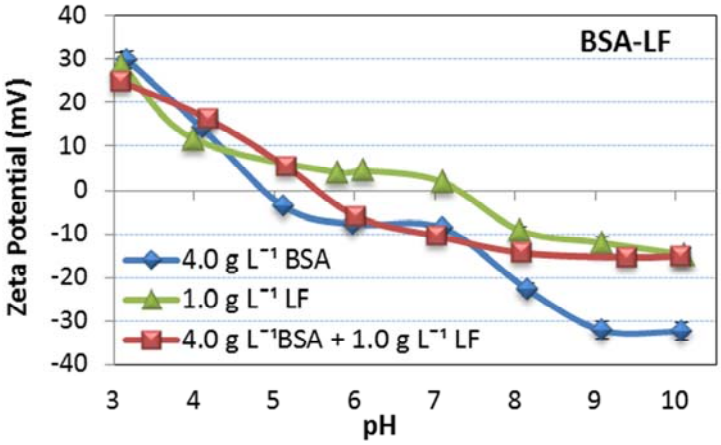

Figure 3.12. Change in zeta potential with pH for different protein concentrations using 0.025 M KCl and BSA-LF mixtures.

Figure 3.12 shows that the zeta potential of the protein mixture exhibited an intermediate behavior between both individual curves but, different from the expected result according to the concentration ratio of the proteins.

Summarizing, the influence of the electrolyte medium and concentration as well as the BSA and LF protein concentration have been experimentally determined, leading to values of the isoelectric

point (Ip) of BSA that lie in the range 3.82 - 5.52, whereas for LF, the measured values fall in the range 5.66 - 9.33. Thus, the obtained results highlight the influence of the characteristics of the solution medium on the protein properties. These results will be applied in Chapter 4 in order to determine the best operating conditions to carry out the separation process.

Isoelectric points: Experimental versus calculated values

With the aim to determine if the Charge Regulation Model (CRM) previously described is a useful tool to determine the isoelectric points without the need of experimentation. Applying the model equations 3.8 to 3.13, the Ip obtained were compared to those experimentally obtained by the zeta potential measurements. The results are indicated in Table 3.2.

Table 3.2. Experimental, calculated and literature values of Isoelectric Point for BSA and LF proteins.

BSA Protein		Isoelectric point (Ip)		
Medium	**Concentration (g L^{-1})**	**Measured**	**Calculated**	**Literature**
KCl 0.01 M	**4.0**	4.96	5.00	4.68[a]
NaCl 0.01 M		5.14	5.00	5.15[c]
$CaCl_2$ 0.01 M		5.52	4.93	4.69[a]
KCl 0.025 M		4.90	4.90	---
KCl 0.05 M		4.94	4.85	---
KCl 0.1 M		4.65	4.78	4.68[e]
KCl 0.025 M	**0.4**	4.36	4.90	4.68[a]
	0.04	3.87	4.90	5.10[g]
LF Protein		**Isoelectric point (Ip)**		
Medium	**Concentration (g L^{-1})**	**Measured**	**Calculated**	**Literature**
KCl 0.01 M	**1.0**	9.33	9.46	9.00[b]
NaCl 0.01 M		9.16	9.46	---
$CaCl_2$ 0.01 M		9.38	9.34	---
KCl 0.025 M		7.25	9.28	7.2[d]
KCl 0.05 M		5.99	9.14	---
KCl 0.1 M		5.66	8.87	5.6[f]
KCl 0.025 M	**0.1**	7.32	9.28	---
	0.01	6.74	9.28	---

[a]0.5 g L^{-1} BSA in 0.001 M KCl, NaCl, or $CaCl_2$ [51]; [b]0.1 g L^{-1} LF in 0.01 M KCl [46]; [c]1.0 g L^{-1} BSA in 0.01 M NaCl [33]; [d]0.2 g L^{-1} LF in 0.01 M NaCl [47]; [e]0.5 g L^{-1} BSA in 0.1 M KCl [52]; [f]0.4 g L^{-1} LF in 0.15 M NaCl [48]; [g]0.006 g L^{-1} BSA in NaCl [53].

As seen in Table 3.2 the mean measured isoelectric points obtained are 4.79 ± 0.50 for the BSA and 7.60 ± 1.51 for LF. The theoretical and experimentally determined isoelectric points of BSA are in agreement to previously reported values in the literature. However, for LF the experimental results at high electrolyte concentrations deviate considerably from the theoretical data (5.66 - 7.25 for the measured values in contrast to 8.87 - 9.28 for the calculated values). Although the literature provides few data of this protein, most of the values already reported are in agreement with those experimentally measured in this work. On the one hand, the CRM can be used to determine the isoelectric point of BSA in the range of concentration 0.4 - 4.0 g L^{-1} and salt concentration 0.01 - 0.1M KCl. Nevertheless, this calculation cannot be applied to the determination of the isoelectric point of LF.

3.3.3 BSA AND LF PROTEIN SIZE

Protein separation processes are strongly affected by protein size as it is one of the differential properties in which separation is based. This property is even more important when membranes technologies are applied, due to the narrow distribution of commercial membrane pores. Far from being constant, protein size is highly influenced by pH and protein concentration. In this study, BSA and LF size values have been determined at different pH (3.0 - 10.0) and protein concentrations (4.0 g L^{-1} for BSA and 1.0 g L^{-1} for LF and corresponding dilutions: 1/10, 1/100) in 0.025M KCl.

Influence of pH

The effective size of the protein molecules was measured by DLS at different pH values in the range 3.0 to 10.0 using 0.025 M KCl solution working with individual solutions containing 4.0 g L^{-1} BSA and 1.0 g L^{-1} LF, respectively. Using the CONTIN approximation [54], graphs of intensity distribution versus particle diameter were obtained for both proteins (Figure 3.13).

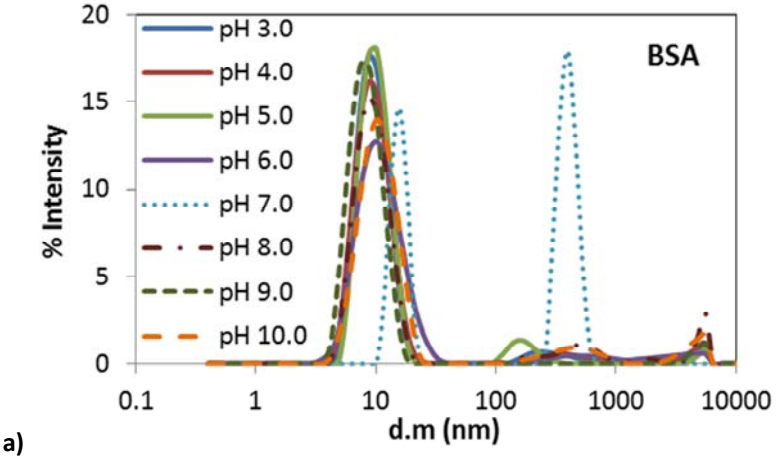

a)

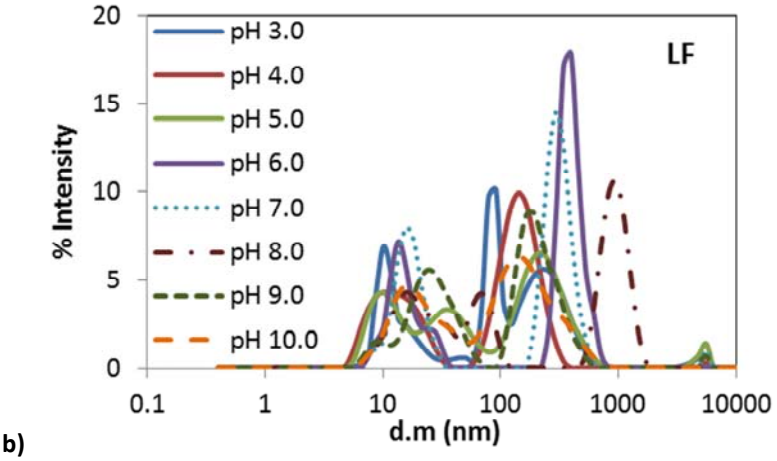

b)

Figure 3.13. Intensity-size distribution at different pH: a) 4.0 g L^{-1} BSA protein and b) 1.0 g L^{-1} LF protein.

BSA samples (Figure 3.13a) exhibited almost monomodal and stable curves (with the exception of pH 7.0); for this reason, the z-average size can be considered the hydrodynamic size. The broad peak shape may be caused by the presence of some aggregates, which will be confirmed by the polydispersity index (PdI) analysis. On the other hand, LF intensity distribution (Figure 3.13b) showed a polydisperse behavior. Thus, it is necessary to study the particle volume distribution for the correct analysis of the data and the proper determination of the

hydrodynamic size. The polydisperse intensity curves for LF suggest the presence of aggregates [54].

The z-average size of BSA versus pH is plotted in Figure 3.14a. Figure 3.14b presents the change in PdI with the pH for this protein. An experimental error of 5.0 % was achieved in both cases.

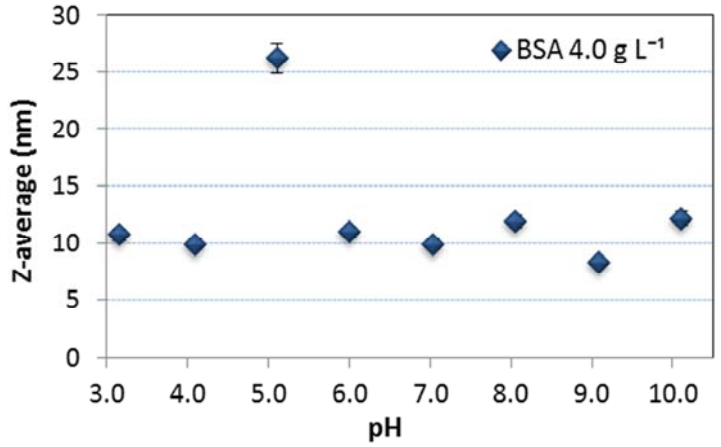

a)

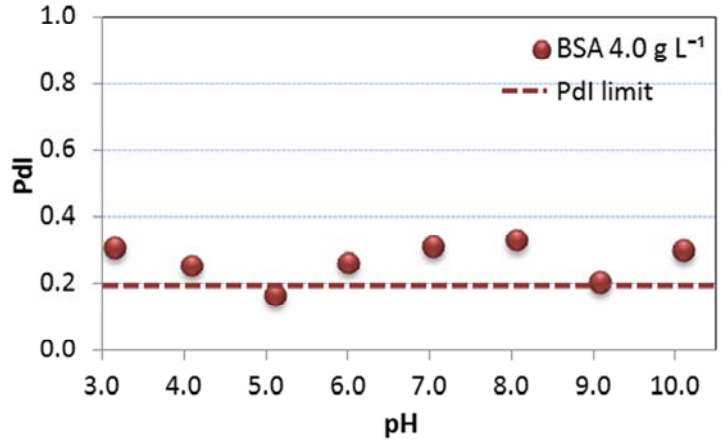

b)

Figure 3.14. Change in a) Z-average size and b) PdI for 4.0 g L^{-1} of BSA at 0.025 M KCl and different pH values.

Figure 3.14a shows no significant change in size with pH, except at the Ip value. This result is consistent with the behavior found in many protein solutions where aggregation under nondenaturing (no

temperature or pressure applied) conditions at pHs close to the isoelectric point [55]. Figure 3.14b presents the change in PdI with pH for this protein; most of the values lie above the recommended PdI value (0.2), suggesting the presence of oligomers and/or aggregates.

As both proteins do not fit the criteria for an Intensity analysis the conversion to volume distribution was performed. Figure 3.15 depicts the size of both proteins using the volume/mass distribution.

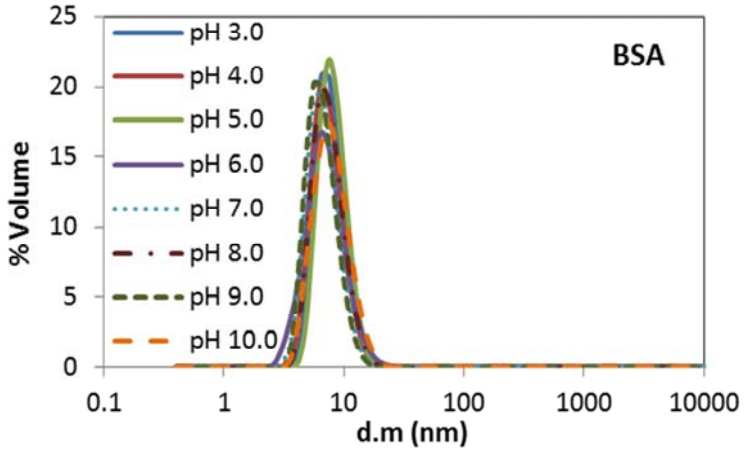

a)

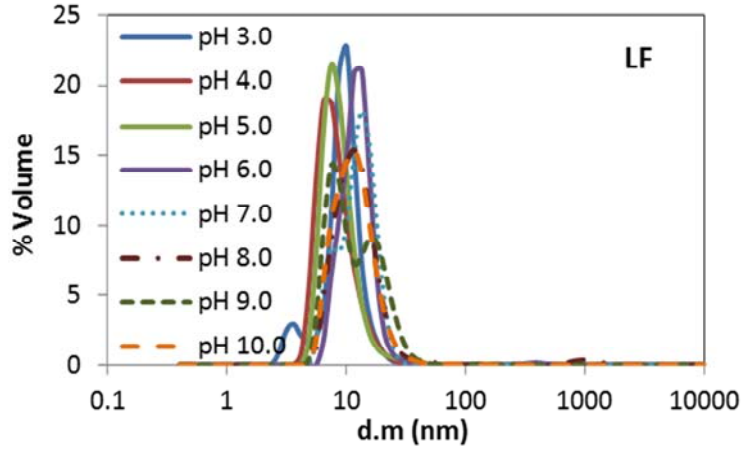

b)

Figure 3.15. Volume distribution: a) 4.0 g L^{-1} BSA protein and b) 1.0 g L^{-1} LF protein.

Figure 3.15a shows that there is no significant influence of pH on the hydrodynamic diameter of BSA, which has an average value of 7.54 nm. As showed in Figure 3.15b, LF tends to increase in size from pH 4.0 to pH 7.0 (8.53 - 12.28 nm) and slightly decrease in size from pH 8.0 to pH 9.0 (12.00 - 8.86 nm). At pH 3.0, this protein exhibits an intermediate size (10.17 nm). Nevertheless, there is not a large difference, as all the values fell in the range between 8.50 nm and 12.30 nm.

Additionally the experimental results of the hydrodynamic size of BSA and LF in volume distribution showed in Figure 3.15 are noted in Table 3.4 for BSA protein and Table 3.5 for LF protein.

Table 3.4. BSA experimental hydrodynamic sizes in volume distribution

BSA 4.0 g L^{-1} 0.025M KCl					
pH	**Peak**	**Size (nm)**	**% Mass**	**kDa estimated**	**% Pd**
3.0	1	7.79 ± 2.50	99.99	105.60	28.50
	2	146.50 ± 39.78	0.00	284000.00	25.17
	3	0.00	0.00	0.00	0.00
4.0	1	7.72± 2.54	99.99	105.60	31.77
	2	902.00± 109.50	0.00	565000.00	29.80
	3	0.00	0.00	0.00	0.00
5.0	1	8.42 ± 2.17	99.99	148.80	26.07
	2	86.01 ± 20.52	0.00	101000.00	17.40
	3	0.00	0.00	0.00	0.00
6.0	1	7.37 ± 3.27	99.99	105.60	39.53
	2	694.20 ± 302.80	0.00	1120000.00	50.63
	3	0.00	0.00	0.00	0.00
7.0	1	6.94 ± 2.68	99.99	105.60	31.40
	2	209.00 ± 96.12	0.00	1580000.00	30.63
	3	0.00	0.00	0.00	0.00
8.0	1	7.35 ± 2.61	99.99	105.60	29.93
	2	267.80 ± 130.30	0.00	565000.00	29.90
	3	0.00	0.00	0.00	0.00
9.0	1	6.74 ± 1.94	99.99	74.90	29.93
	2	2426.00 ± 541.50	0.00	385000000.00	14.37
	3	0.00	0.00	0.00	0.00
10.0	1	8.17 ± 2.77	99.99	148.80	33.10
	2	891.90 ± 222.90	0.00	1120000.00	32.00
	3	0.00	0.00	0.00	0.00

Table 3.5. LF experimental hydrodynamic sizes in volume distribution.

LF 1.0 g L^{-1} 0.025M KCl					
pH	**Peak**	**Size (nm)**	**% Mass**	**kDa estimated**	**% Pd**
3.0	1	10.17 ± 3.16	99.00	209.80	31.40
	2	50.75 ± 11.59	0.60	6500.00	26.60
	3	272.50 ± 104.90	0.40	284000.00	36.30
4.0	1	8.53 ± 3.59	99.80	148.80	41.70
	2	171.70 ± 62.53	0.20	110000.00	30.80
	3	0.00	0.00	0.00	0.00
5.0	1	9.21 ± 4.48	99.80	148.80	32.30
	2	43.82 ± 13.68	0.20	4610.00	42.40
	3	0.00	0.00	0.00	0.00
6.0	1	13.63 ± 1.62	99.30	295.80	14.53
	2	368.00 ± 42.97	0.60	565000.00	15.00
	3	0.00	0.00	0.00	0.00
7.0	1	14.33 ± 2.74	99.50	295.80	17.67
	2	288.80 ± 52.59	0.40	284000.00	19.37
	3	0.00	0.00	0.00	0.00
8.0	1	13.74 ± 3.72	96.70	295.80	21.63
	2	60.79 ± 15.16	1.30	9170.00	22.23
	3	1107.00 ± 236.40	2.00	6250000.00	20.57
9.0	1	8.72 ± 2.89	92.50	105.60	25.07
	2	28.21 ± 9.00	6.97	1650.00	28.47
	3	238.10 ± 109.30	0.50	202000.00	15.60
10.0	1	12.46 ± 3.44	99.53	295.80	23.80
	2	255.87 ± 42.02	0.47	51000.00	32.50
	3	0.00	0.00	0.00	0.00

The accurate particle size value is the average value of the volume distribution with size due to the contribution of at least 90.00 % of each peak to the total volume of the sample [54], being for the BSA of 99.99 % (Table 3.4). The estimated molecular weights considering globular shape lie in the range 74.90 - 148.80 kDa. Although these values are significantly higher than the true monomer mass, in this case the discrepancy is not assigned to the aggregation phenomenon, but to the

fact that the monomer does not have a compact globular shape [56]. Moreover, the hydrodynamic diameter and molecular weight values lead to the conclusion that BSA samples show no aggregation while a percentage in mass from 0.2 - 4.0 % of aggregates is found in the LF samples (Table 3.5). The estimated molecular weights considering globular shape lie in the range 105.60 - 295.80 kDa. Thus, it can be concluded that LF suspensions contained a minor fraction of protein dimers.

Influence of protein concentration

The change in hydrodynamic diameter of the proteins with pH was evaluated in the following concentration ranges: 0.04 - 4.0 g L^{-1} for BSA and 0.01 - 1.0 g L^{-1} for LF in 0.025M KCl. The results obtained are shown in Figure 3.16 with an experimental error lower than 11.0 %.

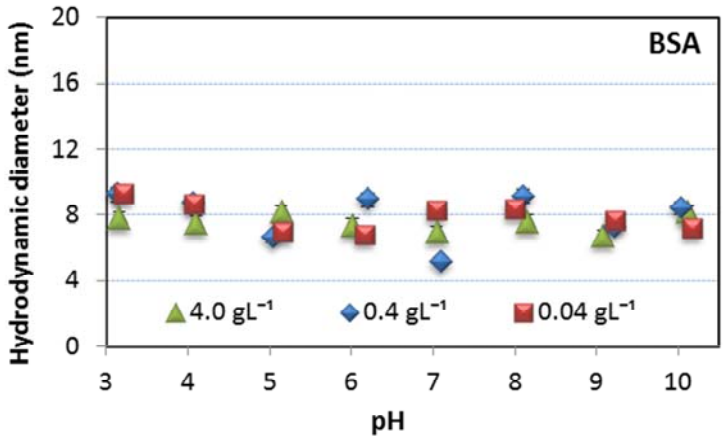

a)

Figure 3.16. Change in protein molecular size with pH for different protein concentrations: a) BSA protein.

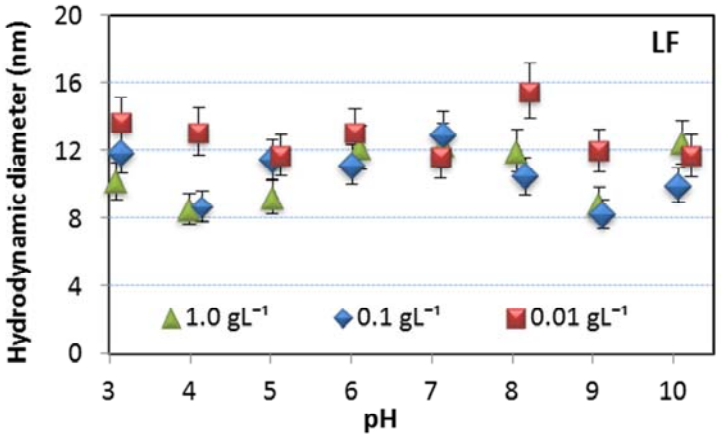

b)

Figure 3.16. Change in protein molecular size with pH for different protein concentrations: b) LF protein.

Figure 3.16a shows that there was no influence of either the protein concentration or the pH on the protein size of BSA (almost all values fell between 7.00 and 9.20 nm, with the average hydrodynamic size previously determined of 7.54 nm (4.0 g L^{-1} BSA)). Although increases in the protein concentration commonly result in an increase in protein aggregation [52,57], some authors consider the opposite behavior due to the repulsion-attraction forces. The increase in concentration reduces the attraction forces, resulting in decreased protein-protein interactions and therefore the formation of aggregates [58,59].

The hydrodynamic size of LF, Figure 3.16b, showed a similar behavior with pH for 0.1 g L^{-1} and 1.0 g L^{-1} LF solutions (with the exception of pH 10.0), with values that fell between 8.00 nm and 12.00 nm, but as the protein concentration decreased (0.01 g L^{-1}), the hydrodynamic diameter increased (values between 11.50 nm and 15.00 nm). It can be due to the fact that a percentage in mass from 0.2 - 4.0 % of aggregates is found in the LF solutions.

Finally, the change in hydrodynamic diameter of the proteins with pH was measured for 4.0 g L^{-1} for BSA, 1.0 g L^{-1} of LF and their mixture in 0.025 M KCl. The results obtained are shown in Figure 3.17 with an experimental error lower than 11.0 %.

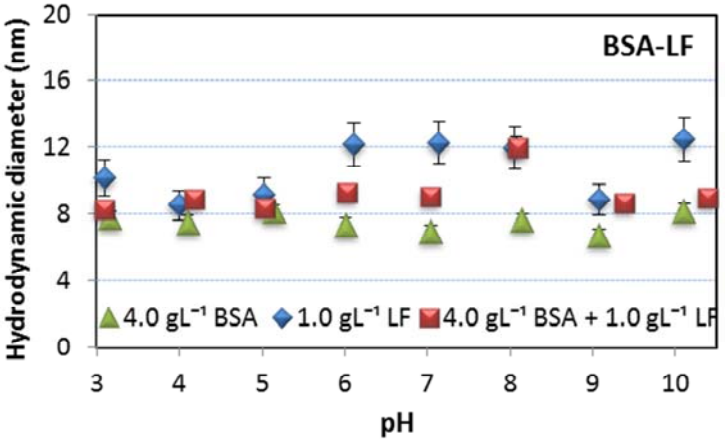

Figure 3.17. Change in protein molecular size with pH for protein mixtures and individual proteins at 0.025 M KCl.

The hydrodynamic size changes with pH for the both individual proteins and their mixture are depicted in Figure 3.17. BSA is present in higher concentration than the LF in the mixture, so the expected change would be expected to approach to BSA hydrodynamic size. Nevertheless, the experimental data showed an intermediate value, with the exception of the values corresponding to both isoelectric points, for which the mixture exhibited the same hydrodynamic diameter as the individual proteins [59].

Hydrodynamic sizes: Experimental versus calculated values

The calculated Stokes (or hydrodynamic) diameters determined by equation 3.16 were compared to the experimentally determined size of 4.0 g L^{-1} of BSA and 1.0 g L^{-1} of LF in 0.025 M KCl (Figure 3.18).

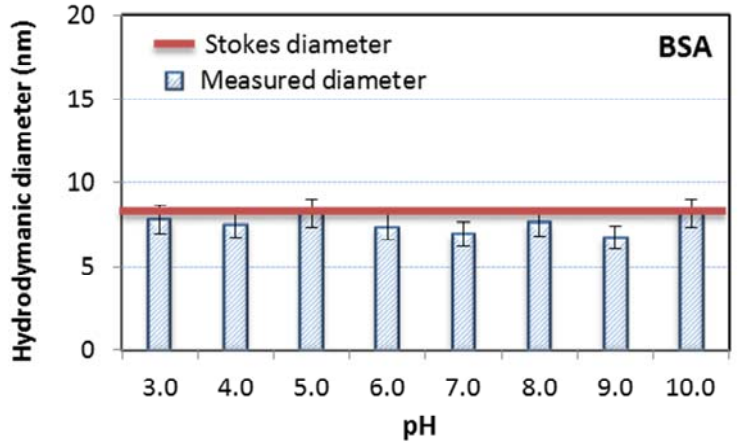

a)

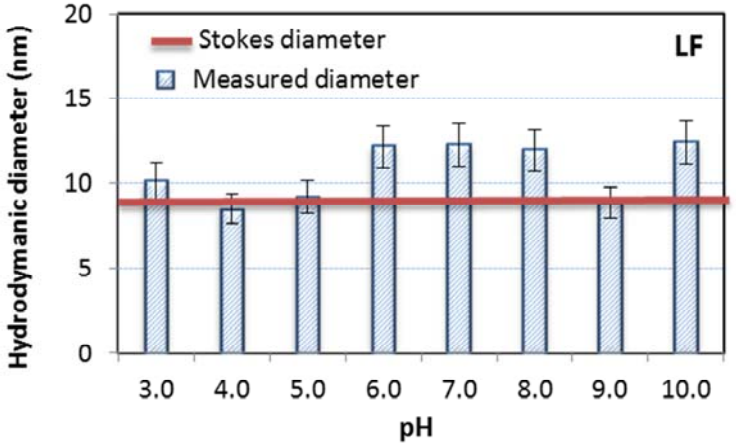

b)

Figure 3.18. Calculated and measured protein molecular size with pH at 0.025 M KCl solutions: a) BSA protein and b) LF protein.

Figure 3.18a shows the similarity between the calculated and experimental diameters. All the results are close to the Stokes diameter (6.92 nm), taking into account the experimental error. This behavior agrees with the fact that the % PdI value is close to the standard value for aggregation (28.0 % PdI) and the measured molecular weight is slightly higher than a single BSA molecule as the technique considered spherical shape molecules (Table 3.4). LF shows measured diameters higher than stokes diameters, Figure 3.18b, due to the formation of aggregates as showed in Table 3.5.

3.4 MEMBRANE CHARACTERIZATION: ZETA POTENTIAL AND MEMBRANE ADSORPTION CAPACITY

The zeta potential of the membranes used in the viability study of the separation processes was measured under different operational conditions. Five membranes were tested, two Polysulfone membranes and three Composited Regenerated Cellulosic membranes (CRC), unmodified charged positively (membrane+) and charged negatively (membrane-). Additionally, the protein adsorption in the membranes was evaluated by means of the model developed by Jones and O'Melia, 2000 [60].

3.4.1 MEMBRANE ZETA POTENTIAL

The zeta potential of the two different cut-off Polysulfone membranes (0.2 µm and 100.0 kDa) used in the separation studies (Chapter 4), was studied in the pH range from 2.0 to 10.0, employing 0.01M NaCl as electrolyte. The results are shown in Figure 3.19 with an experimental error lower than 12.0 %.

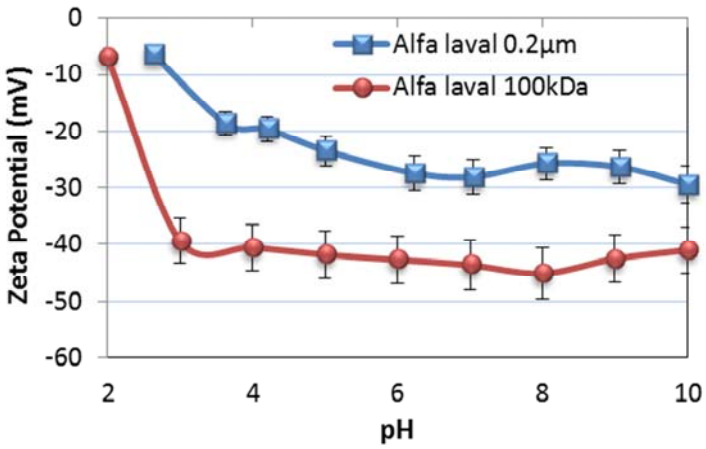

Figure 3.19. Evolution of zeta potential vs. pH for Polysulfone membranes.

The results showed in Figure 3.19 are in good agreement with the zeta potential values (negative) expected due to its sulfonated composition. No isoelectric point is found for the range of pH 2.0 to 10.0. The measurement zeta potential are also in good agreement with the literature reported values that range from -55.0 mV to 5.0 mV [61–65]. Despite the same polymeric composition of both membranes, the difference in cut-off leads to different zeta potential curves as it is shown in Figure 3.19. In the range of pH studied the charge of the 100.0 kDa membrane is always twice negative than the 0.2 µm one.

The zeta potential of the Composited Regenerated Cellulosic membrane (CRC), unmodified, charged positively (membrane+) and charged negatively (membrane-) was studied in the range of pH from 2.0 to 10.0, employing 0.01 M NaCl as electrolyte (Figure 3.20). The values of zeta potential were obtained with a measurement error lower than 7.0 %.

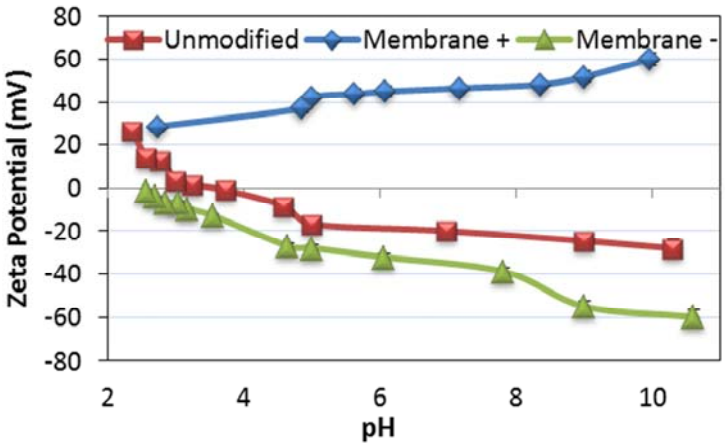

Figure 3.20. Evolution of zeta potential vs. pH for Composited Regenerated Cellulosic membrane membranes.

Figure 3.20 shows the different behavior of the positive and negative membrane charged compared to the unmodified membrane. The unmodified membrane zeta potential ranges from 26.0 to -28.0 mV showing an isoelectric point around pH 3.5. These values are in good

agreement (same order of magnitude) with other measurements reported previously for cellulosic membranes, such as the values of zeta potential of -7.8 mV reported by Babu and Gaikar [66] or zeta potential of -10.0 mV for unmodified membranes at pH 7.0 given by Thekkedath et al [67]. The zeta potential of the positive membrane changes from 30 to 60.0 mV in the range of pH studied, while the zeta potential of the negative membrane ranges from -2.0 to -60.0 mV in the same range of pH. None of them showed isoelectric point. Finally, the effective surface density of the membrane was calculated by means of equation 3.17 leading to the following values, -0.0005 C m^{-2} for the unmodified membrane, -0.0023 C m^{-2} for the negative and 0.0364 C m^{-2} for the positive membrane respectively, in good agreement with data previously reported by Rao and Zydney, [29].

3.4.2 MEMBRANE ADSORPTION CAPACITY

The total amount of protein adsorbed with time for three CRC membranes in different adsorption scenarios (4.0 g L^{-1} BSA, 1.0 g L^{-1} LF and BSA-LF mixture of 4.0 g L^{-1} BSA and 1.0 g L^{-1} LF, at pH 5.0 and pH 9.0) was determined following the method described in section 3.2.2 with the objective of determining the membrane adsorption capacity. These results are shown in Figures 3.21 and 3.22.

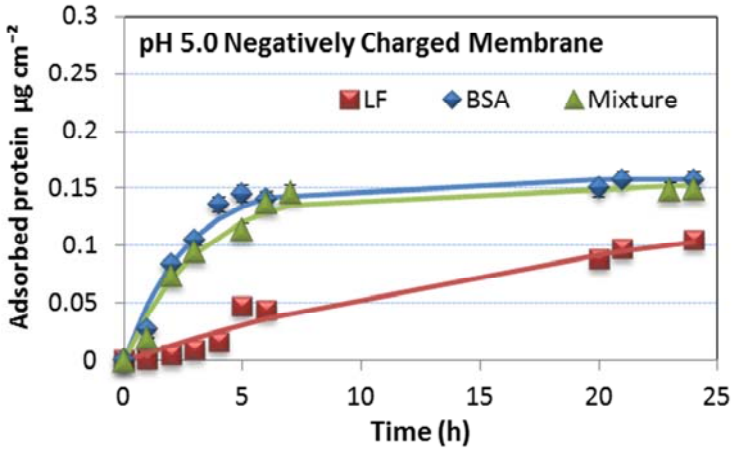

a)

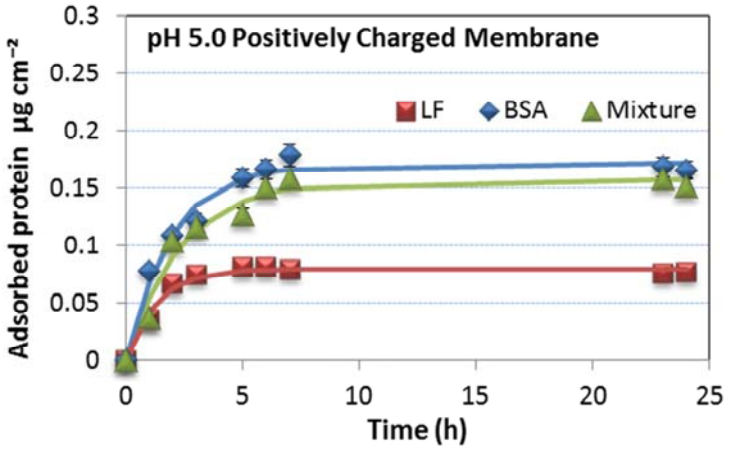

b)

Figure 3.21. Protein adsorbed (4.0 g L^{-1} BSA, 1.0 g L^{-1} LF and their mixture) with time at pH 5.0 a) negatively charged membrane b) positively charged membrane.

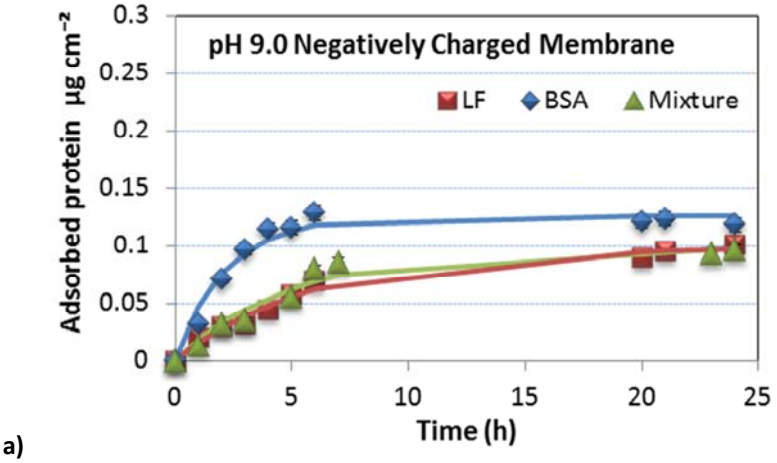

a)

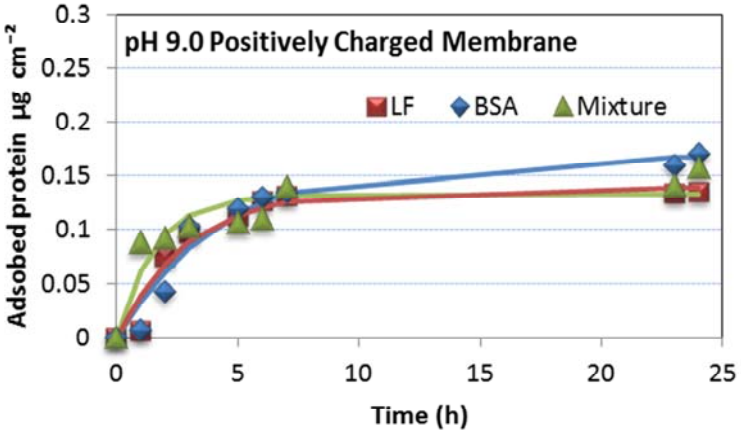

b)

Figure 3.22. Protein adsorbed (4.0 g L^{-1} BSA, 1.0 g L^{-1} LF and their mixture) with time at pH 9.0 a) negatively charged membrane b) positively charged membrane.

In all the cases the amount of BSA adsorbed is greater than LF protein, being this different lower at pH 9.0 and working with positively charged membrane (Figure 3.22b). The total amount adsorbed of BSA was around 0.2 10^{-6} g cm^{-2}, these values are in good agreement with values reported 0.05 to 0.8 10^{-6} g cm^{-2} in the literature [60,68,69]. The total amount adsorbed of LF was in the interval 0.1 10^{-6} to 0.14 10^{-6} g cm^{-2} [70]. No data has been reported till know regarding the LF or mixture adsorption onto ultrafiltration membranes in literature.

The static adsorption between proteins and membranes has been described as a two-steps mechanism in the literature [60,71–77]. The first step is due to the molecular diffusion of proteins from the solution to the membrane surface and it is driven by its concentration gradient. The second step is the transfer of molecules from this nearby position to the adsorbed state. The adsorption process is controlled by diffusion if the first step is slower than the second one, whereas in the opposite case the adsorption would be the rate controlling step [74]. When there is a kinetic control of the adsorption process the rate is determined by the model developed by Jones and O'Melia, 2000 [60]:

$$\Gamma(t)=\Gamma_e(1-e^{-k_0 t}) \qquad (3.18)$$

where Γ_e (μg cm^{-2}), k_0 (1 s^{-1}) are respectively the equilibrium amount adsorbed per membrane surface area and the overall reaction rate constant. Using the nonlinear least-square fit and values showed in Figures 3.21 and 3.22, the values Γ_e y k_0 can be obtained (Table 3.6).

Table 3.6. Parameters obtained in the fitting of the experimental adsorption values to equation 3.18.

			Negatively charged membrane			Positively charged membrane		
		Protein zeta potential (mV)	T_e (μg cm^{-2})	k_0 (s^{-1})	r^2	T_e (μg cm^{-2})	k_0 (s^{-1})	r^2
pH 5.0	BSA	~+1.0	0.16	0.38	0.99	0.17	0.51	1.00
	LF	~+0.5	0.16	0.04	0.98	0.08	0.77	1.00
	Mixture	--	0.15	0.31	0.99	0.16	0.43	1.00
pH 9.0	BSA	~ -16.0	0.13	0.46	1.00	0.18	0.15	0.99
	LF	~ -9.0	0.10	0.17	1.00	0.15	1.33	1.00
	Mixture	--	0.10	0.21	0.99	0.20	2.48	1.00

Although the equilibrium amounts adsorbed are in a narrow range in all the considered conditions, data in Table 3.6 indicate that the equilibrium adsorption is enhanced when the electrostatic repulsive interactions between protein molecules and the membrane is smaller.

Summary

In this Chapter, BSA and LF proteins were characterized by means of foam stability, zeta potential and size, aggregation. Polysulfone and CRC membranes were characterized by means of zeta potential and adsorption capacity.

Protein zeta potential was measured by ELS. The influence of the concentration (0.01 - 0.1 M), electrolyte and buffer type (KCl, NaCl and $CaCl_2$ and 3 buffers: sodium acetate/acetic acid pH 5.0, sodium phosphate/dipotassium phosphate pH 7.0, and borax-hydrocloridic acid buffer pH 9.0) and the protein concentration (0.04-4.0 g L^{-1} BSA and 0.01-1.0 g L^{-1} LF) were evaluated.

BSA zeta potential lay in the range 35.0 mV to -70.0 mV and the isoelectric points (Ip) were in the range 3.82 - 5.52, working with electrolytic solutions. LF zeta potential lay in the range 45.0 mV to -30.0 mV and the isoelectric points (Ip) were in the range 5.66 - 9.33, working with electrolytic solutions.

The difference in the zeta potential values of BSA when using different electrolytes (1:1 and 1:2) appeared to be significant at pHs above the isoelectric point, whereas in the case of LF this difference is found at pHs below the isoelectric point.

Working with buffer solutions, in the case of the BSA protein, the highest zeta potential (absolute value), -35.0 mV, was obtaining in sodium phosphate/dipotassium phosphate buffer working at pH 7.0. For LF protein, the highest zeta potential (absolute value), -8.0 mV, was found working with borax/hydrochloric acid buffer and KCl solutions at pH 9.0.

The measured zeta potential decreased with increasing electrolyte concentration for both proteins.

The decrease in protein concentration in the case of BSA was translated into an increase in the absolute value of the zeta potential and a decrease in the isoelectric point, which changed from 4.90 to 3.87 in the studied range of protein concentrations. However, in the case of

LF, the decrease in the protein concentration did not lead to significant changes in the zeta potential behavior. The zeta potential of the protein mixture exhibited an intermediate behavior between both individual curves but, different from the expected result according to the concentration ratio of the proteins.

The Charged Regulation Model can be used to predict BSA Ip in the conditions studies in this Thesis. On the other hand, Ip of LF is not adequately predicted using studied this tool.

BSA and LF size values were determined by DLS at different pH (3.0-10.0) and protein concentrations (4.0 g L^{-1} for BSA and 1.0 g L^{-1} for LF and corresponding dilutions: 1/10, 1/100) in 0.025M KCl.

Measured hydrodynamic diameter of BSA presented an average value of 7.54 nm. Measured hydrodynamic diameter of LF tends to increase in size from pH 4.0 to pH 7.0 (8.53-12.28 nm) and slightly decrease in size from pH 8.0 to pH 9.0 (12.00 - 8.86 nm). At pH 3.0, this protein exhibits an intermediate size (10.17 nm). BSA samples no aggregation (99.0 %) while a percentage in mass from 0.2-4.0 % of aggregates is found in the LF samples. The estimated molecular weights of BSA considering globular shape lay in the range 74.90- 148.80 kDa. The estimated molecular weights of LF considering globular shape lay in the range 105.60- 295.80 kDa.

No influence of either the protein concentration or the pH on the protein size of BSA was found. The hydrodynamic size of LF showed a similar behavior, but as the protein concentration decreased the hydrodynamic diameter increased (11.50 nm to 15.00 nm).

The hydrodynamic size of both individual proteins in the protein mixtures showed an intermediate value with the exception of the values corresponding to both isoelectric points whatever the pH used.

BSA showed measured diameters equal to calculated stokes diameters (6.92 nm), due to the no formation of aggregates. LF showed measured diameters higher than calculated stokes diameters, due to the formation of aggregates.

The zeta potential of the two polysulfone membranes and three Composited Regenerated Cellulosic membrane (CRC) (unmodified charged positively (membrane+) and charged negatively (membrane-)) was measured in the pH range from 2.0 to 10.0, employing 0.01 M NaCl as electrolyte.

The measured zeta potential values of polysulfone membranes are also in good agreement with the literature reported values that range from -55.0 mV to 5.0 mV. In the range of pH studied the charge of the 100.0 kDa membrane is always twice negative than the 0.2 µm one. The unmodified membrane zeta potential ranges from 26.0 to -28.0 mV showing an isoelectric point around pH 3.5. The zeta potential of the positive membrane changes from 30.0 to 60.0 mV in the range of pH studied, while the zeta potential of the negative membrane ranges from -2.0 to -60.0 mV in the same range of pH. None of them shown isoelectric point.

The total amount of protein adsorbed with time for three CRC membranes in different adsorption scenarios (4.0 g L^{-1} BSA, 1.0 g L^{-1} LF and BSA-LF mixture of 4.0 g L^{-1} BSA and 1.0 g L^{-1} LF, at pH 5.0 and pH 9.0) was determined.

The total amount adsorbed of BSA was close to 0.2 10^{-6} g cm^{-2}. The total amount adsorbed of LF was in the interval 0.1 10^{-6} to 0.14 10^{-6} g cm^{-2}. In all the cases the amount of BSA adsorbed is greater than LF protein, being this difference lower at pH 9.0 and working with positively charged membrane.

The static adsorption is fitted to the Jones and O'Melia Model kinetic: $\Gamma(t)=\Gamma_e\,(1-e^{-k_0 t})$. Using the nonlinear least-square fit and the experimental values, the parameters Γ_e y k_0 was obtained with a correlation coefficient higher than 0.99 in all cases.

3.5 REFERENCES

The references in this section were managed by the Mendeley reference software applying the Separation Science and Technology style.

[1] T.R. Gaborski, J.L. Snyder, C.C. Striemer, D.Z. Fang, M. Hoffman, P.M. Fauchet, et al., High-performance separation of nanoparticles with ultrathin porous nanocrystalline silicon membranes, ACS Nano. 4 (2010) 6973–81.
[2] S. Rouimi, C. Schorsch, C. Valentini, S. Vaslin, Foam stability and interfacial properties of milk protein?surfactant systems, Food Hydrocoll. 19 (2005) 467–478.
[3] J. Noel, A. Prokop, R.D. Tanner, Foam fractionation of a dilute solution of bovine lactoferrin, Appl. Biochem. Biotechnol. 98-100 (2002) 395–402.
[4] J. Clarkson, Z. Cui, R. Darton, Protein denaturation in foam., J. Colloid Interface Sci. 215 (1999) 333–338.
[5] F. Vardar-Sukan, Foaming: consequences, prevention and destruction, Biotechnol. Adv. 16 (1998) 913–948.
[6] A. Berthold, H. Schubert, N. Brandes, L. Kroh, R. Miller, Behaviour of BSA and of BSA-derivatives at the air/water interface, Colloids Surfaces A Physicochem. Eng. Asp. 301 (2007) 16–22.
[7] J. Zawala, R. Todorov, A. Olszewska, D. Exerowa, K. Malysa, Influence of pH of the BSA solutions on velocity of the rising bubbles and stability of the thin liquid films and foams, Adsorption. 16 (2010) 423–435.
[8] A.L. Zydney, Protein separations using membrane filtration: new opportunities for whey fractionation, Int. Dairy J. 8 (1998) 243–250.
[9] S. Aksay, G. Mazza, Optimization of protein recovery by foam separation using response surface methodology, J. Food Eng. 79 (2007) 598–606.
[10] M. Arulmozhi, C. Sudha, K.M. Meera, S. Begum, N. Anantharaman, Foam separation of proteins, Int. J. Chem. Sci. 8 (2010) 68–76.
[11] S. Damodaran, Food proteins and their applications, 1st Ed, Taylor & Francis, New York, USA, 1997.
[12] J. Noel, A. Prokop, R.D. Tanner, Foam fractionation of a dilute solution of bovine lactoferrin, Appl. Biochem. Biotechnol. 98-100 (2002) 395–402.
[13] P. Zhou, X. Liu, T.P. Labuza, Moisture-induced aggregation of whey proteins in a protein/buffer model system, J. Agric. Food Chem. 56 (2008) 2048–54.
[14] H.A. Patel., Studies on heat-and pressure-induced interactions of milk proteins, Thesis work. Massey University. New Zealand, 2007.
[15] E. Ibanoglu, Effect of hydrocolloids on the thermal denaturation of proteins, Food Chem. 90 (2005) 621–626.
[16] T. Arakawa, Y. Kita, Stabilizing effects of caprylate and acetyltryptophanate on heat-induced aggregation of bovine serum albumin, Biochim. Biophys. Acta. 1479 (2000) 32–36.

[17] L. Sánchez, J.M. Peiró, R. Oria, H. Castillo, J.H. Brock, M. Calvo, Kinetic parameters for the heat denaturation of bovine lactoferrin in milk, and its effect on interaction with monocytes., Adv. Exp. Med. Biol. 357 (1994) 253–7.
[18] V. V Mozhaev, K. Heremans, J. Frank, P. Masson, C. Balny, High pressure effects on protein structure and function, Proteins. 24 (1996) 81–91.
[19] N. V Di Russo, D.A. Estrin, M.A. Martí, A.E. Roitberg, pH-Dependent conformational changes in proteins and their effect on experimental pKas: the case of Nitrophorin 4, PLoS Comput. Biol. 8 (2012) e1002761.
[20] F. Ferreira Machado, J.S.R. Coimbra, E.E. Garcia Rojas, L.A. Minim, F.C. Oliveira, R. de C.S. Sousa, Solubility and density of egg white proteins: Effect of pH and saline concentration, Food Sci. Technol. 40 (2007) 1304–1307.
[21] M. Dissanayake, L. Ramchandran, O.N. Donkor, T. Vasiljevic, Denaturation of whey proteins as a function of heat, pH and protein concentration, Int. Dairy J. 31 (2013) 93–99.
[22] D. Fairhurst, An overview of the zeta potential, Am. Pharm. Rev. February 0 (2013).
[23] M. Kaszuba, J. Corbett, F.M. Watson, A. Jones, High-concentration zeta potential measurements using light-scattering techniques, Philos. Trans. 368 (2010) 4439–51.
[24] A. Sze, D. Erickson, L. Ren, D. Li, Zeta-potential measurement using the Smoluchowski equation and the slope of the current-time relationship in electroosmotic flow, J. Colloid Interface Sci. 261 (2003) 402–10.
[25] R.J. Hunter, Zeta potential in colloid science: principles and applications, 2nd Ed, Academic Press, London, UK, 1981.
[26] R.J. Hunter, Foundations of colloid science, 2nd Ed, Oxford University Press Inc., New York, USA, 2001.
[27] A. V Delgado, F. González-Caballero, R.J. Hunter, L.K. Koopal, J. Lyklema, Measurement and interpretation of electrokinetic phenomena, J. Colloid Interface Sci. 309 (2007) 194–224.
[28] M. Elimelech and Amy E. Childress, Zeta potential of reverse osmosis membranes: implicstions for membrane performance, 1996.
[29] S. Rao, A.L. Zydney, High resolution protein separations using affinity ultrafiltration with small charged ligands, J. Memb. Sci. 280 (2006) 781–789.
[30] I. Gitlin, J.D. Carbeck, G.M. Whitesides, Why are proteins charged? Networks of charge-charge interactions in proteins measured by charge ladders and capillary electrophoresis, Angew. Chemie Int. Ed. 45 (2006) 3022–60.
[31] C. Tanford, S.A. Swanson, W.S. Shore, Hydrogen ion equilibria of bovine serum albumin, J. Am. Chem. Soc. 77 (1955) 6414–6421.
[32] G. Scatchard, Y.V. Wu, A.L. Shen, Physical chemistry of protein solutions. X. The binding of small anions by serum albumin, J. Am. Chem. Soc. 81 (1959) 6104–6109.
[33] A. Salis, M. Boström, L. Medda, F. Cugia, B. Barse, D.F. Parsons, et al., Measurements and theoretical interpretation of points of zero charge/potential of BSA protein, Langmuir. 27 (2011) 11597–604.

[34] W.R. Bowen, P.M. Williams, The osmotic pressure of electrostatically stabilized colloidal dispersions, J. Colloid Interface Sci. 184 (1996) 241–250.
[35] V.M. Starov, Nanoscience: colloidal and interfacial aspects, 1st Ed, CRC Press, Boca Raton, Florida, USA, 2011.
[36] A.A.R. Teixeira, M. Lund, F.L.B. da Silva, Fast proton titration scheme for multiscale modeling of protein solutions, J. Chem. Theory Comput. 6 (2010) 3259–3266.
[37] G. Unterhaslberger, C. Schmitt, S. Shojaei-Rami, C. Sanchez, Beta-lactoglobulin aggregates from heating with charged cosolutes: formation, characterization and foaming, in: E. Dickinson, M.E. Leser (Eds.), Food Colloids Self-Assembly Mater. Sci., 1st Ed, Royal Society of Chemistry, Cambridge, UK, 2007: p. 515.
[38] C.A. Smith, Estimation of sedimentation coefficients and frictional ratios of globular proteins, Biochem. Educ. 16 (1988) 104–106.
[39] R.M. Parry, E.M. Brown, Protein-metal interactions. lactoferrin conformation and metal binding properties, Adv. Exp. Med. Biol. 48 (1974) 141–160.
[40] B.J. Compton, Electrophoretic mobility modeling of proteins in free zone capillary electrophoresis and its application to monoclonal antibody microheterogeneity analysis, J. Chromatogr. A. 559 (1991) 357–366.
[41] J. Ku, P. Stroeve, Protein diffusion in charged nanotubes : “On - Off ” behavior of molecular transport, Langmuir. 20 (2004) 2030–2032.
[42] S.A. Moore, B.F. Anderson, C.R. Groom, M. Haridas, E.N. Baker, Three-dimensional structure of diferric bovine lactoferrin at 2.8 A resolution, J. Mol. Biol. 274 (1997) 222–36.
[43] P.G. Thakurta, D. Choudhury, R. Dasgupta, J.K. Dattagupta, Tertiary structural changes associated with iron binding and release in hen serum transferrin: a crystallographic and spectroscopic study, Biochem. Biophys. Res. Commun. 316 (2004) 1124–31.
[44] B. Jachimska, M. Wasilewska, Z. Adamczyk, Characterization of globular protein solutions by dynamic light scattering, electrophoretic mobility, and viscosity measurements, Langmuir. 24 (2008) 6866–72.
[45] Malvern, Zetasizer user manual, Http://www.malvern.com. (2013).
[46] M. Nyström, P. Aimar, S. Luque, M. Kulovaara, S. Metsämuuronen, Fractionation of model proteins using their physiochemical properties, Colloids Surfaces A Physicochem. Eng. Asp. 138 (1998) 185–205.
[47] N. Ndiaye, Y. Pouliot, L. Saucier, L. Beaulieu, L. Bazinet, Electroseparation of bovine lactoferrin from model and whey solutions, Sep. Purif. Technol. 74 (2010) 93–99.
[48] I. Mela, E. Aumaitre, A.-M. Williamson, G.E. Yakubov, Charge reversal by salt-induced aggregation in aqueous lactoferrin solutions, Colloids Surf. B. Biointerfaces. 78 (2010) 53–60.

[49] Y.-I. Lim, S.B. Jørgensen, I.-H. Kim, Computer-aided model analysis for ionic strength-dependent effective charge of protein in ion-exchange chromatography, Biochem. Eng. J. 25 (2005) 125–140.
[50] A. Ho, J. Perera, G. Stevens, The effect of protein concentration on electrophoretic mobility, J. Colloid Interface Sci. 224 (2000) 140–147.
[51] F. Zhang, M.W.A. Skoda, R.M.J. Jacobs, R.A. Martin, C.M. Martin, F. Schreiber, Protein interactions studied by SAXS: effect of ionic strength and protein concentration for BSA in aqueous solutions, J. Phys. Chem. B. 111 (2007) 251–9.
[52] S. Salgin, U. Salgin, S. Bahadir, Zeta potentials and isoelectric points of biomolecules: the effects of ion types and ionic strengths, Int. J. Electrochem. Sci. 7 (2012) 12404–12414.
[53] Y. Mukai, E. Iritani, T. Murase, Effect of protein charge on cake properties in dead-end ultrafiltration of protein solutions, J. Memb. Sci. 137 (1997) 271–275.
[54] M.J. Treuheit, A.A. Kosky, D.N. Brems, Inverse relationship of protein concentration and aggregation, Pharm. Res. 19 (2002) 511–516.
[55] M.G. Carneiro-da-Cunha, M.A. Cerqueira, B.W.S. Souza, J.A. Teixeira, A.A. Vicente, Influence of concentration, ionic strength and pH on zeta potential and mean hydrodynamic diameter of edible polysaccharide solutions envisaged for multinanolayered films production, Carbohydr. Polym. 85 (2011) 522–528.
[56] T. Arakawa, J.S. Philo, D. Ejima, K. Tsumoto, F. Arisaka, Aggregation analysis of therapeutic proteins, Bioprocess Int. (2007) 36–47.
[57] H.-C. Mahler, W. Friess, U. Grauschopf, S. Kiese, Protein aggregation: pathways, induction factors and analysis., J. Pharm. Sci. 98 (2009) 2909–2934.
[58] P.R. Majhi, R.R. Ganta, R.P. Vanam, E. Seyrek, K. Giger, P.L. Dubin, Electrostatically driven protein aggregation: beta-lactoglobulin at low ionic strength, Langmuir. 22 (2006) 9150–9159.
[59] A. Hawe, W.L. Hulse, W. Jiskoot, R.T. Forbes, Taylor dispersion analysis compared to dynamic light scattering for the size analysis of therapeutic peptides and proteins and their aggregates, Pharm. Res. 28 (2011) 2302–2310.
[60] J.L. Kimberly, C.R. O'Melia, Protein and humic acid adsorption onto hydrophilic membrane surfaces: effects of pH and ionic strength, J. Memb. Sci. 165 (2000) 31–46.
[61] D. Möckel, E. Staude, M. Dal-Cin, K. Darcovich, M. Guiver, Tangential flow streaming potential measurements: Hydrodynamic cell characterization and zeta potentials of carboxylated polysulfone membranes, J. Memb. Sci. 145 (1998) 211–222.
[62] M. Ariza, Streaming potential along the surface of polysulfone membranes: a comparative study between two different experimental systems and determination of electrokinetic and adsorption parameters, J. Memb. Sci. 190 (2001) 119–132.

[63] K.S. Kim, K.H. Lee, K. Cho, C.E. Park, Surface modification of polysulfone ultrafiltration membrane by oxygen plasma treatment, J. Memb. Sci. 199 (2002) 135–145.
[64] A. Martín, Zeta potential of membranes as a function of pH optimization of isoelectric point evaluation, J. Memb. Sci. 213 (2003) 225–230.
[65] A.W. Zularisam, A.F. Ismail, M.R. Salim, M. Sakinah, O. Hiroaki, Fabrication, fouling and foulant analyses of asymmetric polysulfone (PSF) ultrafiltration membrane fouled with natural organic matter (NOM) source waters, J. Memb. Sci. 299 (2007) 97–113.
[66] P. Ramesh Babu, V.G. Gaikar, Membrane characteristics as determinant in fouling of UF membranes, Sep. Purif. Technol. 24 (2001) 23–34.
[67] A. Thekkedath, W.M. Naceur, K. Kecili, M. Sbai, A. Elana, L. Auret, et al., Macroscopic and microscopic characterizations of a cellulosic ultrafiltration (UF) membrane fouled by a humic acid cake deposit: First step for intensification of reverse osmosis (RO) pre-treatments, Comptes Rendus Chim. 10 (2007) 803–812.
[68] W. Norde, J. Lyklema, The adsorption of human plasma albumin and bovine pancreas ribonuclease at negatively charged polystyrene surfaces, J. Colloid Interface Sci. 66 (1978) 257–265.
[69] V. Bloomfield, The structure of bovine serum albumin at low pH, Biochemistry. 5 (1966) 684–9.
[70] F. Lampreave, A. Piñeiro, J.H. Brock, H. Castillo, L. Sánchez, M. Calvo, Interaction of bovine lactoferrin with other proteins of milk whey, Int. J. Biol. Macromol. 12 (1990) 2–5.
[71] J.L. Kimberly, C.R. O'Melia, Protein and humic acid adsorption onto hydrophilic membrane surfaces: effects of pH and ionic strength, J. Memb. Sci. 165 (2000) 31–46.
[72] S.M.G. Demneh, B. Nasernejad, H. Modarres, Modeling investigation of membrane biofouling phenomena by considering the adsorption of protein, polysaccharide and humic acid, Colloids Surf. B. Biointerfaces. 88 (2011) 108–14.
[73] P. Aimar, S. Baklouti, V. Sanchez, Membrane—solute interactions: influence on pure solvent transfer during ultrafiltration, J. Memb. Sci. 29 (1986) 207–224.
[74] Z.-P. Zhao, Z. Wang, S.-C. Wang, Formation, charged characteristic and BSA adsorption behavior of carboxymethyl chitosan/PES composite MF membrane, J. Memb. Sci. 217 (2003) 151–158.
[75] M.K. Ko, J.J. Pellegrino, R. Nassimbene, P. Marko, Characterization of the adsorption-fouling layer using globular proteins on ultrafiltration membranes, J. Memb. Sci. 76 (1993) 101–120.
[76] E. Matthiasson, The role of macromolecular adsorption in fouling of ultrafiltration membranes, J. Memb. Sci. 16 (1983) 23–36.
[77] J. Toth, Adsorption, 1st Ed, Taylor & Francis, New York, USA, 2002.

4

BSA-LF SEPARATION VIABILITY

Abstract

The aim of this chapter faces the separation of two high added value minor whey proteins with similar properties: Bovine serum albumin (BSA) and Lactoferrin (LF) by means of two membrane technologies. In a first step the viability of the electrodialysis with ultrafiltration membranes (EDUF) was evaluated. The electrophoretic mobility of BSA and LF in different media measurements were used to determine the EDUF experimental conditions. The Diafiltration separation viability, assessed by means of R_v recovery, considered the influence of the operation variables. Adequate separation was achieved for the highest BSA/LF concentration ratio of 4.0/1.0, corresponding to milk whey conditions, and at pH 5.0, BSA isoelectric point. Membrane fouling was studied at both pHs by the DLVO theory; the total interaction energies are attractive and the Van der Waals attraction dominates the overall interaction curve in both cases. The values of the interaction forces next to the zeta potential as well as the size and adsorption results lead to the conclusion that the fouling is also similar at both pHs.

4.1 INTRODUCTION

The isolation and purification of proteins is widely recognized to be technically and economically challenging and in some cases this last step in the production of high added value biomolecules accounts in some cases up to the 80.0 % of the total cost. Colum Chromatography processes are the most commonly applied nevertheless, this methodology has several disadvantages as low recovery and many elution steps. Compared to resin-based chromatography, membrane separations are simple, energy efficient and readily scalable from the laboratory to industrial settings [1]

In this study two emerging technologies have been selected for the viability study of BSA-LF separation: Electrodialysis with ultrafiltration membrane (EDUF), an electrically enhaced membrane separation process which has been satisfactorily applied for low molecular weight proteins [2] and Diafiltration, an ultrafiltration operation mode that has been used for the isolation of similar size proteins for different sources [3].

4.1.1 ELECTRICALLY ENHANCED MEMBRANE SEPARATION

In 2005 Bazinet et al. developed and patented a new filtration process called electrodialysis with ultrafiltration membrane (EDUF) [4], an electrically driven membrane separation technology. EDUF is basically a batch process in which one or more filtration membranes are stacked into a conventional electrodialytic cell, as a molecular barrier, and allows the separation of molecules according to their charge and molecular size in an electric field (Figure 4.1).

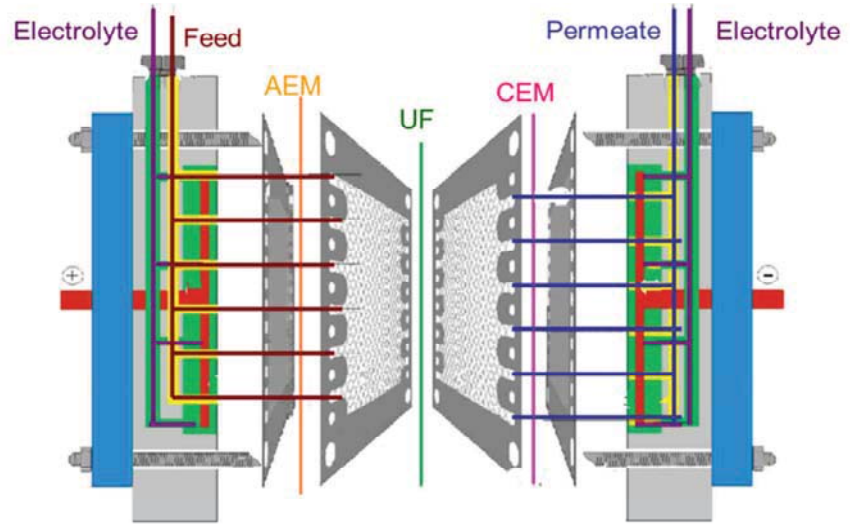

Figure 4.1. Conventional electrodialytic cell with ultrafiltration membrane: EDUF technology (Figure based on PCcell technical description brochure).

This technology has been shown to be efficient for the separation and purification of charged molecules with low molecular weights (MW) such as polyphenols (MW≤610.0 Da [5]), chitosan oligomers (MW≤800.0 Da [6]), green tea catechism (MW≤458.0 Da [7]) and peptides (MW≤3315.0 Da [8–13]). It has been mainly used as a strategy to improve protein solutions permeation flux (JP) by preventing concentration polarization and membrane fouling [14–26]. This technology allows two types of configuration described in Figure 4.2.

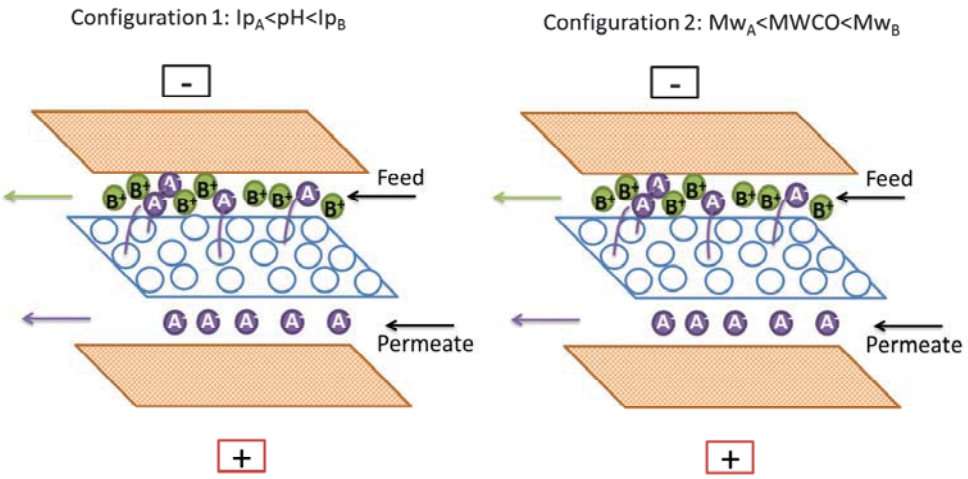

Figure 4.2. Electrodialytic cell with ultrafiltration membrane configurations.

Figure 4.2 shows the two configuration modes than can be applied when an Electrodialytic cell with ultrafiltration membrane is used. The first configuration is based on the difference in charge of the proteins and the membrane used must be higher enough to allow the permeation of the desirable species. The second configuration takes into account charge and size and the molecular weight of the membrane selected should have a value between the two molecular weights of the species.

Since 2005, several studies have applied this technology to the separation of charged molecules with low molecular weights Table 4.1 includes relevant applications of EDUF to separation of milk protein mixtures in the literature. As it is shown in Table 4.1, this technology has been also satisfactory applied to the separation of low molecular weight proteins or serum proteins [2,27,28] with high fluxes and selectivities. The results obtained for the BSA and LF mixture [29,30] had not satisfactorily achieved the separation, obtaining in the best conditions a selectivity is of 4.4 for a flux of 8.9 g m^{-2} h^{-1}[30].

Table 4.1. Relevant applications of EDUF to the separation of milk protein mixtures compiled in the literature.

Ref.	Compound g L^{-1}	Contractor	Membrane	Conditions	Flux g m^{-2} h^{-1}	Selectivity
[2]	β-Lactoglobulim (β-Lg) = 0.2 (Mw=18.4 kDa) α-Lactoglobulim (α-La) = 0.1 (Mw=14.2 kDa)	EMC 4.4-17.6V	CMX-SB cationic AMX-SB anionic Cellulose acetate 30 kDa and 100 kDa	Tris-Mes pH 8.0 Meshistidine pH 6.0 L-alanine-acetic acid at pH 4.8 140-220 µS cm-1	-7.1 β-lg -28.6 L m^{-2} h^{-1}	1.25
[27]	Hemoglobin Bovine (HB) = 1.0 (Mw=64.0 kDa) Bovine Serum Albumin (BSA) = 1.0 (Mw=65.5 kDa)	IEM-FFIEF 60.0-200.0V	Cation exchange Anion exchange Homemade polysulfone-based cation-exchange membrane	No data of composition and conductivity pH 4.8	-9.3 HB -31.1 L m^{-2} h^{-1}	Total BSA
[28]	Bovine Serum Albumin (BSA) = 5.0 (Mw=65.5 kDa) Myoblobin(MYO) blood=5.0 (Mw=17.7 kDa)	IEM-FFIEF 200.0V	Cation exchange Anion exchange Homemade polysulfone-based cation-exchange membrane	0.02M HAC-Tris Buffer pH 4.8 No conductivity data	2.1 20.0 L m^{-2} h^{-1}	Total BSA
[30]	Synthetic and real Whey. 200.0ml of whey +2.0mg of commercial Bovine Lactoferrin (LF). (Mw=79.0 kDa)	EDUF 20.0V	CMX-SB cationic membrane AMX-SB anionic membrane Polyethersulfone 500kDa	2.0 g L^{-1} KCl pH 3.0 3.3mS cm^{-1}	LF = 8.9 α-la = 8.0 β-lg = 41.0 BSA = 2.0	LF/α-LA =1.1 LF/BSA= 4.45 LF/β-LG = 0.2
[29]	Mixture: 1.3 Bovine Lactoferrin (normal or holo-LF) (Mw=79 kDa)+ 1.3 Whey Protein Isolated: β-Lactoglobulim (β-Lg) (Mw=18.36 kDa) + α-Lactoglobulim (α-La) (Mw=14.17 kDa)	EFM 5.0-10.0V	Polyvinylidene fluoride 0.5 µm membranes	deionized water at pH 7.0 16.0 µS cm^{-1}	130.0 L m^{-2} h^{-1}	$S_{LF/\beta\text{-}LG}$ =3.0–6.7 $S_{LF/\alpha\text{-}LA}$=9.0–62.2 (**)

EMC: Electrophoretic membrane contactor; EDUF: electrodialysis with ultrafiltration membrane; EFM: Electrically-enhanced membrane filtration. IEM-FFIEF : Ion-exchange-membrane-partitioned free-flow. IEFTris: tris(hydroxymethyl)aminomethane); Mes:2-(N-morpholino)ethanesulfonic acid; HAC: acetic acid.

(**) $S_{x/y}= Tr_x/Tr_y$ $Tr= (C_{Permeate}/C_{Feed})$ x1

4.1.2 ULTRAFILTRATION IN DIAFILTRATION MODE

Diafiltration is an alternative method of operating an ultrafilter (in any filtration range from microfiltration to reverse osmosis) where fresh solvent (without protein) is added to the filtration system continuously [3] with the goal of "washing out" a permeable specie (Figure 4.3).

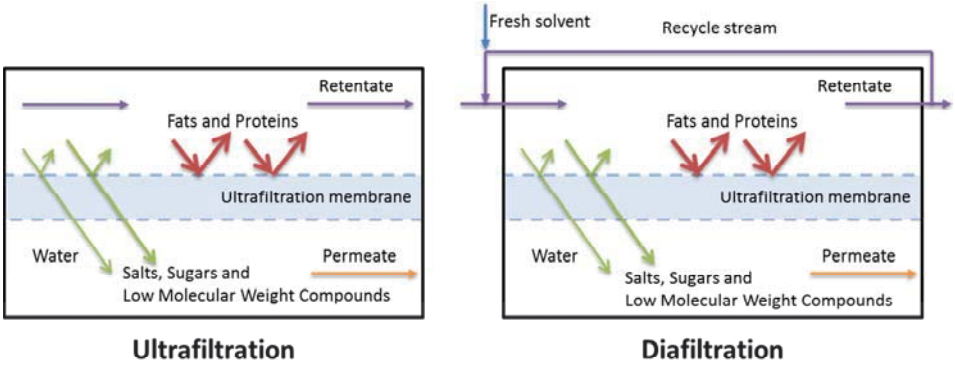

Figure 4.3. Comparison of ultrafiltration and diafiltration operational mode.

Some of the major applications of diafiltration include:

- Removal of precipitating salts (e.g. ammonium sulfate, sodium chloride) from protein solutions [31]
- Removal of precipitating solvents (e.g. ethanol, acetone) from protein solutions [32]
- Removal of peptide fragments from protein solutions [33]
- Buffer exchange before and after chromatographic separation [34]
- Removal of toxic metabolites from blood (e.g. hemodiafiltration) [35]
- Removal of inhibitors from enzyme solutions [36]
- Protein refolding/renaturation [37]
- Protein fractionation [3,38–43].

Diafiltration at low concentrations (<1.0 g L^{-1}) produces high fluxes but the volume that has to be removed is also large. At high concentrations (>5.0 g L^{-1}) permeate fluxes are low, but the volume to be removed is also low. Then, it is usually preceded by a concentration step to reduce process volume.

Diafiltration is an emerging technique as it is quick, efficient and uses the same equipment as ultrafiltration and it increases the recovery of solute or a retentate with a higher level of purity [44]. Conventional techniques used for salt removal or buffer exchange such as membrane dialysis and column-based gel filtration can be effective but have limitations. Dialysis procedures can take up to several days, require large volumes of water for equilibration and risk product loss through manual manipulation of the dialysis bags. Gel filtration results in a dilution of the sample and often requires an additional ultrafiltration step to concentrate it back. Adding steps in a process can risk sample loss or possible contamination. Using diafiltration, salt or solvent removal as well as buffer exchange can be performed quickly and conveniently. Another big advantage of diafiltration is that the sample is concentrated on the same system, minimizing the risk of sample loss or contamination [45].

4.1.3 MEMBRANE FOULING STUDY

The use of filtration membranes in the separation processes is unavoidable linked to the production of undesirable fouling [46]. These phenomena translate into pore blockage, a decline in flux, and modifications to the membrane surface properties [47] and results in an increase of maintenance and operational costs, being the major obstacle to the wide application of membrane separation processes.

In the latest years a big effort has been made to control or eliminate membrane fouling, including fabrication of antifouling membranes [48–52], the use of shear-enhanced processes [53,54] and pretreatment of the feed solutions [55–58]. However, operate at the best conditions is technically sound and economically attractive to maximize both,

permeate flux (or minimize membrane fouling) and the quality of the permeate. To minimize the fouling phenomena, parameters influencing decline in flux, and their contribution, must be determined.

Two types of fouling are usually distinguished in filtration processes [59]. The first one, called *"static fouling"*, is due to the macromolecule adsorption that occurs even in the absence of filtration. It is referred to the specific intermolecular interactions between the particles and the membrane and is often irreversible, adhesive fouling. Some of the mechanisms of this adhesive fouling are the hydrogen bonding, hydrophobic interactions, van der Waals interaction (Ew, J) and extracellular macromolecular interactions [60–67]. The second type is the so called *"dynamic fouling"*, known as filtration-induced marcosolute or particle deposition and it is usually reversible, nonadhesive fouling, where the accumulation of rejected particles on the top of the surface membrane is prominent (cake formation) [68].

Proteins generally are a few nanometers in dimension and have sizes comparable to colloidal particle sizes. The theories that may be used to characterize colloidal systems in terms of colloid interactions and stability can also be applied to proteins [66]. Evaluation of energies of protein–protein and protein–membrane interactions forms a basis for understanding a wide range of colloidal phenomena, such as fouling. In this context, the Derjaguin, Landau, Verwey, and Overbeek (DLVO) theory [69] describes the chemical interactions that lead to colloidal membrane fouling and considers two types of protein–protein and protein–membrane interaction: van der Waals and electrostatic interactions.

According to the DLVO theory, the electrostatic energies (Ee, J) are governed by the interactions between the diffuse ion atmosphere outside the charged surfaces of the proteins. The electrostatic energy between an infinitely thick flat surface (i.e., the membrane) and a protein, or between proteins, are evaluated using the following equations [63,66,67,70]:

Electrostatic protein–membrane interaction energy:

$$E_e = \varepsilon\varepsilon_0 r\left(\zeta_1{}^2 + \zeta_2{}^2\right)\left[\frac{2\zeta_1\zeta_2}{\zeta_1{}^2 + \zeta_2{}^2}\ln\left(\frac{1+\exp(-\kappa D)}{1-\exp(-\kappa D)}\right) + \ln(1-\exp(-2\kappa D)\right] \quad (4.1)$$

Electrostatic protein–protein interaction energy:

$$E_e = \Pi\varepsilon\ \varepsilon_0 \frac{R_1 R_2}{R_1 + R_2}\zeta_1\zeta_2 \ln[1+\exp(-\kappa D] \quad (4.2)$$

The van der Waals protein–membrane and protein–protein energies [70] were calculated according to equations 4.3 and 4.4, respectively:

$$E_w = \frac{-AR}{6D}\left(1 + \frac{D}{2R+D} + \frac{D}{R}\ln\left[\frac{D}{(2R+D)}\right]\right) \quad (4.3)$$

$$E_w = \frac{-A}{6}\left(\frac{2R_1R_2}{(2R_1+2R_2+D)D} + \frac{2R_1R_2}{(2R_1+D)(2R_2+D)} + \ln\left[\frac{(2R_1+2R_2+D)D}{(2R_1+D)(2R_2+D)}\right]\right). \quad (4.4)$$

Here, ε_o and ε_r are the electrical permittivity of a vacuum (C V^{-1} m^{-1}) and the dielectric constant of the fluid, respectively, ζ_1 is the zeta potential of the membrane, ζ_2 is the zeta potential of the protein (V), κ is the inverse of the Debye length (m), R is the radius of the protein or the membrane (m), D is the separation distance between particles (m), and A is the Hamaker constant (J) that can be roughly defined as a material property that represents the strength of van der Waals interactions between macroscopic bodies [67].

Interaction energies can be repulsive or attractive, depending on the chemical structure, the media properties, the membrane charge, and the protein charge. The total interaction energy E_T (J), which is equal to the sum of the electrostatic and van der Waals energies, predicts whether repulsive or attractive forces are dominant between the membrane and protein:

$$E_t = E_e + E_w \quad (4.5)$$

4.2 MATERIALS AND METHODS

4.2.1 MATERIALS

Proteins and Buffers

In this study measurements were performed using individual and mixtures standards of the native BSA (Catalog A-6003 Sigma Chemical, Spain) and native LF (NutriScience Innovations, USA). BSA is readily soluble in water and requires high concentrations of neutral salts, such as ammonium sulfate, to induce precipitation. Bovine LF is highly soluble in water (2.0 %, 20°C) and has an Fe^{3+} content of 3.0 mg/100 g protein. The isoelectric point of BSA is close to 4.9, its molecular weight is 66.5 kDa, and the protein shape is a prolate ellipsoid with dimensions of 14.0 x 3.8 x 3.8 nm [71]. LF has an isoelectric point around 9.0, a molecular weight of 78 kDa, and a globular shape with dimensions of 4.0 x 5.1 x 7.1 nm, as determined using the lattice cell parameter data [72,73].

Protein standards of BSA, LF and their mixture in the range of concentrations of 0.1 - 4.0 g L^{-1} were prepared by adding the protein powder to the desired buffer solution, pH 5.0 (sodium acetate/acetic acid Analytical grade, Merk), pH 7.0 (sodium phosphate/dipotassium phosphate, Analytical grade, Merk); pH 9.0 (borax/hydrochloric acid (Fluka, Spain)) or different electrolyte solutions (KCl, NaCl or $CaCl_2$ Analytical grade, Merk). Shaking was avoided to prevent foam formation, which can seriously interfere with analytical procedure. Protein standards were used within the subsequent 24 h.s to minimize the likelihood of protein aggregation. NaOH and HCL 0.1M (Analytical grade, Merk) were employed to rise or reduce the pH of the electrolytic protein solutions.

4.2.2 EXPERIMENTAL METHODOLOGY

4.2.2.1. Electrically enhanced membrane separation (EDUF) set-up

Two different cells, with different effective areas, consisted in two electrode compartments separated by a defined number of spacers were used in this study. The cell configuration is described in Figure 4.4.

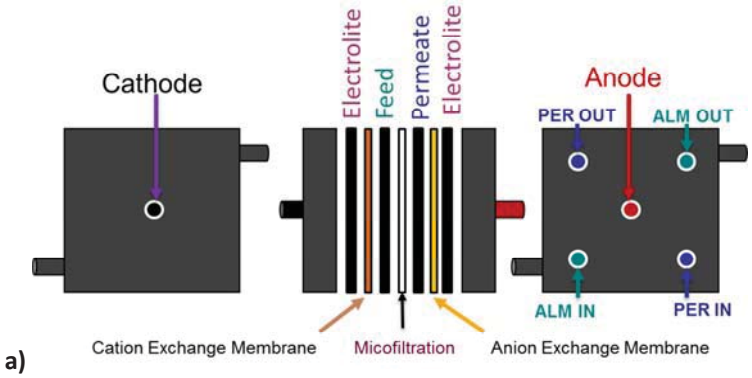

Figure 4.4. EDUF cell configuration used in this study a) Cell diagram b) PcCell Picture, c) ED Cell Picture.

In the Figure 4.4a the general two- compartment arrangement configuration of the cell is described. Commercial cationic (CEM), anionic membranes (AEM) and polysulfone microfiltration membranes of 0.2 µm (MF1) and 100.0 kDa (MF2) were used in a two-compartment arrangement. The characteristics of the membranes applied are given in Table 4.2. The two ion exchange membranes were used to keep the

electrolytic stream while the separation was performed through a micro/ultrafiltration membrane placed between the feed phase and the permeate. In Figure 4.4 the feed is placed on the right side of the membrane, in this way, protein negatively charged will permeate through the membrane (BSA transfer mode). When the permeation of positively charged proteins is required the feed should be placed on the left side of the ultrafiltration membrane (LF transfer mode). The first cell used (PC, cell system) has an effective area of 64.0 cm^2 and the electrodes were made of Pt/Ir- coated Ti stretched metal (Anode) and Ti stretched metal (cathode) and the spacer were of Polypropylene (0.1 mm) (Figure 4.4b). The second cell applied (ED Cell) has electrodes (100.0 cm^2 effective area) made of titanium coated with ruthenium oxide and spacers of 3.0 mm-thick Viton gaskets (Figure 4.4c). The EDUF experimental system used in this study is described in Figure 4.5.

Table 4.2. Membranes used in the electrically enhanced process.

Parameters	AEM	CEM	MF1	MF2
Reference	PC SFA	PC SFK	GRM0.2PP	GR40PP
General use	Electrodialysis	Electrodialysis	Microfiltration	Ultrafiltration
Membrane type	Strongly alkaline ammonium	Strongly acidic ammonium	Polysulphone 0.2 µm	Polysulphone 100.0 kDa
Transference nº	> 0.95	>0.94	---	---
Resistance, W cm^2	~1.0	~1.0	---	---
Water content (wt%)	~24.0	~21.0	---	---
Maximum operating Temp, °C	60.0	50.0	75.0	75.0
Thickness µm	30.0-120.0 (adjustable)	30.0-50.0	---	---
Ionic form	Cl^-	Na^+	---	---
pH range	---	---	1.0-13.0	1.0-13.
Pressure, bar (psi)	---	---	1.0-10.0 (15.0-145.0)	1.0-10.0 (15.0-145.0)

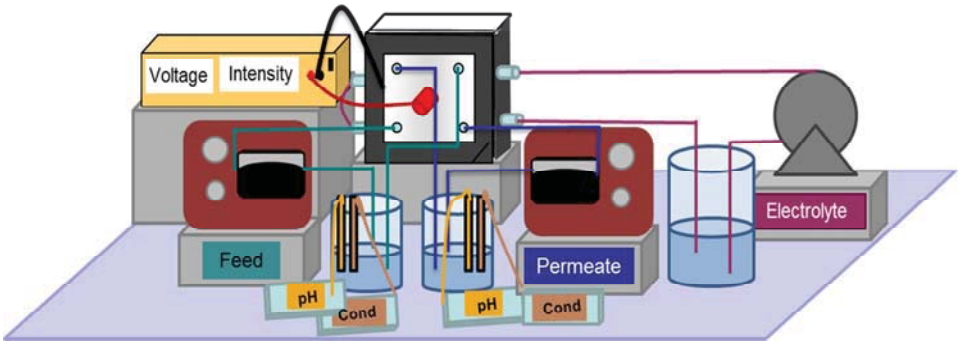

Figure 4.5. Diagram of the experimental EDUF system used in this work.

In Figure 4.5 describes the experimental system of EDUF consisted in: three closed loops with Electrode rinse liquid (500 mL), Free solution (300 mL) and permeate solutions (300 mL); two peristaltic pumps (Watson-Marlow 323 SD) with a capacity of 120.0 L h^{-1} and one centrifugal pump (PCcell BED1-4) with a capacity of 120.0 L h^{-1} and a variable power source (0.0-36.0 V / 0.0-16.0 A) (PCcell BED1-4) DC generator that supplied the desired fixed current or voltage in the stack.

At the beginning of each experiment the cell was filled with the three working solutions (feed, permeate and electrolyte) with fluxes of 28.0 mL min^{-1}, 11.0 mL min^{-1} and 55.0 mL min^{-1} for the feed, permeate and electrolyte and the power supply was not connected until the complete filly of the cell. Changes of conductivity, pH and concentration in feed and permeate were recovered with time and the pH was kept constant with the addition of the required amount of NaOH or HCl 0.1M. The study of the influence of principal variables (membrane, protein media and intensity/voltage) on the process performance was carried out through the analysis of the protein concentration profiles and the selectivity. All the experiments were replicated. The results reported in this work are the average values of the two experiments, and the relative experimental error is indicated by the error bars.

Protein quantification

When the electrolytic medium was applied the measurement of both proteins in the binary mixture was performed by the spectroscopic methodology for protein determination in complex medium developed in the Chapter 3. Samples were adjusted at pH 3.0 and the profiles of fluorometric and UV-vis absorbance were obtained. The curves were analyzed by Fityk software and the center (fluorescence) and height of the common Gaussian (UV-vis) were obtained. By comparing the results with the calibration curves the percentage of each protein in the mixture as well as the total protein concentration was determined.

4.2.2. Ultrafiltration system in Diafiltration mode set-up

The diafiltration experiments were performed in the Amicon ultrafiltration system (Millipore) shown in the Figure 4.6.

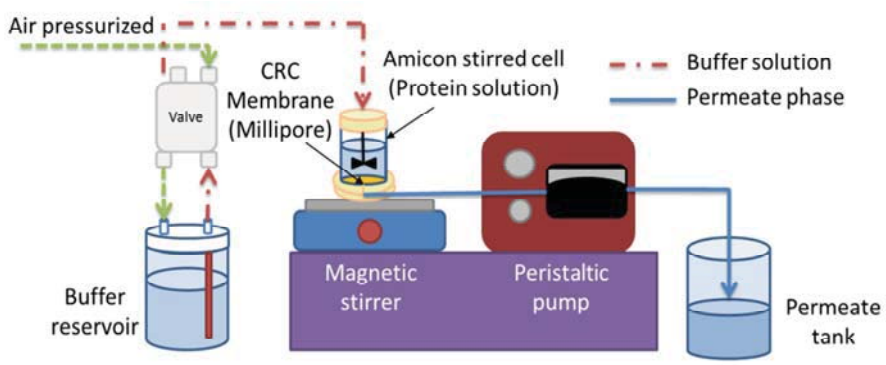

Figure 4.6. Diagram of the experimental diafiltration system used in this study.

The 44.5 mm diameter Amicon-stirred airtight UF cell (Figure 4.6, Model 8050, Millipore) was initially filled with 50.0 mL of the protein mixture. The buffer solution flowed from a separate reservoir (Model 6028, Millipore, Spain). All experiments were run for 3 h corresponding to 6–7 diavolumes (V_d) and replicated. It is important to understand the term Diafiltration Volume, V_d. Each diafiltration volume is a volume of buffer equal to the volume of process solution in the reservoir. The membranes were used only once.

All ultrafiltration experiments were performed using 100.0 kDa composite regenerated cellulose membranes (CRC, Millipore, Madrid, Spain) with an effective membrane surface area of 13.4 cm^2. These membranes were charge lightly negative in their unmodified form and displayed very low rates of protein adsorption due to their high degree of hydrophilicity [3]. The estimated average pore size was 6.20 nm (data provided by Millipore Costumer Service, Madrid, Spain). Membranes were charged according to the methodology described in the literature [74] and there were stored in NaOH 0.05 N 24 h.s before its use.

Protein quantification

Both proteins in the binary mixture were quantitatively analyzed using high performance liquid chromatography, (HPLC) according to the method adapted from Adam et al. [75] using an HPLC Waters 2690 Separation Module (Waters) fitted with a CIMac™-SO_3 analytical column (BiaSeparations) and a Waters 996 diode array spectroscopic detector with a wavelength range of 210.0 – 400.0 nm (UV, Waters). The method was sensitive to protein concentrations below 0.03 g L^{-1}, and the detection limit was still lower.

4.3 RESULTS AND DISCUSSION

4.3.1 EDUF AND DIAFILTRATION VIABILITY STUDIES

The relevance of "whey concentrate" has been pointed out by different authors [40,41,76] due to its higher commercial price (from 3 to 40 times higher than whey powder) and its value as protein source. For this reason the initial concentration (4.0 g L^{-1} BSA and 1.0 g L^{-1} LF) simulated the conditions found in the production of whey concentrate [77].

The viability separation of the high added value protein BSA and LF from their mixture was carried out by two technologies. First the Electrically Enhanced separation was evaluated and secondly the ultrafiltration system operation in diafiltration mode was carried out.

4.3.1.1 Electrically enhanced separation (EDUF) experiments

Electrophoretic mobility determination

The electric field applied in the EDUF systems acts as the driving force of the process. The electrophoretic mobility, which takes into account the velocity of movement of a protein in a medium, function of size and charge; $m^2\ V^{-1}\ s^{-1}$, is the main parameter to determine the best operational conditions in such systems.

EDUF experiments are usually performed in two different media: i) the electrolytic media, high conductivity solutions that assures the proper conduction of the intensity in the stacks [6,10,30] and ii) the buffer media which allows the pH control of the system [2,18,78]. In this work, the electrophoretic mobility analysis will be performed in KCl 0.025M electrolytic solution (most commonly applied solution [6,10,30]) and three different buffers: sodium acetate/acetic acid pH 5.0 (corresponding to Ip BSA), sodium phosphate/dipotassium phosphate pH 7.0 (Ip BSA < pH < Ip LF) and borax-hydrocloridic acid pH 9.0 (corresponding to Ip LF).

Two considerations should be taken into account when the electrophoretic measurement is performed: i) the bigger the electrophoretic mobilities the better transmission is achieved, ii), The greater the differences in electrophoretic mobilities between proteins the higher selectivity is reached. Negative values of electrophoretic mobility imply a migration to the anode while proteins with positive electrophoretic mobility will migrate to the cathode.

The electrophoretic mobilities of 4.0 g L^{-1} of BSA and 1.0 g L^{-1} LF dissolved in the three buffer solutions, sodium acetate/acetic acid pH 5.0, sodium phosphate/dipotassium phosphate pH 7.0 and borax-hydrocloridic acid pH 9.0 are compared in Figure 4.7.

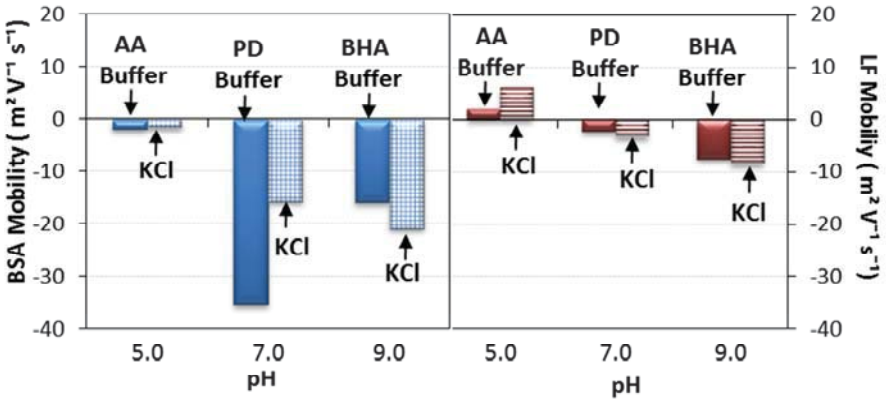

Figure 4.7. Electrophoretic mobility comparison of BSA and LF with pH for Buffers and KCl. AA buffer: sodium acetate/acetic acid, PD buffer: sodium phosphate/dipotassium phosphate and BHA buffer: borax/hydrochloric acid.

As it is depicted in Figure 4.7, BSA electrophoretic mobility has negative values whatever the pH used. Higher mobilities are obtaining in buffer (sodium acetate/acetic acid, sodium phosphate/dipotassium phosphate, borax/hydrochloric acid) solution than a KCl solution at the same pH. Being the highest mobility of 1.6 10^{-8} m^2 V^{-1} s^{-1} working sodium phosphate/dipotassium phosphate buffer solution at pH 7.0. Figure 4.7 shows that LF presents positive electrophoretic mobility at pH 5.0 while pH 7.0 and 9.0 are associated to negative electrophoretic mobility. Being

the highest mobility (absolute) of -6.0 10^{-9} m^2 V^{-1} s^{-1} working KCl solution at pH 9.0.

As a result of previous obtained mobility values, the electrophoretic mobility of 4.0 g L^{-1} BSA and 1.0 g L^{-1} LF versus the pH was determined in KCl 0.025 M. Figure 4.8 shows the experimental results. The experiments were duplicates being the experimental error lower than the 10.0 %.

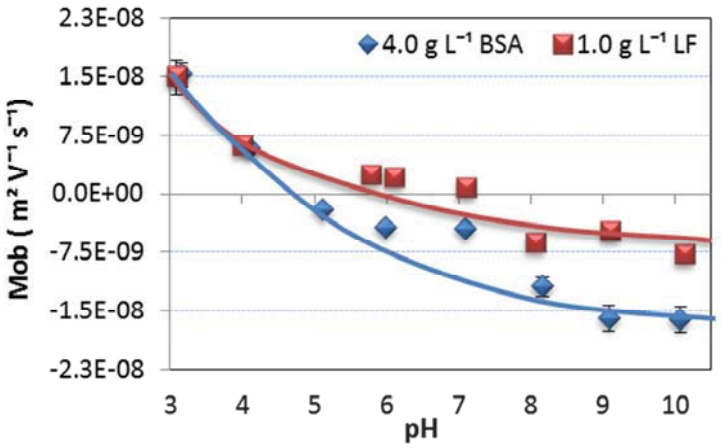

Figure 4.8. Electrophoretic mobility profiles with pH at 0.025M KCl.

Figure 4.8 shows the evolution electrophoretic mobility vs. in the pH range 3.0 to 10.0. Three different scenarios can be found: i) the highest electrophoretic mobilities for both proteins (1.5 10^{-8} m^2 V^{-1} s^{-1}) is found at pH 3.0, ii) In the range of pH from 5.5 to 7.0 BSA presents negative electrophoretic mobility and LF presents positive electrophoretic mobility and iii) the differences in electrophoretic mobilities are considerable for pH 9.0 and 10.0 but the charge of both proteins in this range is the same. According to these results the selected operating conditions were 0.025 M KCl solution at pH 6.0.

The experimental results of electrophoretic mobility of 4.0 g L^{-1} BSA and 1.0 g L^{-1} LF in the phosphate/dipotassium phosphate buffer vs the ionic strength are shown in Figure 4.9 with an experimental error lower than 7.0 %.

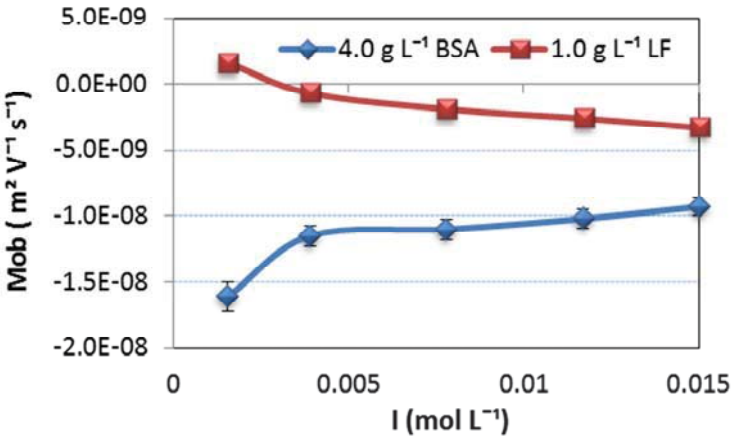

Figure 4.9. Electrophoretic mobility profiles of BSA and LF vs. ionic strength at phosphate/dipotassium phosphate buffer pH 7.0.

The LF electrophoretic mobility decreases with increasing ionic strength from 2.5 10^{-9} m^2 V^{-1} s^{-1} to -2.5 10^{-9} m^2 V^{-1} s^{-1} (Figure 4.9). The BSA electrophoretic mobility increases with increasing ionic strength from -1.6 10^{-8} m^2 V^{-1} s^{-1} to -1.0 10^{-8} m^2 V^{-1} s^{-1} (Figure 4.9). The best operational conditions selected corresponds to ionic strength 1mM where electrophoretic mobility presents highest difference in charge and in absolute value.

Finally, the following operational conditions were selected: 0.025 M KCl solution at pH 6.0 (μ_{BSA} =-0.32 10^{-8} m^2 V^{-1} s^{-1} and μ_{LF} 0.21 10^{-8} m^2 V^{-1} s^{-1}) and phosphate/dipotassium phosphate buffer 0.001M pH 7.0 (μ_{BSA} =-1.61 10^{-8} m^2 V^{-1} s^{-1} and μ_{LF} 0.24 10^{-8} m^2 V^{-1} s^{-1}), in order to perform the EDUF viability experiments.

Experimental assessment of the separation of BSA/LF mixtures

Once the most suitable experimental conditions were established, the viability of BSA and LF separation by means of EDUF technology were evaluated. Table 4.3 describes the experimental conditions applied in this study.

Table 4.3. Experimental conditions in EDUF viability study.

	PHASES			Protein	EDUF SYSTEM	
Exp	Feed	Electrolyte	Permeate	Transfered	Membrane	Voltage
1	4.0 g L^{-1} BSA 1.0 g L^{-1} LF 2.0 g L^{-1} KCl pH 6.0 3.4 mS cm^{-1}	20.0 g L^{-1} NaCl 21.9 mS cm^{-1}	2.0 g L^{-1} KCl pH 6.0 3.3 mS cm^{-1}	BSA	100.0 kDa	0.3 A fixed 46.9 A m^{-2}
2					0.2 µm	
3				LF		
4				BSA		0.5 A fixed 50.0-9.0 A m^{-2}
5				LF		
6	4.0 g L^{-1} BSA 1.0 g L^{-1} LF Phosphate Buffer 1mM pH 7.0 0.7 mS cm^{-1}	Phosphate Buffer 1mM pH 7.0 0.7 mS cm^{-1}	Phosphate Buffer 1mM pH 7.0 0.7 mS cm^{-1}	BSA		20 V fixed 10.0-5.0 A m^{-2}
7						30 V fixed 33.0-3.0 A m^{-2}

The separation performance of the Exp1, 2, 4, 5 and 6 was not satisfactory enough. The best results corresponded to Exp3 and Exp6 whose results are shown in Figure 4.10. The experiments were duplicates being the experimental error lower than the 10.0 %.

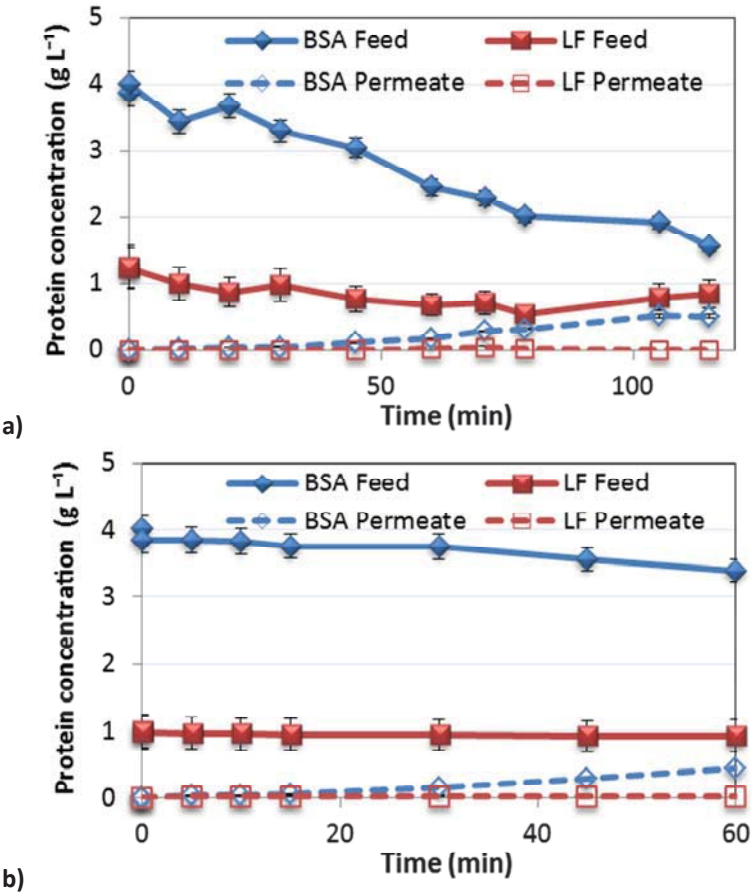

Figure 4.10. Evolution of BSA and LF concentration profiles in the feed and permeate vs. time in the experiments a) Exp3 and b) Exp6.

As it is shown in Figure 4.10, only BSA in low concentration is found in the permeate phase. Additionally, the concentration in the feed solution also decreased, indicating that a certain amount of BSA should be adsorbed in the membrane. The results reported in this thesis suggest the viability of the BSA-LF separation by means of EDUF, but further research needs to be addressed to completely achieve competitive conditions in terms of fluxes and selectivities. In a future work, the research and development of new electrolyte media able to guarantee higher electrophoretic mobilities and better control of the operational conditions are needed, but this future research is out of the scope of this thesis.

4.3.1.2 Pressure enhanced separation (Diafiltration) experiments

Protein characterization

The influence size and charge of proteins in the viability of the separation process by Diafiltration was evaluated in the buffer working media: sodium acetate/acetic acid pH 5.0 (corresponding to Ip BSA) and borax-hydrocloridic acid buffer pH 9.0 (corresponding to Ip LF).

Zeta potential and size values of 4.0 g L^{-1} BSA and 1.0 g L^{-1} LF in the buffer solutions of pH 5.0 and pH 9.0 were compared to membrane pore size in Figure 4.11. The experiments were duplicates being the experimental error lower than the 10.0 %.

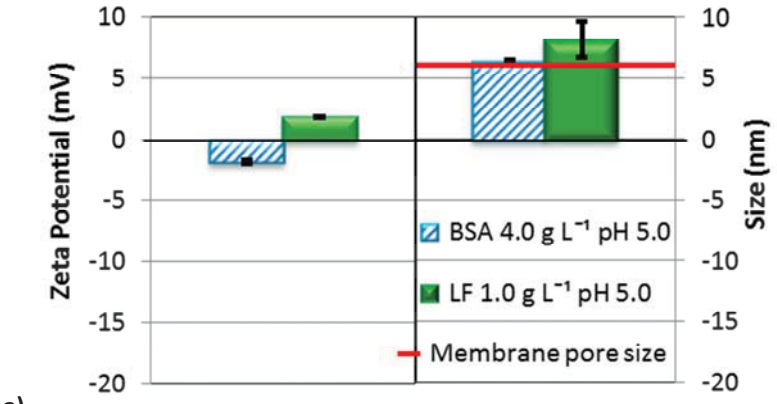

a)

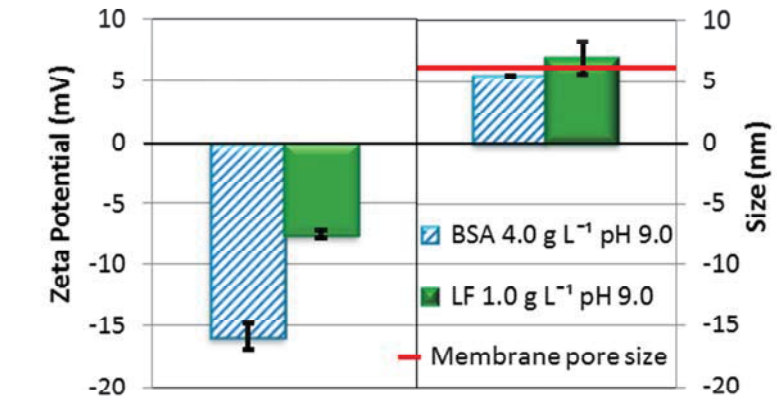

b)

Figure 4.11. Zeta potentials and molecular sizes of BSA and LF in a) buffer solution pH 5.0 and, b) buffer solution pH 9.0

In Figure 4.11a BSA zeta potential was slightly negatively at the isoelectric point, 5.0. This pH corresponds to the theoretical isoelectric point of BSA reported previously in the literature (BSA Ip range from 4.68 (for 0.5 g L^{-1} BSA in 0.001 M KCl) [79] to 5.15 (for 1.0 g L^{-1} BSA in 0.01 M NaCl) [80]). LF zeta potential was slightly positively at this pH. This value was lower than expected based on the results of Nyström et al. [81] who reported a ζ-potential of 20mV at this pH. At pH 9.0, BSA and LF proteins zeta potential were negative (Figure 4.11b). This behavior was unexpected in the case of LF zeta potential because this pH corresponds to the theoretical isoelectric point of LF. In contrast with the general agreement in the literature on the value of Ip for BSA, the reported Ip values for LF span a broader range, from 5.6 (for 0.4 g L^{-1} LF in 0.15 M NaCl) [82] to 8.0 – 9.0 (for 0.1 g L^{-1} LF in 0.01 M NaCl) [81].

With regard to the hydrodynamic diameter, a value of 6.6 nm was resported for BSA [83,84] in good agreement with the measured value at pH 5.0 in this study, 6.64 nm (Figure 4.11a) and slightly higher than the measured value at pH 9.0, 5.52 nm (Figure 4.11b). Nyström et al reported the hydrodynamic diameter of LF 7.20 nm [81], lower than the value measured at pH 5.0, 8.21 nm (Figure 4.11a) and higher than 6.99 nm (Figure 4.11b) measured at pH 9.0.

The measured polydispersity index (PdI) was less than 0.2 for BSA, indicating that aggregation did not occur. Higher values were obtained for LF, 0.6 < PdI < 0.8, thus indicating the formation of aggregates of this protein.

Experimental assessment of the viability of BSA/LF mixtures

The separation viability was assessed studying the influence of the operation variables, i.e., the BSA/LF initial concentration ratio (4.0/1.0 and 2.0/1.0) and the solution pH (5.0 and 9.0), using 100.0 kDa composite regenerated cellulose membranes (CRC, Millipore, Madrid, Spain). The evaluation of the separation process was analyzed by means of the parameter percentage of recovery, “% Rv”, expressed in the equation 4.1:

$$R_v = 100 * \frac{g\,protein\,in\,permeate(Q)}{g\,initial\,protein(Q_o)} \quad (4.1)$$

Table 4.4 shows the experimental conditions used in the experimental assessment of the separation of BSA/LF mixtures.

Table 4.4. Experimental conditions in Diafiltration viability study.

Exp	Membrane	pH	Buffer disolution	BSA (g L^{-1})/LF (g L^{-1}) Initial Ratio
Exp 1	Unmodified	5.0	Sodium acetate/ Acetic acid	4.0/1.0
Exp 2	Unmodified	9.0	Borax/ Hydrochloric acid	4.0/1.0
Exp 3	Unmodified	5.0	Sodium acetate/ Acetic acid	4.0/1.0
Exp4	Unmodified	9.0	Borax/ Hydrochloric acid	4.0/1.0

Figures 4.12 and 4.13 show the R_v results versus the diavolume for experiments Exp1–Exp4 with an experimental error lower than 10.0 % (error bars).

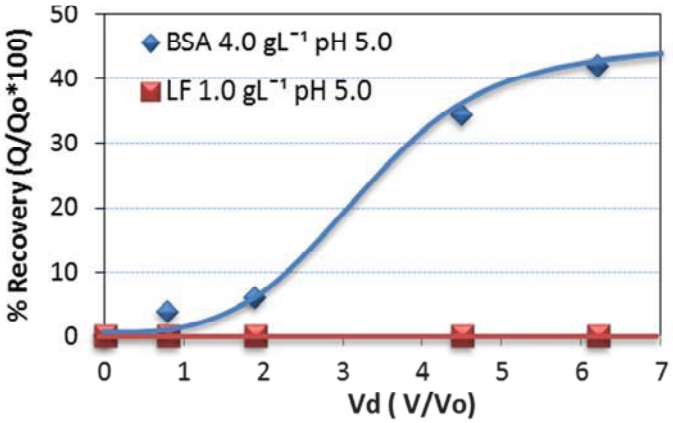

a)

Figure 4.12. R_v of BSA and LF from the diafiltration process
a) Exp1

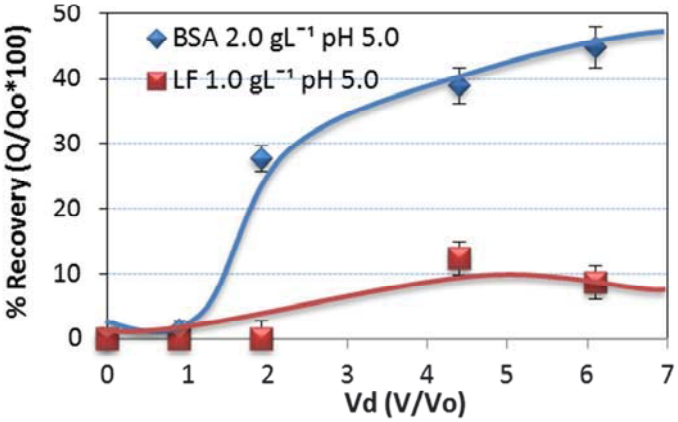

b)

Figure 4.12. R_v of BSA and LF from the diafiltration process b) Exp 2.

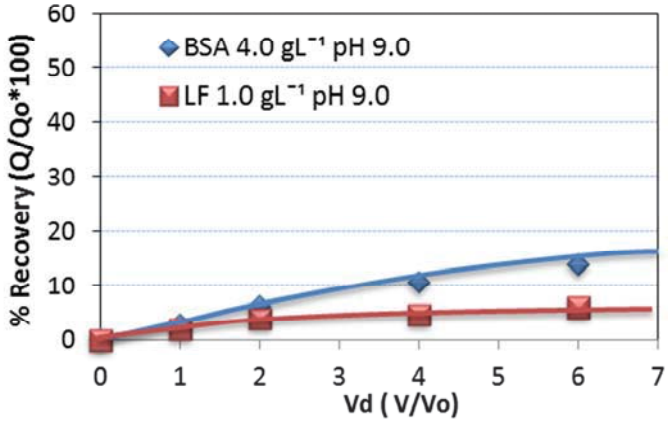

a)

Figure 4.13. R_v of BSA and LF from the diafiltration process a) Exp3.

b)

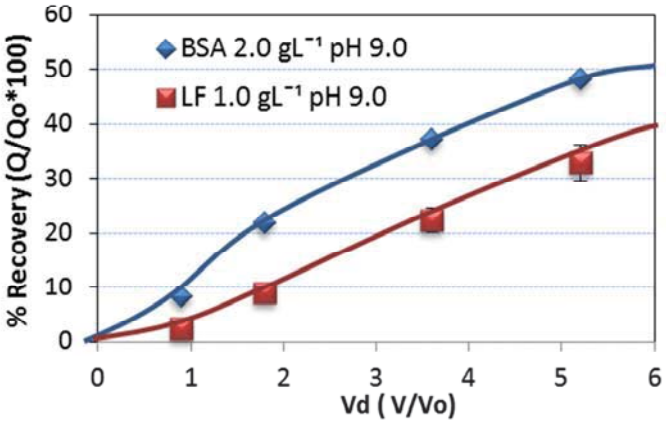

Figure 4.13. R_v of BSA and LF from the diafiltration process b) Exp 4.

The data shown in Figure 4.12a confirmed the viability of the separation of BSA/LF mixtures, with a BSA recovery of approximately 40.0 %, whereas the LF concentration in the permeate remained negligible after 3 h. On the other hand, Figures 4.12, 4.13a and 4.13b showed operational conditions less suitable. The highest recovery percentage of LF was obtained under the experimental conditions given in Exp4, with a 2.0/1.0 protein ratio and a pH of 9.0; however, this gain in recovery was accompanied by a loss in the separation selectivity. Results shown in Figures 4.12 and 4.13 are in good agreement with the size results obtained in Figure 4.11. At pH 5.0 the BSA has lower size than the LF so its permeation is promoted. At pH 9.0 both proteins have similar size and close to the pore of the membrane, for this reason both can permeate.

Figures 4.12 and 4.13 give information whose rationale is currently under study. F. Lampreave et al, in a previous work [85] reported the formation of stoichiometric complexes between BSA and LF whose presence might modify the permeation flux; this possibility that could depend on the concentration of both proteins needs further research.

The experimental results suggested that the viability of the a BSA/LF mixture was demonstrated. Adequate separation was achieved for the highest BSA/LF concentration ratio of 4.0/1.0, corresponding to milk whey conditions, and at pH 5.0, BSA isoelectric point. At pH 9.0, feasible separation conditions could not be identified, and the influence of the various operational conditions must be further evaluated.

4.3.2 IMPROVED SEPARATION OF BOVINE SERUM ALBUMIN AND LACTOFERRIN MIXTURES USING CHARGED ULTRAFILTRATION MEMBRANES

The viability of the separation process of the BSA/LF protein was previously determined. This section analyses the influence of the principal operational conditions, namely the membrane charge and buffer pH on the protein recovery.

4.3.2.1 Influence of the membrane charge and the buffer pH on the separation process

Table 4.5 shows the experimental conditions selected in Exp5-Exp8 to evaluate the influence of the membrane charge and the buffer pH on the separation process.

Table 4.5. Experimental conditions of Exp5-Exp8.

Exp	Membrane Charge (mV)	pH	Buffer disolution	BSA (g L^{-1})/LF (g L^{-1}) Initial Ratio
Exp 5	Negative (-27.8)	5.0	Sodium acetate/ Acetic acid	4.0/1.0
Exp 6	Negative (-55.1)	9.0	Borax/ Hydrochloric acid	4.0/1.0
Exp 7	Positive (42.4)	5.0	Sodium acetate/ Acetic acid	4.0/1.0
Exp 8	Positive (51.8)	9.0	Borax/ Hydrochloric acid	4.0/1.0

The influence of the membrane charge on the separation process was examined in Figures 4.14 and 4.15 show the recovery, R_v BSA/LF results of the experiments Exp5-Exp8 versus Diavolumes, V_d. The experiments were duplicates being the experimental error lower than the 10.0 %.

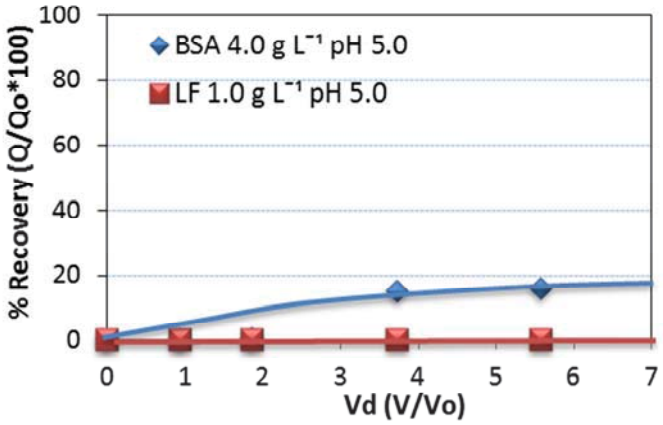

a)

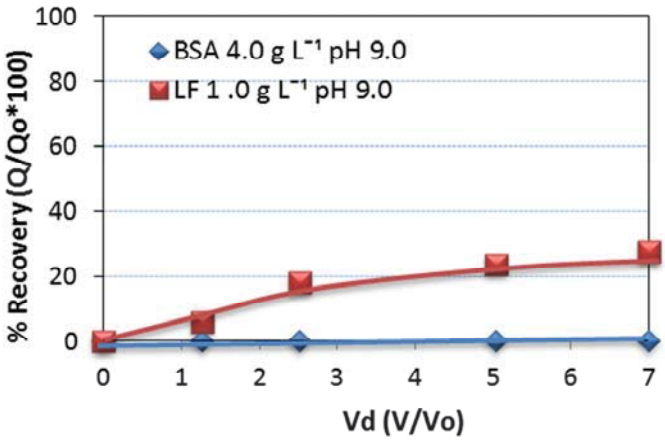

b)

Figure 4.14. Rv of BSA and LF in the diafiltration process using negatively charge membrane a) Exp5 (pH 5.0) b) Exp6 (pH 9.0).

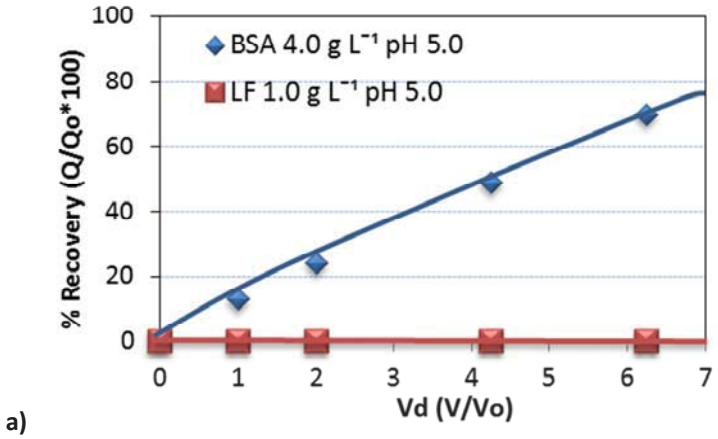

a)

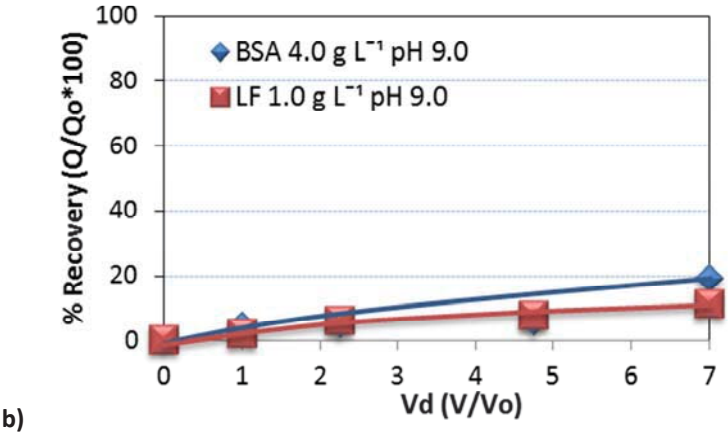

b)

Figure 4.15. Rv of BSA and LF in the diafiltration process using positively charge membrane a) Exp5 (pH 5.0) b) Exp6 (pH 9.0).

Figure 4.14 shows that the negative membrane allows the separation of BSA and LF at the select pH values, being the recoveries of 20.0 % for BSA at pH 5.0 and of 30.0 % for LF at pH 9.0. When the positive membrane is used the separation (Figure 4.15) of BSA at pH 5.0 is improved obtaining a recovery of 70.0 % (Figure 4.15a). On the contrary, at pH 9.0 (Figure 4.15b) the separation of BSA and LF was not achieved and the recoveries of both proteins were also low (20.0 % BSA and 11.0 % LF).

In order to establish a relationship between the recovery results and the size and charge of the protein and membranes, the observed sieving coefficient [81,86–97] is defined as follows:

$$S_o = \frac{C_p}{C_t} \tag{4.2}$$

where C_p and C_t are the protein concentrations (mol m^{-3}) in the permeate and diafiltration tanks measured when steady state conditions were reached, respectively.

Figure 4.16 shows the observed sieving coefficients of both proteins working with positive, negative, and unmodified CRC membranes at pH 5.0 and 9.0. The results obtained with unmodified membrane correspond to the viability analysis reported in the previous section.

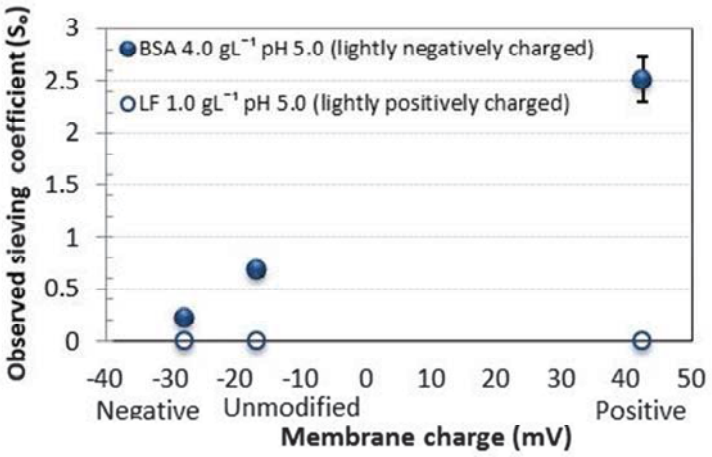

a)

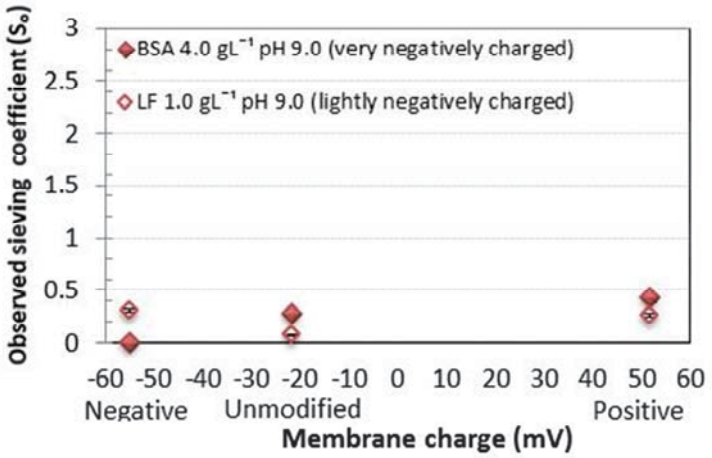

b)

Figure 4.16. S_0, observed sieving coefficient vs. the initial membrane charge a) buffer solution pH 5.0 b) buffer solution pH 9.0.

At pH 5.0 (Figure 4.16a), BSA was close to its isoelectric point, being the protein size the smallest possible, 6.64 nm. The size of LF under these conditions was 8.21 nm. The estimated average pore size of the unmodified membrane was 6.20 nm (Figure 4.11a). Therefore, LF was rejected by the membrane due to size exclusion independently of the membrane and protein charge. The low sieving coefficient of LF at pH 5.0 agreed well with the tendency of LF to form aggregates at this working pH, which prevented its permeation through the membrane

pores. In the case of BSA, the more positive the membrane charge, the higher the sieving coefficient, S_o= 0.3-2.5. This behavior was explained by the electrostatic interactions between the lightly negatively charged proteins and the different charged membranes and the similar size of the protein and the membrane pore.

At pH 9.0 (Figure 4.16b), LF was close to its isoelectric point, being the protein size 6.99 nm. The estimated average pore size of the unmodified membrane was 6.20 nm (Figure 4.11b). Therefore, LF was rejected by the membrane due to size exclusion independently of the membrane and protein charge, as reported in Chapter 3, where LF aggregation was evaluated as 0.2 - 4.0 % in mass (molecular weights between 105.60 and 295.80 kDa). The size of BSA under these conditions was 5.52 nm. At pH 9.0, BSA was strongly negatively charged, and the use of the negatively charged membrane resulted in the rejection of BSA molecules due to protein–membrane charge repulsion [98]. The use of a positively charged membrane at pH 9.0 did not significantly improve the protein mixture separation. The likely formation of complex species between BSA and LF in a stoichiometric ratio of 1:1 at pH 9.0, as reported previously [85], may explain this experimental behavior.

4.3.2.2 Permeation flux and separation selectivity

The most important parameters for the design of a membrane separation process are the permeation flux and selectivity. These parameters determine the economy of the process. The selectivity (α) is defined by equation (4.3) [91].

$$\alpha_{i/j} = \frac{S_{o\,i}}{S_{o\,j}} \tag{4.3}$$

Here, S_o are the sieving coefficients referred to both the target protein (i) and the competitive protein, j. The results of permeation flux experiments, the observed sieving coefficients of the proteins, and the corresponding selectivity values calculated using equation (4.3) are listed in Table 4.6.

Table 4.6. Selectivity and permeation fluxes for BSA and LF.

Exp.	pH	Membrane	BSA flux g $m^{-2}h^{-1}$	LF flux g $m^{-2}h^{-1}$	So (BSA)	So (LF)	αBSA/LF
5	**pH 5.0**	Negative	6.6	n. f.	0.2	0.0	BSA enriched permeate
1		Unmodified	21.1	n. f.	0.7	0.0	BSA enriched permeate
7		Positive	30.3	n. f.	2.5	0.0	BSA enriched permeate
Exp.	**pH**	**Membrane**	**BSA flux g $m^{-2}h^{-1}$**	**LF flux g $m^{-2}h^{-1}$**	**So (BSA)**	**So (LF)**	**αBSA/LF**
6	**pH 9.0**	Negative	n. f.	1.1	0.0	0.4	LF enriched permeate
3		Unmodified	8.1	0.1	0.3	0.1	0.3
8		Positive	8.7	1.3	0.4	0.3	0.6

n. f.: no flux quantified.

The data listed in Table 4.6 reveal that the separation of BSA or LF from their mixtures can be selectively achieved under the appropriate experimental conditions. At pH 5.0, the permeate phase was enriched with BSA, and LF was completely retained in the feed solution. The positively charged membrane provided the highest flux value under these conditions. At pH 9.0, the negatively charged membrane provided a good separation selectivity, although the flux was very low.

The obtained results were compared in Table 4.7 with data previously reported for this particular mixture of proteins or protein mixtures having similar sizes and shapes. Some studies were focused on improving the separation rate by applying an electric field [29,30]. Despite the fluxes obtained are quite high the selectivities are lower than 70.0 for all the cases of study. The highest permeate flux values were reported by Ndiaye et al. [30], with a maximum LF/BSA selectivity of 4.5 for an initial LF/BSA concentration ratio of 11.1, which is dissimilar from the ratio present in milk whey. This work employed an initial BSA/LF concentration ratio of 4.0/1.0. The maximum BSA permeation flux of 30.3 g $m^{-2}h^{-1}$ was achieved at pH 5.0 using a positively charged membrane, while the maximum LF permeation flux of 1.1 g $m^{-2}h^{-1}$ was

obtained under maximum selectivity conditions involving the use of a negatively charged membrane and a solution pH of 9.0. These results constitute improvements of more than a factor of 1000 over the best selectivity results reported in literature thus far for the separation of these two minor proteins with similar or improved flux values. Thus, two different methods of recovering the target LF protein from the binary mixtures may be anticipated: i) maximizing the permeate flux and further isolating the retained LF using a commercial UF membrane, or ii) optimizing the permeation flux using a negatively charged UF membrane followed by recovery of the LF from the permeate solution.

Table 4.7. Comparison of the flux and selectivity values reported in the literature for mixtures of the BSA/LF milk proteins.

ARTICLE	MEMBRANE/ PROCESS	PROTEIN MIXTURE ($g\ L^{-1}$)	FLUX $L\ m^{-2}h^{-1}$/ $g\ m^{-2}h^{-1}$	SELECTIVITY
[99]	• Membrane: Composite regenerated cellulose, unmodified, negatively charged, and positively charged 100 kDa membranes. • Process: Diafiltration Amicon 8050 conf. Millipore.	Synthetic mixture: BSA=4.0-2.0 LF= 1.0	-BSA: 77.7 / 30.3 -LF: 95.78 / 1.1	$\alpha_{BSA/LF} = \infty$ $\alpha_{LF/BSA} = \infty$
[100]	• Membrane Ceramic 300 kDa membrane, tubular module from Tami (France) • Process: Ultrafiltration	Acid bovine whey pre-treated for the removal of casein. No concentration data.	No data	• 90.0% LF in permeate pH 5.0 (mixture minor proteins). • α-LA and β-LG fully retained.
[29]	• Membrane: PVDF 0.5 µm • Process: Electrically-enhanced crossflow microfiltration. The system was homemade.	Mixture: • LF (normal/holo-LF).=1.3 • whey proteins isolate (62.8% β-LG + 27.1% α-LA).=1.3	Total flux • 80.0 (1667 mV) • 130.0 (3333 mV)	$S_{LF/\beta\text{-}LG}$=3.0–6.7 $S_{LF/\alpha\text{-}LA}$=9.0–62.2 (**)
[30]	• Membrane: CMX-SB cationic and AMX-SB anionic membranes-Neosepta, polyethersulfone membrane –Millipore. • Process: Electro-ultrafiltration system.	Synthetic and real whey: • 200 mL whey • 0.002 g commercial LF LF/BSA=11.1	Flux at max pH 3.0 -LF = /8.9 -α-LA = /8.0 -β-LG = /41.0 -BSA = /2.0	$\alpha_{LF/\alpha\text{-}LA}$ =1.1 $\alpha_{LF/BSA}$= 4.5 $\alpha_{LF/\beta\text{-}LG}$ = 0.2
[81]	• Membrane: RC 100 kDa membranes. • Process: Ultrafiltration system.	Mixture: LF= 0.1 BSA=0.1	Total flux: -240 .0	$\alpha_{LF/BSA}$= 2.5

(**) $S_{x/y} = Tr_x/Tr_y$ $Tr = (C_{Permeate}/C_{Feed})$ x100

4.3.3 EVALUATION OF FOULING ON CHARGED ULTRAFILTRATION MEMBRANES DURING THE SEPARATION OF MILK WHEY PROTEINS

In this work the interaction between proteins and protein-membrane were evaluated by the equations (4.1 – 4.5). The zeta potentials, the relative sizes of the proteins and membrane pores and other parameters obtained from the literature were used to calculate them. The experimental values of the Hamaker constants of the proteins and membranes were difficult to identify. The order of this constant is kT, where k is the Boltzmann constant and T is the temperature. The values used to model the protein–protein interactions and the protein–membrane interactions were 13.0 10^{-21} J (an intermediate value within the reported range 10.0–16.0 10^{-21}J for protein–protein interactions [101]) and7.8 10^{-21} J, respectively (BSA and polytetrafuoroetilene) [102]

The total energies were calculated as the addition of the BSA-BSA, the BSA-LF and the BSA-Membrane and LF-Membrane electrostatic and van der Waals forces balanced by mass ratio.

The best operational conditions in terms of selectivity and fluxes had been established in the section (4.3.3), then, in this section the study of the main major obstacle to the wide application of membrane separation processes, the fouling, will be performed.

4.3.3.1 Static adsorption of protein solutions

Figure 4.17 shows the membrane ζ-potential before and after use in the adsorption experiments performed with individual proteins and their mixtures for the positively charged membrane at pH 5.0 and the negatively charged membrane at pH 9.0. The ζ-potentials were measured with 0.01M NaCl as electrolyte at the pH of study.

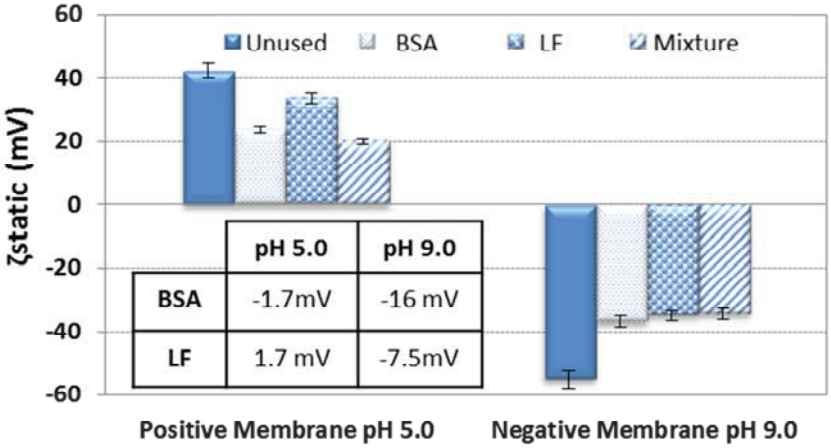

Figure 4.17. Membrane zeta potential before and after the adsorption experiments

As it is shown in Figure 4.17, at pH 5.0, the ζ-potential of the membrane after use decreased with the three solutions and the relative reduction follows the same tendency that the adsorption of the proteins for positive membranes, BSA ≈ Mixture > LF as shown in Figure 3.21b (Chapter 3).

At pH 9.0, Figure 4.17, the three adsorption experiments behaved in a similar way in terms of ζ-potential, being the charge of the membrane reduced by approximately 37.0 %. The amount of protein adsorbed is similar for LF and the mixture and slightly higher for the BSA, as shown in Figure 3.22a. These results are consistent with the results reported previously by Robertson and Zydney [103], who concluded that BSA can adsorbed quite strongly to surfaces having the same charge as the protein.

4.3.3.2 Dynamic diafiltration experiments

The changes in the membrane ζ-potential before and after each diafiltration experiment (section 4.3.2) were experimentally measured and compared to the values obtained in the static experiments (Figure 4.18).

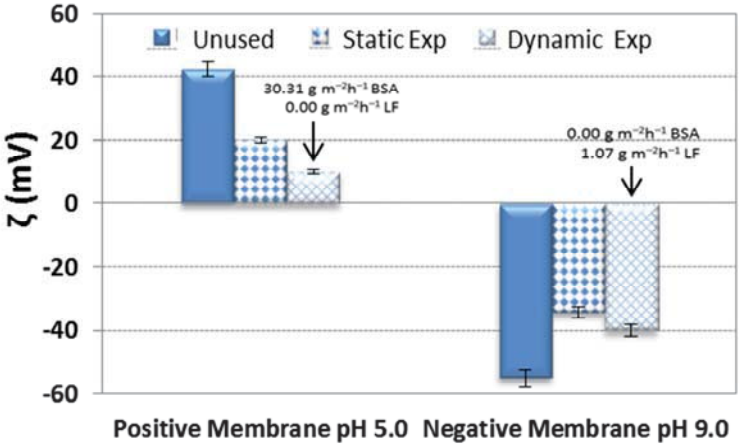

Figure 4.18. zeta potential of the unused membrane, the membrane used after adsorption (Static Exp.) and after diafiltration (Dynamic Exp.) for experiments performed with protein mixtures and positively charged membrane at pH 5.0 and negatively charged membrane at pH 9.0.

Figure 4.18 shows the comparison of membrane ζ-potential before and after protein static adsorption and diafiltration experiments at pH 5.0 and at pH 9.0. At pH 5.0 ζ-potential was reduced by 50.0 % in the static adsorption experiments increasing up to 70.0 % in the diafiltration experiments due to the contribution of the dynamic adsorption (20.0 %). In the case of the negatively charged membrane, almost the same reduction of charge is found in the case of the membranes used for the mixture adsorption and the diafiltration experiments; therefore the reduction of the membrane ζ-potential is also due to the static adsorption process.

According to the previous results, static adsorption is the main responsible for the membrane fouling under the experimental conditions selected in this Thesis.

4.3.3.3 Determination of interaction energies between surfaces through the DLVO theory

The fouling produced in the diafiltration experiments could be explained by considering the electrostatic (E_e) and Van der Walls energy (E_w) of the BSA-membrane and LF-membrane and the BSA-BSA, LF-LF,

and BSA-LF interactions calculated according to the DLVO theory. E_e depends mainly on the ζ-potential of the species, whereas Ew is influenced by the size of the protein and the membrane size. The total energy E_t is the value resulting from the addition of E_e and E_w interactions forces. The Electrostatic (E_e), van der Waals (E_w) and total (E_t) energies were calculated by the equations 4.1-4.5 for each diafiltration experiment.

The zeta potentials and the relative sizes of BSA and LF protein were experimentally obtained in this study (Chapter 3). The experimental values of the Hamaker constants of the proteins and membranes were difficult to obtain. The values Hamaker constant found in the literature to model the protein–protein interactions and the protein–membrane interactions were 13 10^{-21} J, an intermediate value within the reported range 10–16 10^{-21}J for protein–protein interactions [101], and 7.84 10^{-21} J protein–membrane interaction (BSA and polytetrafuoroetilene membrane), respectively [102]. The equilibrium distance (D) was assumed to be of 0.156 nm. This equilibrium distance corresponds to the minimum equilibrium cut-off distance and must be regarded as the distance between the outer electron shells of adjacent non-covalently interacting molecules [66].

Protein–protein energy interactions calculated according to equations 4.2 and 4.4 resulted in the range 10^{-24}-10^{-22} J. These values can be considered negligible compared to membrane–protein energy interactions, 10^{-21}-10^{-20} J, calculated according to equations 4.1 and 4.3. Figure 4.19 shows electrostatic (E_e), Van der Walls energy (E_w) and total energy (E_t) between BSA and LF proteins and the positively charged membrane at pH 5.0 (Figure 4.19a) and the negatively charged membrane at pH 9.0.

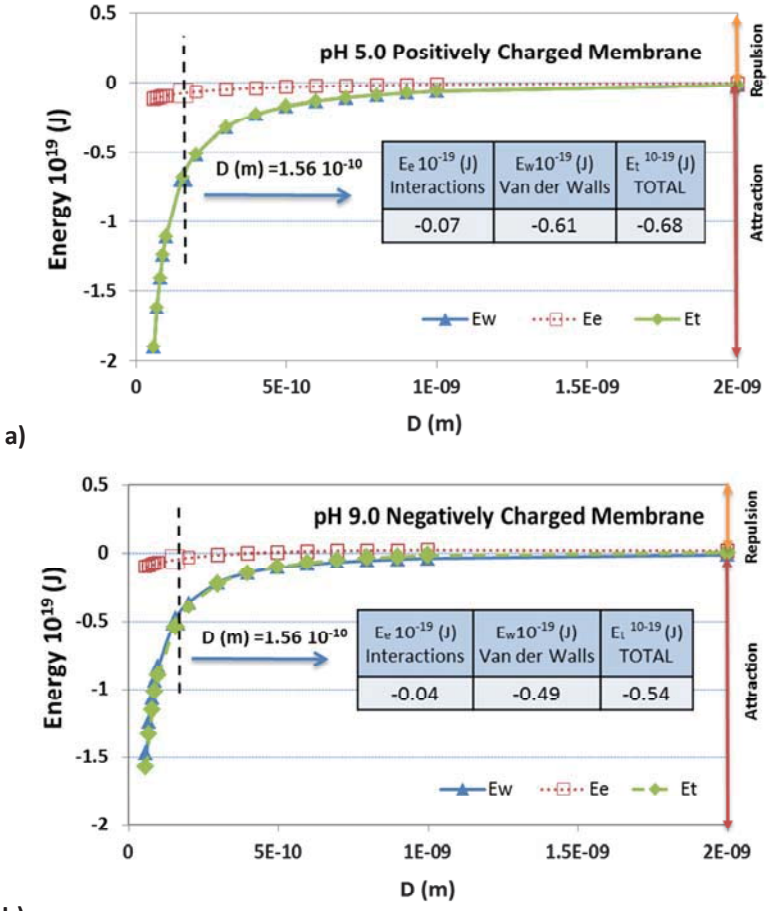

Figure 4.19. E_e, E_w E_t between BSA and LF proteins and the membrane. a) Positively charged at pH 5.0, b) Negatively charged at pH 9.0.

As it is depicted in Figure 4.19a, at pH 5.0 the total interaction energies are attractive and the Van der Waals attraction dominates the overall interaction curve. This attractive interaction energies promoted protein adsorption onto the membrane surface and facilitated membrane fouling. These results agreed with the experimental change in the ζ-potential observed for the positively charged membrane after adsorption and diafiltration (Figure 4.18) at pH 5.0. The higher concentration of BSA in the feed solution suggested that this protein was responsible for much of the membrane fouling under these

conditions [103], the adsorption measurements with values of BSA adsorbed amount higher than the founded for LF or the mixture confirms this hypothesis (Figure 3.21b). These results are consistent with the results reported previously by Robertson and Zydney [103], who concluded that proteins can adsorb quite strongly to surfaces having the same charge as the protein. In this work, protein–membrane adsorption was favored by the low surface potential of BSA compared to that of the membranes, as well as to the hydrophobic, hydrophilic, structural, and steric protein–membrane interactions [103].

In Figure 4.19b the energies depicted were in the same order of magnitude but slightly lower than those founded for pH 5.0. Although, at this pH membrane, BSA and LF were charged negatively, sizes of both proteins were in the same range than the membrane size allowing the filtration process and consequently, the fouling to occur [103]. On the other hand, although initial BSA concentration was higher than LF´s, its contribution to fouling is similar due to its closer charge to the membrane.

The values of the interaction forces described by the DLVO theory next to the zeta potential as well as the size and adsorption results lead to the conclusion that the fouling is similar at both pHs. Thus, the most suitable experimental conditions for BSA-LF separation obtained in this Thesis are pH 5.0, positively charged membrane and concentration ratio of 4.0 g L^{-1} of BSA and 1.0 g L^{-1} of LF as they achieved the highest fluxes and selectivity (section 4.3.2).

Summary

In this Chapter the viability study of BSA and LF proteins separation by means electrically enhanced membrane separation (EDUF) and Ultrafiltration system in Diafiltration mode has been performed.

The following EDUF operational conditions were selected performing a previous electrophoretic mobility test: i) 0.025M KCl solution at pH 6.0 (μ_{BSA} =-0.32 10^{-8} m^2 V^{-1} s^{-1} and μ_{LF} 0.21 10^{-8} m^2 V^{-1} s^{-1}) and ii) phosphate/dipotassium phosphate buffer 0.001M pH 7.0 (μ_{BSA} =-1.61 10^{-8} m^2 V^{-1} s^{-1} and μ_{LF} 0.24 10^{-8} m^2 V^{-1} s^{-1}).

Working with EDUF system, only BSA in low concentration was found in the permeate phase. Additionally, the concentration in the feed solution also decreased, indicating that a certain amount of BSA should be adsorbed in the membrane.

The influence size and charge of proteins in the viability of the separation process by Diafiltration was evaluated in the buffer working media: sodium acetate/acetic acid pH 5.0 (corresponding to Ip BSA) and borax-hydrocloridic acid buffer pH 9.0 (corresponding to Ip LF). At pH 5.0, BSA zeta potential was slightly negatively at the isoelectric point, 5.0. LF zeta potential was slightly positively at this pH BSA hydrodynamic diameter was of 6.64 nm and 8.21 nm for LF. At pH 9.0, BSA and LF proteins zeta potential were negative and both hydrodynamic diameters decreased to 5.52 nm and 6.99 nm respectively.

The Diafiltration separation viability, assessed by means of R_v recovery, considered the influence of the operation variables, i.e., the BSA/LF initial concentration ratio (4.0/1.0 and 2.0/1.0) and the solution pH (5.0 and 9.0), using 100.0 kDa composite regenerated cellulose membranes (CRC, Millipore). Adequate separation was achieved for the highest BSA/LF concentration ratio of 4.0/1.0, corresponding to milk whey conditions, and at pH 5.0, BSA isoelectric point.

In order to obtain the optimal conditions of the BSA/LF Diafiltration the influence of the negatively charged and positively charged membranes and buffer pH on the protein recovery was studied. At pH 5.0 working with positively membrane LF was completely retained in the feed mixture and a maximum BSA permeation flux of 30.3 g $m^{-2}h^{-1}$ was achieved. At pH 9.0 working, with negatively charged membrane, BSA was completely retained in the feed mixture and a maximum LF permeation flux of 1.1 g $m^{-2}h^{-1}$ was obtained.

Membrane fouling was studied at both pHs by the DLVO theory; the total interaction energies are attractive and the Van der Waals attraction dominates the overall interaction curve in both cases. The values of the interaction forces next to the zeta potential as well as the size and adsorption results lead to the conclusion that the fouling is also

similar at both pHs. Thus, the most suitable experimental conditions for BSA-LF separation obtained in this Thesis are pH 5.0, positively charged membrane and concentration ratio of 4.0 g L^{-1} of BSA and 1.0 g L^{-1} of LF as they achieved the highest fluxes and selectivity.

4.4 REFERENCES

The references in this section were managed by the Mendeley reference software applying the Separation Science and Technology style.

[1] T.R. Gaborski, J.L. Snyder, C.C. Striemer, D.Z. Fang, M. Hoffman, P.M. Fauchet, et al., High-performance separation of nanoparticles with ultrathin porous nanocrystalline silicon membranes, ACS Nano. 4 (2010) 6973–81.
[2] S. Galier, H.R. Balmann, The electrophoretic membrane contactor: A mass-transfer-based methodology applied to the separation of whey proteins, Sep. Purif. Technol. 77 (2011) 237–244.
[3] S. Rao, A.L. Zydney, High resolution protein separations using affinity ultrafiltration with small charged ligands, J. Memb. Sci. 280 (2006) 781–789.
[4] L. Bazinet, J. Amiot, J.-F. Poulin, D. Labbe, A. Tremblay, Patent Invention. Process and system for separation of organic charged compounds, 2008, US20080017513 A1.
[5] E. Husson, M. Araya-Farias, Y. Desjardins, L. Bazinet, Selective anthocyanins enrichment of cranberry juice by electrodialysis with ultrafiltration membranes stacked, Innov. Food Sci. Emerg. Technol. 17 (2013) 153–162.
[6] M. Aider, S. Brunet, L. Bazinet, Electroseparation of chitosan oligomers by electrodialysis with ultrafiltration membrane (EDUF) and impact on electrodialytic parameters, J. Memb. Sci. 309 (2008) 222–232.
[7] D. Labbe, M. Arayafarias, A. Tremblay, L. Bazinet, Electromigration feasibility of green tea catechins, J. Memb. Sci. 254 (2005) 101–109.
[8] L. Firdaous, P. Dhulster, J. Amiot, A. Gaudreau, D. Lecouturier, R. Kapel, et al., Concentration and selective separation of bioactive peptides from an alfalfa white protein hydrolysate by electrodialysis with ultrafiltration membranes, J. Memb. Sci. 329 (2009) 60–67.
[9] J.-F. Poulin, J. Amiot, L. Bazinet, Simultaneous separation of acid and basic bioactive peptides by electrodialysis with ultrafiltration membrane, J. Biotechnol. 123 (2006) 314–28.
[10] C. Roblet, A. Doyen, J. Amiot, L. Bazinet, Impact of pH on ultrafiltration membrane selectivity during electrodialysis with ultrafiltration membrane (EDUF) purification of soy peptides from a complex matrix, J. Memb. Sci. 435 (2013) 207–217.
[11] O.M. Kattan Readi, M. Gironès, K. Nijmeijer, Separation of complex mixtures of amino acids for biorefinery applications using electrodialysis, J. Memb. Sci. 429 (2013) 338–348.
[12] A. Doyen, L. Saucier, L. Beaulieu, Y. Pouliot, L. Bazinet, Electroseparation of an antibacterial peptide fraction from snow crab by-products hydrolysate by electrodialysis with ultrafiltration membranes, Food Chem. 132 (2012) 1177–1184.
[13] M. Vanhoute, L. Firdaous, L. Bazinet, R. Froidevaux, D. Lecouturier, D. Guillochon, et al., Effect of haem on the fractionation of bovine haemoglobin

peptic hydrolysate by electrodialysis with ultrafiltration membranes, J. Memb. Sci. 365 (2010) 16–24.
[14] G.M. Rios, P. Freund, Design and performance of ceramic EUF process for protein concentration, Key Eng. Mater. 61-62 (1992) 255–260.
[15] C.W. Robinson, M.H. Siegel, A. Condemine, C. Fee, T.Z. Fahidy, B.R. Glick, Pulsed-electric-field crossflow ultrafiltration of bovine serum albumin, J. Memb. Sci. 80 (1993) 209–220.
[16] G.M. Rios, H. Rakotoarisoa, B. Tarodo de la Fuente, Basic transport mechanisms of ultrafiltration in the presence of an electric field, J. Memb. Sci. 38 (1988) 147–159.
[17] S. Lentsch, P. Aimar, J.L. Orozco, Enhanced separation of albumin-poly(ethylene glycol) by combination of ultrafiltration and electrophoresis, J. Memb. Sci. 80 (1993) 221–232.
[18] W.R. Bowen, R.S. Kingdon, H.A.M. Sabuni, Electrically enhanced separation processes: the basis of in situ intermittent electrolytic membrane cleaning (IIEMC) and in situ electrolytic membrane restoration (IEMR), J. Memb. Sci. 40 (1989) 219–229.
[19] R.J. Wakeman, Electrically enhanced microfiltration of albumin suspensions, Food Bioprod. Process. 76 (1998) 53–59.
[20] Y.G. Park, Improvement of dead-end filtration during crossflow electro-microfiltration of proteins, J. Ind. Eng. Chem. 11 (2005) 692–699.
[21] E. Iritani, Y. Mukai, Y. Kiyotomo, Effects of electric field on dynamic behaviors of dead-end inclined and downward ultrafiltration of protein solutions, J. Memb. Sci. 164 (2000) 51–57.
[22] J.M. Radovich, B. Behnam, C. Mullon, Steady-State modeling of the Electroultrafiltration at constant concentration, Sep. Sci. Technol. 20 (1985) 315–329.
[23] S. Oussedik, D. Belhocine, H. Grib, H. Lounici, D.L. Piron, N. Mameri, Enhanced ultrafiltration of bovine serum albumin with pulsed electric field and fluidized activated alumina, Desalination. 127 (2000) 59–68.
[24] G. Brunner, E. Okoro, Reduction of membrane fouling by means of an electric field during ultrafiltration of protein solutions, Phys. Chem. Chem. Phys. 93 (1989) 1026–1032.
[25] P. Zumbusch, W. Kulcke, G. Brunner, Use of alternating electrical fields as anti-fouling strategy in ultrafiltration of biological suspensions – Introduction of a new experimental procedure for crossflow filtration, J. Memb. Sci. 142 (1998) 75–86.
[26] H.M. Huotari, G. Trägårdh, I.H. Huisman, Crossflow membrane filtration rnhanced by an rxternal DC rlectric field: a review, Chem. Eng. Res. Des. 77 (1999) 461–468.
[27] J. Cheng, Y. Li, T.S. Chung, S.-B. Chen, W.B. Krantz, High-performance protein separation by ion exchange membrane partitioned free-flow isoelectric focusing system, Chem. Eng. Sci. 63 (2008) 2241–2251.

[28] J.-H. Cheng, T.S. Chung, S.H. Neo, Investigation of mass transfer in the ion-exchange-membrane-partitioned free-flow IEF system for protein separation, Electrophoresis. 30 (2009) 2600–12.
[29] G. Brisson, M. Britten, Y. Pouliot, Electrically-enhanced crossflow microfiltration for separation of lactoferrin from whey protein mixtures, J. Memb. Sci. 297 (2007) 206–216.
[30] N. Ndiaye, Y. Pouliot, L. Saucier, L. Beaulieu, L. Bazinet, Electroseparation of bovine lactoferrin from model and whey solutions, Sep. Purif. Technol. 74 (2010) 93–99.
[31] U. Kulozik, Variation of the calcium content in skim milk by diafiltration and ion exchange – Effects on permeation rate and structure of deposited layers in the RO, J. Memb. Sci. 145 (1998) 91–97.
[32] J.F. Kim, G. Székely, I.B. Valtcheva, A.G. Livingston, Increasing the sustainability of membrane processes through cascade approach and solvent recovery—pharmaceutical purification case study, Green Chem. 16 (2014) 133.
[33] L. Zhao, H. Zhao, P. Nguyen, A. Li, L. Jiang, Q. Xia, et al., Separation performance of multi-components solution by membrane technology in continual diafiltration mode, Desalination. 322 (2013) 113–120.
[34] A.T. Phillips, M.W. Signs, Desalting, concentration, and buffer exchange by dialysis and ultrafiltration, in: J.E. Coligan, B.M. Dunn, D.W. Speicher, P.T. Wingfield (Eds.), Curr. Protoc. Protein Sci., 4th Ed, John Wiley & Sons, Inc, 2005.
[35] F. Miao, A. Velayudhan, E. DiBella, J. Shervin, M. Felo, M. Teeters, et al., Theoretical analysis of excipient concentrations during the final ultrafiltration/diafiltration step of therapeutic antibody, Biotechnol. Prog. 25 (2009) 964–72.
[36] Z. Li, W. Youravong, A. H-Kittikun, Separation of proteases from yellowfin tuna spleen by ultrafiltration, Bioresour. Technol. 97 (2006) 2364–2370.
[37] H. Yoshii, T. Furuta, T. Yonehara, D. Ito, Y.Y. Linko, P. Linko, Refolding of denatured/reduced lysozyme at high concentration with diafiltration, Biosci. Biotechnol. Biochem. 64 (2000) 1159–65.
[38] A.L. Zydney, Protein separations using membrane filtration: new opportunities for whey fractionation, Int. Dairy J. 8 (1998) 243–250.
[39] B. Cheang, A.L. Zydney, Separation of alpha-lactalbumin and beta-lactoglobulin using membrane ultrafiltration, Biotechnol. Bioeng. 83 (2003) 201–9.
[40] C. Baldasso, T.C. Barros, I.C. Tessaro, Concentration and purification of whey proteins by ultrafiltration, Desalination. 278 (2011) 381–386.
[41] R. Atra, G. Vatai, E. Bekassy-Molnar, A. Balint, Investigation of ultra- and nanofiltration for utilization of whey protein and lactose, J. Food Eng. 67 (2005) 325–332.
[42] M.M.H. El-Sayed, H. a Chase, Trends in whey protein fractionation, Biotechnol. Lett. 33 (2011) 1501–11.
[43] E. Tsakali, K. Petrotos, A.D. Allessandro, A review on whey composition and the methods used for its utilization for food and pharmaceutical products, in:

6th Int. Conf. Simul. Model. Food Bio-Industry. FOODSIM, Braganca, Portugal, 2010.
[44] G. Walsh, Proteins: biochemistry and biotechnology, 2nd Ed, John Wiley & Sons, New York, USA, 2014.
[45] B.R. Shri Ramaswamy, Huajiang Huang, Separation and purification technologies in biorefineries, 2013.
[46] A. Dakheel, N.A. Darwish, A review of colloidal interactions in membrane separation, Iran. J. Energy Environ. 1 (2010) 144–159.
[47] J.A. Howell, V. Sanchez, R.W. Field, Membranes in bioprocessing: theory and applications, 1st Ed, Chapman & Hall, London, UK, 1993.
[48] M. Kumar, M. Ulbricht, Novel antifouling positively charged hybrid ultrafiltration membranes for protein separation based on blends of carboxylated carbon nanotubes and aminated poly(arylene ether sulfone), J. Memb. Sci. 448 (2013) 62–73.
[49] J. Huang, K. Zhang, K. Wang, Z. Xie, B. Ladewig, H. Wang, Fabrication of polyethersulfone-mesoporous silica nanocomposite ultrafiltration membranes with antifouling properties, J. Memb. Sci. 423-424 (2012) 362–370.
[50] Y. Mo, A. Tiraferri, N.Y. Yip, A. Adout, X. Huang, M. Elimelech, Improved antifouling properties of polyamide nanofiltration membranes by reducing the density of surface carboxyl groups, Environ. Sci. Technol. 46 (2012) 13253–61.
[51] Y.-L. Su, W. Cheng, C. Li, Z. Jiang, Preparation of antifouling ultrafiltration membranes with poly(ethylene glycol)-graft-polyacrylonitrile copolymers, J. Memb. Sci. 329 (2009) 246–252.
[52] Y. Wang, X. Zhang, B. Shi, L. Jia, X. Zhou, Preparation of anti-fouling polyethersulfone ultrafiltration membrane by an external high voltage electric enhancing method, Sep. Sci. Technol. 45 (2010) 2280–2286.
[53] W. Shi, M.M. Benjamin, Effect of shear rate on fouling in a Vibratory Shear Enhanced Processing (VSEP) RO system, J. Memb. Sci. 366 (2011) 148–157.
[54] O. Akoum, R. Chotard-Ghodsnia, L.H. Ding, M.Y. Jaffrin, Ultrafiltration of low-heat and UHT skim milks with a shear-enhanced vibrating filtration system, Sep. Sci. Technol. 38 (2003) 571–589.
[55] Y.H. Choi, J.H. Kweon, D.I. Kim, S. Lee, Evaluation of various pretreatment for particle and inorganic fouling control on performance of SWRO, Desalination. 247 (2009) 137–147.
[56] Y. Zhiqing, L. Xiaolong, W. Chunrui, W. Xuan, Effect of pretreatment on membrane fouling and VMD performance in the treatment of RO-concentrated wastewater, Desalin. Water Treat. 51 (2013) 6994–7003.
[57] S.-O. Baek, I.-S. Chang, Pretreatments to control membrane fouling in membrane filtration of secondary effluents, Desalination. 244 (2009) 153–163.
[58] C.-H. Lai, Y.-H. Chen, H.-H. Yeh, Effects of feed water quality and pretreatment on NF membrane fouling control, Sep. Sci. Technol. 48 (2013) 1609–1615.

[59] N. Hilal, O.O. Ogunbiyi, N.J. Miles, R. Nigmatullin, Methods employed for control of fouling in MF and UF membranes: a comprehensive review, Sep. Sci. Technol. 40 (2005) 1957–2005.
[60] C.Y. Tang, T.H. Chong, A.G. Fane, Colloidal interactions and fouling of NF and RO membranes: a review, Adv. Colloid Interface Sci. 164 (2011) 126–43.
[61] N.S. Pujar, A.L. Zydney, Electrostatic and electrokinetic interactions during protein transport through narrow pore membranes, Ind. Eng. Chem. Res. 33 (1994) 2473–2482.
[62] C.M. Roth, B.L. Neal, A.M. Lenhoff, Van der Waals interactions involving proteins, Biophys. J. 70 (1996) 977–87.
[63] Y. Chen, H. Kim, Monte Carlo simulation of pore blocking and cake formation by interfacial interactions during membrane filtration, Desalination. 233 (2008) 258–266.
[64] P. Aimar, S. Baklouti, V. Sanchez, Membrane—solute interactions: influence on pure solvent transfer during ultrafiltration, J. Memb. Sci. 29 (1986) 207–224.
[65] S. Lee, S. Kim, J. Cho, E.M.V. Hoek, Natural organic matter fouling due to foulant–membrane physicochemical interactions, Desalination. 202 (2007) 377–384.
[66] J.A. Brant, A.E. Childress, Membrane–colloid interactions: comparison of extended DLVO predictions with AFM force measurements, Environ. Eng. Sci. 19 (2002) 413–427.
[67] S. Salgın, S. Takaç, T.H. Özdamar, A parametric study on protein membrane ionic environment interactions for membrane fouling, Sep. Sci. Technol. 40 (2005) 1191–1212.
[68] L. Huang, M.T. Morrissey, Fouling of membranes during microfiltration of surimi wash water: Roles of pore blocking and surface cake formation, J. Memb. Sci. 144 (1998) 113–123.
[69] A.-S. Jönsson, B. Jönsson, Colloidal fouling during ultrafiltration, Sep. Sci. Technol. 31 (1996) 2611–2620.
[70] R.J. Hunter, Zeta potential in colloid science: principles and applications, 2nd Ed, Academic Press, London, UK, 1981.
[71] J. Ku, P. Stroeve, Protein diffusion in charged nanotubes : “On - Off ” behavior of molecular transport, Langmuir. 20 (2004) 2030–2032.
[72] S.A. Moore, B.F. Anderson, C.R. Groom, M. Haridas, E.N. Baker, Three-dimensional structure of diferric bovine lactoferrin at 2.8 A resolution, J. Mol. Biol. 274 (1997) 222–36.
[73] P.G. Thakurta, D. Choudhury, R. Dasgupta, J.K. Dattagupta, Tertiary structural changes associated with iron binding and release in hen serum transferrin: a crystallographic and spectroscopic study, Biochem. Biophys. Res. Commun. 316 (2004) 1124–31.
[74] R. van Reis, Charged filtration membranes and uses therefore, WO 01/08792 A2, 2001.

[75] V. Adam, O. Zitka, P. Dolezal, L. Zeman, A. Horna, J. Hubalek, et al., Lactoferrin isolation using monolithic column coupled with spectrometric or micro-amperometric detector, Sensors. 8 (1995) 464–487.
[76] A. Rektor, G. Vatai, Membrane filtration of Mozzarella whey, Desalination. 162 (2004) 279–286.
[77] K.W.K. Yee, D.E. Wiley, J. Bao, Whey protein concentrate production by continuous ultrafiltration: Operability under constant operating conditions, J. Memb. Sci. 290 (2007) 125–137.
[78] A. Ho, J. Perera, G. Stevens, The effect of protein concentration on electrophoretic mobility, J. Colloid Interface Sci. 224 (2000) 140–147.
[79] A. Salis, M. Boström, L. Medda, F. Cugia, B. Barse, D.F. Parsons, et al., Measurements and theoretical interpretation of points of zero charge/potential of BSA protein, Langmuir. 27 (2011) 11597–604.
[80] F. Zhang, M.W.A. Skoda, R.M.J. Jacobs, R.A. Martin, C.M. Martin, F. Schreiber, Protein interactions studied by SAXS: effect of ionic strength and protein concentration for BSA in aqueous solutions, J. Phys. Chem. B. 111 (2007) 251–9.
[81] M. Nyström, P. Aimar, S. Luque, M. Kulovaara, S. Metsämuuronen, Fractionation of model proteins using their physiochemical properties, Colloids Surfaces A Physicochem. Eng. Asp. 138 (1998) 185–205.
[82] I. Mela, E. Aumaitre, A.-M. Williamson, G.E. Yakubov, Charge reversal by salt-induced aggregation in aqueous lactoferrin solutions, Colloids Surf. B. Biointerfaces. 78 (2010) 53–60.
[83] B. Jachimska, M. Wasilewska, Z. Adamczyk, Characterization of globular protein solutions by dynamic light scattering, electrophoretic mobility, and viscosity measurements, Langmuir. 24 (2008) 6866–72.
[84] W.R. Bowen, P.M. Williams, The osmotic pressure of electrostatically stabilized colloidal dispersions, J. Colloid Interface Sci. 184 (1996) 241–250.
[85] F. Lampreave, A. Piñeiro, J.H. Brock, H. Castillo, L. Sánchez, M. Calvo, Interaction of bovine lactoferrin with other proteins of milk whey, Int. J. Biol. Macromol. 12 (1990) 2–5.
[86] S. Bhushan, M.R. Etzel, Charged ultrafiltration membranes increase the selectivity of whey protein separations, J. Food Sci. 74 (2009) E131–9.
[87] S. Cowan, S. Ritchie, Modified polyethersulfone (PES) ultrafiltration membranes for enhanced filtration of whey proteins, Sep. Sci. Technol. 42 (2007) 2405–2418.
[88] M.M. Rohani, A.L. Zydney, Effect of surface charge distribution on protein transport through semipermeable ultrafiltration membranes, J. Memb. Sci. 337 (2009) 324–331.
[89] D. Lucas, M. Rabiller-Baudry, L. Millesime, B. Chaufer, G. Daufin, Extraction of α-lactalbumin from whey protein concentrate with modified inorganic membranes, J. Memb. Sci. 148 (1998) 1–12.

[90] H.U. Osmanbeyoglu, T.B. Hur, H.K. Kim, Thin alumina nanoporous membranes for similar size biomolecule separation, J. Memb. Sci. 343 (2009) 1–6.
[91] R. van Reis, J.M. Brake, J. Charkoudian, D.B. Burns, A.L. Zydney, High-performance tangential flow filtration using charged membranes, J. Memb. Sci. 159 (1999) 133–142.
[92] P.D. Peeva, T. Knoche, T. Pieper, M. Ulbricht, Cross-flow ultrafiltration of protein solutions through unmodified and surface functionalized polyethersulfone membranes – effect of process conditions on separation performance, Sep. Purif. Technol. 92 (2012) 83–92.
[93] C. Ho, A. Zydney, A combined pore blockage and cake filtration model for protein fouling during microfiltration, J. Colloid Interface Sci. 232 (2000) 389–399.
[94] D. Lucas, M. Rabiller-Baudry, F. Michel, B. Chaufer, Role of the physico-chemical environment on ultrafiltration of lysozyme with modified inorganic membrane, Colloids Surfaces A Physicochem. Eng. Asp. 136 (1998) 109–122.
[95] I. Gitlin, J.D. Carbeck, G.M. Whitesides, Why are proteins charged? Networks of charge-charge interactions in proteins measured by charge ladders and capillary electrophoresis, Angew. Chemie Int. Ed. 45 (2006) 3022–60.
[96] V.T. Kuberkar, R.H. Davis, Modeling of fouling reduction by secondary membranes, J. Memb. Sci. 168 (2000) 243–258.
[97] M. Nyström, P. Aimar, S. Luque, M. Kulovaara, Fractionation of model proteins using their physiochemical properties, 138 (1998) 185–205.
[98] G. Brisson, M. Britten, Y. Pouliot, Effect of iron saturation on the recovery of lactoferrin in rennet whey coming from heat-treated skim milk, J. Dairy Sci. 90 (2007) 2655–64.
[99] V. Valiño, M.F. San Román, R. Ibañez, I. Ortiz, Improved separation of bovine serum albumin and lactoferrin mixtures using charged ultrafiltration membranes, Sep. Purif. Technol. 125 (2014) 163–169.
[100] M.C. Almecija, Obtención de Lactoferrina bovina mediante ultrafiltración de latosuero, Thesis work. Universidad de Granada, 2007.
[101] V.A. Parsegian, Van der Waals forces: a Handbook for biologists, chemists, engineers, and physicists, 1st Ed, Cambridge University, New York, USA, 2006.
[102] A.L. Zydney, N.S. Pujar, Protein transport through porous membranes: effects of colloidal interactions, Colloids Surfaces A Physicochem. Eng. Asp. 138 (1998) 133–143.
[103] B.C. Robertson, A.L. Zydney, Protein adsorption in asymmetric ultrafiltration membranes with highly constricted pores, J. Colloid Interface Sci. 134 (1990) 563–575.

5

CONCLUSIONS AND CHALLENGES FOR FUTURE RESEARCH

5.1. CONCLUSIONS

This thesis assesses the quantification, characterization and separation of two biomolecules with high added value: Bovine serum albumin (BSA) and Lactoferrin (LF). The main results and conclusions are summarized in the following paragraphs:

Development of a quantitative BSA/LF measurement method

A HPLC method based on *ion-exchange Chromatography* has been adapted for the qualitative and quantitative determination of BSA and LF in mixtures *using a Cimac™-SO_3^-* column and sodium phosphate/dipotassium phosphate buffer as mobile phase. This method allows the qualitative and quantitative individual determination of BSA and LF in buffer solutions in the range of 0.01 to 4.0 g L^{-1} with a detection limit lower than 0.01 g L^{-1}.

A quantification method based on Fluorescence and Ultraviolet (UV-vis) techniques has been developed for the qualitative and quantitative determination of BSA and LF in electrolytic solutions in a range up to 1.0 g L^{-1}. The method implies two steps. In a first step the relative percentage of BSA in the sample is obtained by Fluorescence

and in a second step, the total protein concentration is obtained by UV-vis. The fitting of the Fluorescence and UV-vis spectra by the Fityk software is needed to determine the parameters to be applied in the calibration curves.

Protein and membrane characterization

BSA and LF proteins were characterized by means of foam stability, zeta potential and size, aggregation Polysulfone and CRC membranes were characterized by means of zeta potential and adsorption capacity. Both, proteins and membranes, characterizations were performed in different conditions relevant for the proposed separation process.

Zeta potential of BSA/LF proteins

Zeta potential of both proteins was determined by Electrophoretic Light Scattering (ELS):

Under the experimental conditions used in this study, the difference in the zeta potential values of BSA using different electrolytes (KCl, NaCl 1:1 and $CaCl_2$ 1:2) appeared to be significant at pHs above the isoelectric point, whereas in the case of LF this difference in zeta potential is found at pHs below the isoelectric point.

Working with electrolytic solutions (0.01 - 0.1 M KCl), the measured zeta potential decreased with increasing electrolyte concentration for both proteins. BSA zeta potential lay in the range 35.0 mV to -70.0 mV and the isoelectric points (Ip) were in the pH range 3.82 - 5.52 while LF zeta potential lay in the range 45.0 mV to -30.0 mV being the corresponding isoelectric points (Ip) in the pH range 5.66 - 9.33.

Working with buffer solutions, BSA protein reached the highest zeta potential (absolute value) of -35.0 mV, in sodium phosphate/dipotassium phosphate buffer at pH 7.0. This value was -8.0 mV for LF protein working with borax/hydrochloric acid buffer and KCl solutions at pH 9.0.

The decrease in protein concentration in the case of BSA implied an increase in the absolute value of the zeta potential and a decrease in the isoelectric point, from pH 4.90 to pH 3.87. However, in the case of LF, the decrease in the protein concentration did not lead to significant changes in the zeta potential behavior. The zeta potential of the protein mixture exhibited an intermediate behavior between both individual curves.

The Charged Regulation Model can be used to predict BSA Ip. On the other hand, the isoelectric point (Ip) of LF is not adequately predicted using this tool.

Molecular size of proteins

BSA and LF size values were determined by Dynamic Light Scattering (DLS) at different pH and protein concentrations.

Measured hydrodynamic diameter of BSA presented an average value of 7.54 nm. Measured hydrodynamic diameter of LF tends to increase in size from pH 4.0 to pH 7.0 (8.53 - 12.28 nm) and slightly decrease in size from pH 8.0 to pH 9.0 (12.00 - 8.86 nm). BSA molecules did not aggregate while a percentage in mass from 0.2-4.0 % of aggregates is found in the LF samples. The estimated molecular weights lay in the range 74.90 - 148.80 kDa for BSA and 105.60 - 295.80 kDa for LF.

BSA showed measured diameters equal to calculated stokes diameters (6.92 nm). LF showed measured diameters higher than calculated stokes diameters, due to the formation of aggregates.

Zeta potential of the membranes

The zeta potential of the two polysulfone membranes was measured in the pH range from 2.0 to 10.0, employing 0.01M NaCl as electrolyte reporting values in the range from -55.0 mV to 5.0 mV. The CRC unmodified membrane zeta potential ranged from 26.0 to -28.0 mV showing an isoelectric point around pH 3.5. The zeta potential of the positive membrane changed from 30.0 to 60.0 mV, while the zeta

potential of the negative membrane ranges from -2.0 to -60.0 mV. None of them presented isoelectric point.

Membrane adsorption capacity

The total amount of protein adsorbed with time for unmodified, positively and negatively charged membranes in different adsorption conditions was determined.

The total amount adsorbed was 0.2 10^{-6} g cm^{-2} for BSA and 0.1 10^{-6} to 0.14 10^{-6} g cm^{-2} for LF. In all the cases the amount of BSA adsorbed was greater than the amount of LF, being this difference lower at pH 9.0 with positively charged membrane.

The static adsorption was fitted to the Jones and O'Melia Model kinetic: $\Gamma(t)=\Gamma_e\ (1-e^{-k^0 t})$. Using the nonlinear least-square fit and the experimental values, the parameters Γ_e y k_0 were obtained with a correlation coefficient higher than 0.99 in all cases.

BSA/LF separation viability

Electrically enhanced membrane separation

The operation conditions allowing the highest BSA and LF proteins electrophoretic mobilities were determined and applied in the EDUF separation process:

i) 0.025M KCl solution at pH 6.0, μ_{BSA} =-0.32 10^{-8} m^2 V^{-1} s^{-1} and μ_{LF} 0.21 10^{-8} m^2 V^{-1} s^{-1}.

ii) phosphate/dipotassium phosphate buffer 0.001M at pH 7.0, μ_{BSA} =-1.61 10^{-8} m^2 V^{-1} s^{-1} and μ_{LF} 0.24 10^{-8} m^2 V^{-1} s^{-1}.

Working with EDUF system, only BSA at low concentration was found in the permeate phase.

Ultrafiltration system in Diafiltration mode

The diafiltration separation viability, assessed by means of R_v recovery, considered the influence of the operation variables, i.e., the BSA/LF initial concentration ratio (4.0/1.0 and 2.0/1.0) and the solution pH (5.0 and 9.0), using 100.0 kDa CRC membranes. Adequate separation

was achieved for the highest BSA/LF concentration ratio of 4.0/1.0, corresponding to milk whey conditions, and at pH 5.0 (BSA isoelectric point).

In order to obtain the optimal conditions of the BSA/LF diafiltration, the influence of the negatively charged and positively charged membranes and the buffer pH on the protein recovery was studied. At pH 5.0 working with positively membrane, LF was completely retained in the feed mixture and a maximum BSA permeation flux of 30.31 g $m^{-2}h^{-1}$ was achieved. At pH 9.0 working with negatively charged membrane, BSA was completely retained in the feed mixture and a maximum LF permeation flux of 1.07 g $m^{-2}h^{-1}$ was obtained.

Membrane fouling, after diafiltration process, was studied at both pHs (5.0 and 9.0) by the Derjaguin, Landau, Verwey, and Overbeek (DLVO) theory; the total interaction energies were attractive and the Van der Waals attraction dominated the overall interaction curve at both pHs. The values of interaction energies led to the conclusion that the fouling formation was similar in both cases.

5.2. CHALLENGES FOR FUTURE RESEARCH

This thesis intends to open up the possibility of new pathways for the development whey protein isolation assisted by membranes. In spite of the promising results obtained thought the chapters of this thesis, there are still challenges that must be overcome before this process can be scaled up.

BSA isolation from a binary mixture with LF has been satisfactorily performed by positively charged membranes at pH 5.0 but the fluxes obtained for the LF isolations were not satisfactory enough to be considered for higher scale.

The research and development of new electrolyte media able to guarantee higher electrophoretic mobilities and better control of the operational conditions are needed in the BSA/LF separation by means of EDUF, in order to completely achieve competitive conditions in terms of fluxes and selectivities.

Once the isolation of BSA has been satisfactorily achieved, optimization of the separation by means of integration of a serial process is necessary in order to isolate LF.

Finally, being the adequate operational condition requirements fulfilled, the use of real whey effluents would be necessary to optimize the process.

5

CONCLUSIONES Y TRABAJO FUTURO

5.1. CONCLUSIONES

En esta tesis se ha llevado a cabo la cuantificación, caracterización y separación de dos biomoléculas de alto valor añadido: la albúmina sérica bovina (BSA) y la lactoferrina (LF). Las principales aportaciones y conclusiones obtenidas se resumen en los siguientes párrafos:

Desarrollo de un método para la medida cuantitativa de BSA y de LF

La cuantificación individual de las proteínas BSA y LF en mezclas binarias no electrolíticas, en un rango de concentraciones de 0.01 a 4.0 g L^{-1}, se llevó a cabo adaptando un método cromatográfico que utiliza la columna de intercambio iónico *Cimac™-*SO_3^- y el buffer de fosfato sódico/fosfato dipotásico como fase móvil, con un límite de detección menor de 0.01 g L^{-1}.

La necesidad de obtener un método de medida de ambas proteínas en medios con alta concentración de electrolitos impulsó el desarrollo de un método específico de cuantificación basado en absorción en Fluoroscencia y Ultravioleta Visible (UV-vis). El método

implica dos etapas: En una primera etapa el porcentaje relativo de la proteína BSA en la muestra se determina mediante Fluorescencia. En una segunda etapa la cantidad total de proteína se determina mediante UV-vis. El software de ajuste Fityc se utiliza para la obtención de los parámetros necesarios de calibración. El método es válido para un rango de concentraciones de hasta 1.0 g L^{-1} de cada proteína individual.

Caracterización de proteínas y membranas

Las proteínas BSA y LF se caracterizaron mediante la medida de su potencial zeta, punto isoeléctrico, tamaño, agregación. Así mismo, las membranas de polisulfona y Celulosa Regenerada Compuesta (CRC) utilizadas en el estudio de la separación de proteínas, se caracterizaron mediante la determinación del potencial zeta y la capacidad de adsorción. Ambas caracterizaciones fueron realizadas en diferentes condiciones relevantes para el proceso de separación propuesto.

Potencial zeta de las proteínas

El potencial zeta de ambas proteínas se determinó mediante Electrophoretic Light Scattering (ELS):

Las diferencias en los valores de potencial zeta de la proteína BSA en función del pH, utilizando diferentes tipo de electrolitos (KCl, NaCl 1:1 y $CaCl_2$ 1:2), no fueron significativas, sin embargo, para el caso de la proteína LF, se encontraron diferencias a pHs por debajo de su correspondiente punto isoeléctrico.

Trabajando con diferentes concentraciones de electrolito, 0.01 - 0.1 M KCl, en función del pH, el potencial zeta de la BSA presentó valores comprendidos entre 35.0 mV a -70.0 mV y sus puntos isoeléctricos se mantuvieron entre los pHs 3.82 - 5.52. En el caso de la LF estos valores se encontraron en el rango de 45.0 mV a -30.0 mV, mientras que los puntos isoeléctricos se encontraron entre los pHs 5.66 - 9.33.

En el caso de utilizar disoluciones buffer, el mayor valor de potencial zeta obtenido (en valor absoluto) para la BSA fue de -35.0 mV para el buffer fosfato sódico/fosfato dipotásico, pH 7.0. Para la LF, el mayor valor (en valor absoluto) de potencial zeta alcanzado, fue de -8.0 mV, trabajando con el buffer bórax/ácido clorhídrico y con la disolución KCl, pH 9.0.

Cuando se utilizó la mezcla binaria de las proteínas BSA y LF, la disminución de la concentración de proteína se tradujo en un crecimiento de los valores de potencial zeta (en términos absolutos) y un decrecimiento de los puntos isoeléctricos de 4.90 a 3.87 para la BSA. En cambio, la concentración de LF no tuvo una influencia significativa ni en los valores de potencial zeta ni en los correspondientes puntos isoeléctricos.

El Modelo de Regulación de Carga predijo satisfactoriamente los puntos isoeléctricos de la proteína BSA. En el caso de la LF el modelo no permitió describir dichos valores.

Tamaño Molecular de Proteínas

El tamaño molecular de las proteínas BSA y LF se determinó mediante Dynamic Light Scattering (DLS):

Los valores de diámetro hidrodinámico obtenidos para la BSA presentaron un tamaño medio de 7.54 nm. Para la LF los valores se incrementaron entre pH 4.0 y pH 7.0 (8.53 - 12.28 nm) y decrecieron entre pH 8.0 y pH 9.0 (12.00 - 8.86 nm). No se encontraron agregados de BSA en las muestras mientras que la LF presentó un porcentaje variable entre 0.2 y 0.4 % en masa de agregados. Los valores estimados de peso molecular fueron respectivamente, 74.90 - 148.80 kDa para la BSA y 105.60 - 295.80 kDa para la LF.

La BSA presentó valores de diámetros medidos similares a los valores calculados de diámetro de Stokes (6.92 nm). La presencia de agregados en la LF dio lugar a valores de diámetro medidos diferentes a los diámetros de Stokes calculados.

Potencial zeta de las membranas

Los valores de potencial zeta obtenidos para las membranas de polisulfona presentaron valores comprendidos entre -55.0 mV y 5.0 mV. Los potenciales zeta de la membrana sin modificar se encontraron en el rango de 26.0 a -28.0 mV, estando su punto isoeléctrico a pH 3.5. El rango de potencial zeta de las membranas cargadas positivamente fue de 30.0 a 60.0 mV y de -2.0 a -60.0 mV para las membranas cargadas negativamente. En el rango de pH estudiado, ninguna de las dos membranas alcanzó su punto isoeléctrico.

Capacidad de adsorción de la membrana

La cantidad total de proteína adsorbida en las membranas cargadas positiva y negativamente se determinó en a diferentes condiciones de pH.

La cantidad total adsorbida fue de 0.2 10^{-6} g cm^{-2} para la BSA y en el rango de 0.1 10^{-6} a 0.14 10^{-6} g cm^{-2} para la LF. Para todos los casos la cantidad de BSA adsorbida fue mayor que la de LF, siendo la diferencia menor a pH 9.0 trabajando con la membrana positivamente cargada.

La adsorción estática se ajustó al modelo cinético de Jones and O'Melia: $\Gamma(t)=\Gamma_e\,(1-e^{-k^0 t})$ con un coeficiente de correlación de 0.99.

Viabilidad de la separación de las proteínas BSA/LF en mezclas binarias

Ultrafiltración combinada con Electrodiálisis (EDUF)

Se determinaron las condiciones de trabajo que permitieron las mayores movilidades electroforéticas de las proteínas BSA y LF, para su aplicación en la tecnología de EDUF:

i) 0.025M KCl a pH 6.0, μ_{BSA} =-0.32 10^{-8} m^2 V^{-1} s^{-1}, μ_{LF} 0.21 10^{-8} m^2 V^{-1} s^{-1}

ii) fosfato sódico-fosfato dipotásico de concentración 0.001M a pH 7.0, μ_{BSA} =-1.61 10^{-8} m^2 V^{-1} s^{-1}, μ_{LF} 0.24 10^{-8} m^2 V^{-1} s^{-1}.

En estas condiciones, solo fue posible separar BSA en bajas concentraciones.

Ultrafiltración operando en modo Diafiltración

La viabilidad del proceso de separación de las proteínas BSA y LF mediante diafiltración se llevó a cabo, teniendo en cuenta las propiedades estructurales de las proteínas, mediante el estudio de las variables de operación; relación de concentración BSA/LF (4.0/1.0 y 2.0/1.0) y el pH del medio utilizando membranas (CRC) de 100.0 kDa. Se obtuvo una adecuada separación para la mayor relación de concentraciones (4.0/1.0) a pH 5.0.

Las mejores condiciones de separación en el proceso de diafiltración de las proteínas BSA/LF, se obtuvieron tras el estudio de la influencia de la carga de las membranas (cargadas positiva y negativamente) y el pH. Utilizando membranas cargadas positivamente a pH 5.0, la LF se retuvo completamente en la alimentación y la BSA permeó con un flujo de 30.3 g m^{-2} h^{-1}. A pH 9.0 trabajando con la membrana negativa, se retuvo la BSA en la alimentación, permeando la LF con un flujo de 1.1 g m^{-2} h^{-1}.

El fouling de la membrana tras el proceso de diafiltración se describió mediante el modelo Derjaguin, Landau, Verwey, and Overbeek (DLVO). Las energías de interacción obtenidas fueron negativas y dominadas por las enegías de Van der Waals para ambos pHs. Los valores de las energías de interacción permitieron concluir que la formación de fouling fue similar en ambos casos.

5.2. RETOS PARA INVESTIGACIONES FUTURAS

Esta tesis pretende abrir la posibilidad de nuevas vías al desarrollo de técnicas de separación de proteínas del suero lácteo mediante membranas. A pesar de los buenos resultados obtenidos durante el desarrollo de este trabajo hay todavía retos que deben ser solucionados antes de que este proceso pueda convertirse en realidad.

La separación de BSA de la mezcla binaria con LF se alcanzó satisfactoriamente, pero la separación de LF, debido a los bajos flujos obtenidos, está lejos de poder ser considerada para un proceso a mayor escala.

En este trabajo se demostró la viabilidad de la separación de las proteínas mediante tecnología de membranas combinada con tecnología de electrodiálisis, sin embargo, se necesita profundizar en el estudio de las condiciones que faciliten unos flujos y selectividades satisfactorios.

Una vez obtenidos valores de separación que puedan cumplir con las necesidades industriales, el uso de efluentes de suero reales será necesario para la optimización del sistema.

NOMENCLATURE

ABBREVIATIONS

A	Hamaker constant (J)
AA buffer	sodium acetate/acetic acid
Ala (A)	Alanine
Arg (R)	Arginine
Asn (N)	Asparagine
Asp (D)	Aspartic acid
BSA	bovine serum albumin
BHA buffer	borax/hydrochloric acid
c_o	concentration (mol m^{-3})
C_p	concentration in the permeate (mol m^{-3})
C_t	concentration in the tank (mol m^{-3})
CRC	composite regenerated cellulose
C	concentration (mol m^{-3})
Cys	Cysteine (C)
d	particle size (nm)
D	separation distance (0.156 nm)
e	electron charge (1.602×10^{-19} C)
Ee	electrostatic interactions (J)
EDUF	electrodialysis with ultrafiltration membrane
EFM	Electrically-enhanced membrane filtration
EMC	Electrophoretic membrane contactor
Et	total interactions (J)
Ew	van der Waals interactions (J)
E_z	transmembrane voltage (V m^{-1})
F	Faraday's constant (96500 C mol^{-1})
Fab DNA	Antigen-binding fragment of DNA
ƒ(κa)	Henry's function
f/f_0	frictional ratio
f	frictional coefficient

f_0	theoretical frictional coefficient
Glu (E)	Glutamic acid
Gly (G)	Glycine
Gln (k)	Glutamine
HAC	acetic acid
Hb	hemoglobin
His (H)	Histidine
HPLC	high-performance liquid chromatography
I	ionic strength (mol L^{-1})
IEM-FFIEF	Ion-exchange-membrane-partitioned free-flow
Ile (I)	Isoleucine
Ip	isoelectric point
k	Boltzmann constant (1.38×10^{-23} J K^{-1})
K^{int}	intrinsic equilibrium constants
K_j	equilibrium constant of Cl^- binding sites
Leu (L)	Leucine
L_D	Debye length (nm)
LF	bovine lactoferrin
LYS	lysozyme
Lys (K)	Lysine
Met (M)	Methionine
Mes	2-(N-morpholino)ethanesulfonic acid
m_j	number of Cl^- binding sites
M_W	molecular weight (kDa)
MYO	myoglobin
N	Avogadro's number (6.022E23 mol^{-1})
n_i	number of titratable amino acids
P	pressure (Pa)
PD buffer	sodium phosphate/dipotassium phosphate
PdI	polydispersity index
Phe (F)	Phenylalanine
Pro (P)	Proline
Q	quantity of protein in permeate (g)
Q_o	initial quantity of protein (g)
R	gas constant (8.314 J mol^{-1} K^{-1})

R_1, R_2	protein and membrane radius (m)
R_v	recovery (%)
r_S	Solute radius (nm)
r	Stokes radius (nm)
Ser (S)	Serine
S_o	observed sieving coefficient (g L^{-1} g^{-1}L)
T	absolute temperature (K)
t	time (h)
T_M	melting point of proteins (°C)
Thr (T)	Threonine
Tr	transmittance (g L^{-1} g^{-1}L)
Tris	tris(hydroxymethyl)aminomethane);
Trp (W)	Tryptophan
Tyr (Y)	Tyrosine
v	partial specific volume (m^3 g^{-1})
V	permeate volume (L)
Val	Valine
Vd	diavolume volume permeate vs initial volume (L L^{-1})
V_o	initial volume (L)
WPI	whey protein isolate
z	protein surface charge (mV)
z_i	ion valence
Z_{ion}^-	anions charge contribution (mV)
Z_H^+	cations charge contribution (mV)
z_{max}	total number of positively charged amino acid residues at very low pH
$Z_{protein}$	protein net charge (mV)

GREEK LETTERS

α-la	alpha lactalbumin
$\alpha_{i/j}$	selectivity, defined as the ratio between the sieving coefficients
β-lg	beta macroglobulin
ε_r	dielectric constant of the fluid (78.5)
ε_o	vacuum electrical permittivity (8.854×10^{-12} C V^{-1} m^{-1})
κ^{-1}	thickness of the electrical double layer, Debye layer (m)
σ_P	effective surface density (C m^{-2})
σ_S^*	effective surface density (C m^{-2})
μ	viscosity (Pa s)
μ_E	electrophoretic mobility (cm s^{-1} V^{-1})
ψ_s^*	electrostatic potential at the protein surface (V)
Λ	solution conductivity (Ω^{-1} m^{-1})
γ	activity coefficient of the ion
η	sample dynamic viscosity (N s m^{-2})
ζ	zeta potential (V, mV)

LIST OF SCIENTIFIC CONTRIBUTIONS

PUBLICATIONS IN INTERNATIONAL JOURNALS AND PATENTS

V. Valiño, M.F. San Román, R. Ibáñez and I. Ortiz. Improved separation of bovine serum albumin and lactoferrin mixtures using charged ultrafiltration membranes, **Sep. Purif. Technol. 125 (2014) 163–169**. IF= 2.894 Chemical Engeneering

V. Valiño, M.F. San Román, R. Ibáñez, J.M. Benito, I. Escudero and I. Ortiz**.** Accurate determination of key surface properties that determine the efficient separation of bovine milk BSA and LF proteins. **Sep. Purif. Technol.** IF= 2.894 Chemical Engeneering .Acepted with minor revisions **(03/06/2014)**

V. Valiño, M.F. San Román, R. Ibáñez and I. Ortiz**.** Evaluation of fouling on charged ultrafiltration membranes during the separation of milk whey proteins. **Desalination.** IF= 3.041. Under Review

V. Valiño, R. Valiente, M.F. San Román, R. Ibáñez e I. Ortiz Método espectroscópico para la determinación de proteínas en medios complejos. **P201400165.** Presented on 28/02/2014 and favorably informed on 02/06/2014 Ref number: **2464440-A1**

CONTRIBUTIONS TO INTERNATIONAL CONFERENCES

Virginia Valiño, Fresnedo San Román, Raquel Ibáñez, Inmaculada Ortiz. "Ultrafiltration Membranes for Protein Separation". **International Congress on Membranes and Membrane Processes ICOM 2011**. July 2011. Amsterdam. Netherlands. Poster.

Virginia Valiño, Fresnedo San Román, Raquel Ibáñez, Inmaculada Ortiz. "Separation of Bovine Serum Albumin and Lactoferrin Using Ultrafiltration with Charged Membranes**". 12th Mediterranean Congress of Chemical Engineering**. November 2011. Barcelona. Spain. Poster.

Virginia Valiño, Fresnedo San Román, Raquel Ibáñez, Inmaculada Ortiz."Improved Isoelectric Separation of Whey Proteins using charged ultrafilter membranes". **Congreso Internacional de Ingeniería Química de ANQUE 2012**. June 2012. Sevilla. Spain. Poster.

Virginia Valiño, Fresnedo San Román, Raquel Ibáñez, Inmaculada Ortiz." Isolation of minor whey proteins by diaultrafiltration with charged membranes". **20th International Congress of Chemical and Process Engineering CHISA 2012**. August 2012. Prague. Czech Republic. Poster.

Virginia Valiño, Fresnedo San Román, Raquel Ibáñez, Inmaculada Ortiz. "Organic membranes for protein separation: characterization of electrical properties by means of Zeta Potential". **Euromembrane 2012**. September 2012. London. UK. Poster.

Virginia Valiño, Fresnedo San Román, Raquel Ibáñez, Jose Manuel Benito, Mª Isabel Escudero e Inmaculada Ortiz. "Medida de Tamaño y Potencial Zeta como herramienta para el correcto diseño de procesos de separación de proteínas" **XXXIV Reunión Bienal de la Real Sociedad Española de Química**. September 2013. Santander. Spain. Oral

Virginia Valiño, Fresnedo San Román, Raquel Ibáñez, Inmaculada Ortiz. "Evaluation of the membrane fouling in the separation of bovine serum albumin and lactoferrin mixtures by ultrafiltration**". IX Ibero-American Congress on Membrane Science and Technology**. May 2014. Santander. Spain. Oral

Virginia Valiño, Fresnedo San Román, Raquel Ibáñez, Jose Manuel Benito, Mª Isabel Escudero e Inmaculada Ortiz. "Improving whey proteins purification by ultrafiltration: Determination of bovine milk BSA and LF optimal surface properties". **International Congress on Membranes and Membrane Processes ICOM 2014**. July 2014. Suzhou China. Poster.